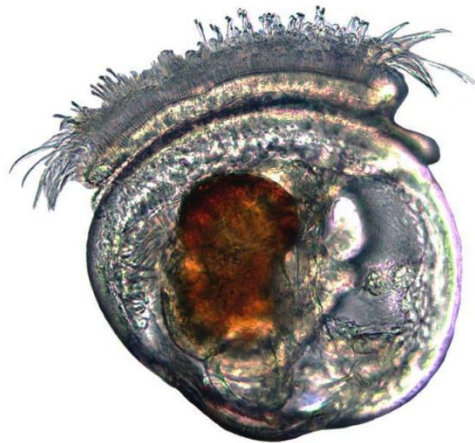


Larval development of the New Zealand mussel *Perna canaliculus* and effects of cryopreservation

Adam B. Rusk



A thesis submitted to
Auckland University of Technology
in partial fulfilment of the requirements for the degree of
Master of Science (MSc)

2012

School of Applied Science

TABLE OF CONTENTS

<i>LIST OF FIGURES</i>	VI
<i>LIST OF TABLES</i>	XI
<i>ATTESTATION OF AUTHORSHIP</i>	XII
<i>ACKNOWLEDGEMENTS</i>	XIII
<i>ABSTRACT</i>	XV
CHAPTER ONE: General Introduction	1
1.1 INTRODUCTION AND LITERATURE REVIEW.....	2
1.1.1 Mussel biology & ecology.....	2
1.1.2 Global & national aquaculture review.....	10
1.1.3 Hatchery rearing of <i>Perna canaliculus</i>	13
CHAPTER TWO: Larval Development	16
2.1 ABSTRACT.....	17
2.2 INTRODUCTION AND LITERATURE REVIEW.....	19
2.2.1 General bivalve larval development.....	19
2.2.2 Bivalve larval shell morphology.....	24
2.2.3 Bivalve larval nervous system.....	26
2.2.4 Larval development of <i>Perna canaliculus</i>	31

2.2.5	Significance of research on Perna canaliculus larvae	35
2.3	AIM & OBJECTIVES.....	36
2.4	METHODS AND MATERIALS.....	36
2.4.1	General larval rearing.....	36
2.4.2	Survivability	40
2.4.3	Shell length.....	40
2.4.4	Feeding consumption	41
2.4.5	Light microscopy.....	41
2.4.6	Scanning electron microscopy	42
2.4.7	Histology.....	43
2.4.8	Confocal microscopy	44
2.4.9	Statistical analyses	45
2.5	RESULTS	46
2.5.1	Survivability analysis	46
2.5.2	Shell length analysis.....	47
2.5.3	Feeding consumption analysis	48
2.5.4	Embryogenesis.....	49
2.5.5	Shell morphology.....	52
2.5.6	Organogenesis	56
2.5.7	Neurogenesis	62

2.6	DISCUSSION.....	70
2.6.1	Survivability	71
2.6.2	Shell morphology and growth.....	73
2.6.3	Feeding consumption	76
2.6.4	Embryogenesis.....	78
2.6.5	Organogenesis	80
2.6.6	Neurogenesis	84
	CHAPTER THREE: Cryopreservation	91
3.1	ABSTRACT.....	92
3.2	INTRODUCTION AND LITERATURE REVIEW.....	93
3.2.1	General bivalve cryopreservation.....	93
3.2.2	Cryopreservation on Perna canaliculus	96
3.2.3	Significance of cryopreserving Perna canaliculus larvae.....	98
3.3	AIM & OBJECTIVES.....	98
3.4	METHODS AND MATERIALS.....	99
3.4.1	Experimental reagents	99
3.4.2	Larval incubation and collection	99
3.4.3	Cryopreservation	100
3.4.4	Larval rearing & sampling.....	102
3.4.5	Statistical analyses	104

3.5	RESULTS	104
3.5.1	Survivability	104
3.5.2	Shell length.....	106
3.5.3	Feeding consumption.....	107
3.5.4	Shell morphology.....	109
	Control larvae.....	109
	Cryopreserved at D-stage.....	109
	Cryopreserved at trochophore stage	110
3.5.5	Organogenesis	117
	Control larvae.....	117
	Cryopreserved at trochophore	123
	Cryopreserved at D-stage.....	126
3.5.6	Neurogenesis	128
	Control larvae.....	128
	Cryopreserved at D-stage.....	134
	Cryopreserved at trochophore	138
3.6	DISCUSSION.....	141
3.6.1	Survivability	142
3.6.2	Shell length.....	145
3.6.3	Feeding consumption	147

3.6.4	Shell morphology.....	148
3.6.5	Organogenesis	150
3.6.6	Neurogenesis	152
	CHAPTER FOUR: General Discussion	156
4.1	DISCUSSION	157
	REFERENCES	164

LIST OF FIGURES

Figure 1.1. Female green-lipped mussel releasing orange oocytes.....	5
Figure 1.2. Male green-lipped mussel releasing white clouds of sperm.	6
Figure 1.3. Unfertilised oocytes of <i>Perna canaliculus</i>	7
Figure 1.4. Life cycle of mussel.....	8
Figure 2.1. General bivalve and freshwater bivalve life cycle	20
Figure 2.2. Diagram of the pediveliger stage of oyster <i>Ostrea edulis</i>	28
Figure 2.4. Experimental design for larval rearing	39
Figure 2.5. Average survivability of mussel larvae over 21 days	46
Figure 2.6. Average shell length of mussel larvae over 21 days	47
Figure 2.7. Average feeding consumption of mussel larvae over 21 days	48
Figure 2.8. Light images of unfertilised egg to umbonate larva	50
Figure 2.9. Embryogenesis of <i>Perna canaliculus</i>	51
Figure 2.10. Late gastrula of <i>Perna canaliculus</i>	52
Figure 2.11. Shell development of <i>Perna canaliculus</i>	54
Figure 2.12. D-stage larva at 4 days old.....	55
Figure 2.13. Post-larva at 20 days old	55
Figure 2.14. Sagittal section of a D-larva at 3 days old	58
Figure 2.15. Sagittal section of an early umbo larva at 7 days old	59
Figure 2.16. Frontal section of an early umbo larva at 7 days old	59

Figure 2.17. Sagittal section of late umbo larva at 11 days old.....	60
Figure 2.18. Sagittal section of late umbo larva at 13 days old.....	60
Figure 2.19. Transverse section of late umbo larva at 15 days old	61
Figure 2.20. Transverse section of pediveliger at 18 days old.....	61
Figure 2.21. Larva of pediveliger at 18 days old	62
Figure 2.22. FMRFamide immunoreactivity in trochophore at 18 hours old.....	65
Figure 2.23. FMRFamide immunoreactivity in D-stage at 2 days old	65
Figure 2.24. FMRFamide immunoreactivity in D-stage at 5 days old	66
Figure 2.25. FMRFamide immunoreactivity in early umbo larva at 10 days old.....	67
Figure 2.26. FMRFamide immunoreactivity in late umbo larva at 14 days old.....	68
Figure 2.27. FMRFamide immunoreactivity in pediveliger larva at 18 days old	69
Figure 3.1. Experimental design of cryopreserved and non-cryopreserved larvae	103
Figure 3.2. Average percent survival of mussel larvae over the 21-day rearing period.....	105
Figure 3.3. Average shell length of larvae over 19 days	107
Figure 3.4. Average percent feeding consumption of larvae over 23 days.....	108
Figure 3.5. SEM images of D-stage to umbonate larvae	112
Figure 3.6. Larva at 5 days old cryopreserved at trochophore stage	113
Figure 3.7. Larva at 7 days old cryopreserved at trochophore stage	113

Figure 3.8. Larva at 7 days old cryopreserved at trochophore stage	114
Figure 3.9. Larva at 11 days old cryopreserved at trochophore stage	114
Figure 3.10. Larva at 8 days old cryopreserved at D-stage	115
Figure 3.11. Larva at 15 days old cryopreserved at D-stage	115
Figure 3.12. Larva at 15 days old cryopreserved at D-stage	116
Figure 3.13. Light images of D-stage to late umbo-stage larvae showing organogenesis and microalgae content	119
Figure 3.14. Frontal section of unfrozen D-stage larva at 3 days old	120
Figure 3.15. Sagittal section of unfrozen D-stage larva at 3 days old	120
Figure 3.16. Sagittal section of unfrozen early-umbo larva at 7 days old.....	121
Figure 3.17. Sagittal section of unfrozen late-umbo larva at 11 days old.....	121
Figure 3.18. Frontal section of unfrozen late-umbo larva at 15 days old	122
Figure 3.19. Sagittal section of unfrozen pediveliger at 20 days old	122
Figure 3.20. Frontal section of unfrozen pediveliger at 20 days old	123
Figure 3.21. Sagittal section of D-stage larva at 3 days old cryopreserved at trochophore	124
Figure 3.22. Frontal section of D-stage larva at 3 days old cryopreserved at trochophore	125
Figure 3.23. Frontal section of late-umbo larva at 13 days old cryopreserved at trochophore	125

Figure 3.24. Sagittal section of D-stage larva at 3 days old cryopreserved at D-stage	127
Figure 3.25. Sagittal section of late-umbo larva at 11 days old cryopreserved at D-stage	127
Figure 3.26. Transverse section of late-umbo larva at 15 days old cryopreserved at D-stage	128
Figure 3.27. FMRFamide immunoreactivity in control larva at 2 days old	131
Figure 3.28. FMRFamide immunoreactivity in control larva at 5 days old	131
Figure 3.29. FMRFamide immunoreactivity in control larva at 10 days old	132
Figure 3.30. FMRFamide immunoreactivity in control larva at 14 days old	133
Figure 3.31. FMRFamide immunoreactivity in control larva at 18 days old	134
Figure 3.32. FMRFamide immunoreactivity in 2 day old larva cryopreserved at D-stage	136
Figure 3.33. FMRFamide immunoreactivity in 5 day old larva cryopreserved at D-stage	136
Figure 3.34. FMRFamide immunoreactivity in 10 day old larva cryopreserved at D-stage	137
Figure 3.35. FMRFamide immunoreactivity in 14 day old larva cryopreserved at D-stage	137
Figure 3.36. FMRFamide immunoreactivity in 2 day old larva cryopreserved at trchophore.....	139

Figure 3.37. FMRFamide immunoreactivity in 5 day old larva cryopreserved at trochophore139

Figure 3.38. FMRFamide immunoreactivity in 10 day old larva cryopreserved at trochophore.140

Figure 3.39. FMRFamide immunoreactivity in 14 day old larva cryopreserved at trochophore140

LIST OF TABLES

Table 1. Different embryonic and larval stages of <i>Perna canaliculus</i> in hours and days	56
Table 2. Different larval stages of cryopreserved and controls of <i>Perna canaliculus</i> in days.....	116

ATTESTATION OF AUTHORSHIP

"I hereby declare that this submission is my own work and that, to the best of my knowledge and belief, it contains no material previously published or written by another person (except where explicitly defined in the acknowledgements), nor material which to a substantial extent has been submitted for the award of any other degree or diploma of a university or other institution of higher learning."

Signed:



Date: 18/10/2012

ACKNOWLEDGEMENTS

To my supervisors

I am grateful to my supervisor Andrea Alfaro, who has provided support and the foundations to succeed which I have immensely appreciated. I wish to thank Serean Adams of Cawthron Institute for supporting me as this research wouldn't have been possible without her involvement.

To my family

Father Brett, mother Wendy, and brother Glen, thank you for your support both financially and motivationally. A special thanks to my wonderful and loving partner Heather, who has supported me through thick and thin, and patiently tolerated my absence during this study. To my extended family the Hodgsons, I wish to thank you all for your generosity in providing a wonderful home, crazy cat, and for raising such a beautiful woman which has made my studies that much easier and enjoyable.

To my colleagues

Thank you to those who have taken their own time to communicate and discuss my findings within the Aquaculture Biotechnology Group (ABG). A special thanks to Tim Young and Annapoorna Ganesan for their help and willingness to share knowledge and expertise in *Perna canaliculus* larvae, and I wish you both well for the future.

To others who have assisted me

I am very grateful to Cawthron Institute for the MBIE funded grant, and to the Glenhaven crew for helping me with the larval rearing experiments. A special thanks to Jonathan Morrish and Ellie Watts of Cawthron who somehow found time out of their very busy days to help me. Thanks Ellie and Nige for accommodating me at your lovely house, your hospitality was very much appreciated.

Toitu te marae a Tane Toitu te marae a Tangaroa Toitu te iwi

If the land is well and the sea is well, the people will thrive

ABSTRACT

The New Zealand green-lipped mussel, *Perna canaliculus*, is an important aquaculture species. This commercially attractive mussel species contributes over 70% of total aquaculture in New Zealand, with exports in excess of \$NZ 220 million. This industry relies heavily on wild-caught spat, which accounts for about 80% of seed requirements in mussel farming. This source of wild spat is unreliable and unpredictable. As a consequence, recent research focus has been directed at successfully rearing larvae to spat within hatchery settings. Previous research has been focussed at achieving high settlement rates, but this is highly variable due to seasonal variations and inconsistent rearing parameters. An alternative approach to utilising seasonally viable larvae is to cryopreserve (freeze) healthy *Perna canaliculus* larvae and thaw them on demand for hatchery production. This allows a year-round spat supply without the need to condition broodstock for out of season production. However, the success of this method also has been variable, often resulting in low survival rates. Part of the reason for this lack of success is that little is known about the thawing and post-thawing effects on larval viability and subsequent development.

Overall, knowledge about the intricate developmental processes involved within the embryo or larval stages is lacking, and no detailed study has characterised these stages of larval development. Therefore, this study is the first to describe, in detail, larval development of *Perna canaliculus* from embryogenesis through to settlement in a hatchery environment. This project also included the first

comprehensive investigation of the effects of cryopreservation for post-thawed trochophore (16 hours post-fertilisation) and D-stage (48 hours post-fertilisation) larvae through subsequent larval development. A multi-technique approach involving visual observations, scanning electron microscopy, histology, and immunochemistry were performed on larval samples collected daily through all stages of larval development over a 21-day rearing period. Cryopreserved and normal larvae were assessed daily through survivability, shell length, feeding consumption, shell morphology, organogenesis, and neurogenesis.

Normally reared larvae had decreasing percent survival with the lowest survival values occurring at the pediveliger and post-settlement stage. Feeding consumption also varied over the 21-day rearing time period with a typically high feeding rate up to 15 days post-fertilisation to metamorphosis. Shell length was positively linear with little deviation except near the settlement stage where variations in shell growth were apparent. A low larval density (< 4%) was observed through to settlement and substrate attachment stages, which normally indicates competent settlement behaviour. For these normally reared larvae, embryogenesis was followed to a gastrula stage at 18 hours post-fertilisation, with the appearance of a blastopore, apical sense organ, and enclosing vegetal pole. D-stage larvae had limited organogenesis with the development of an alimentary and nervous systems. Shell morphology on D-stage larvae (2 days old) revealed a flat hinged, pitted punctuate prodissoconch I shell, followed closely by commarginal growth lines within the prodissoconch II shell at 4 days old. The umbo stage (7–17 days old) had further organogenesis

development with a protruding beating velum, a well-developed posterior and adductor muscle, velum retractor muscles, and further dissoconch II secretion of the shell with a more rounded umbonate appearance. Neurogenesis had significantly progressed at this stage with paired cerebral, pedal, and visceral ganglia observed. Pediveliger larvae (18 days old) developed a complete nervous system with more innervations and fibres extending throughout the larva. During pediveliger development, a rapid metamorphosis transition occurred with the development of a gill rudiment, eye spot, and functioning foot. The first appearance of a dissoconch shell layer appeared during this transition.

Within the cryopreservation study, results showed that there were significant differences in survivability, shell length, and feeding consumption between controls (not cryopreserved) and frozen (cryopreserved) treatments, but no comparable differences were observed among both frozen treatments (cryopreserved at the trochophore stage and cryopreserved at the D-stage) throughout the 21-day development period. At 18 days post-fertilisation, ~23% of control larvae had progressed to competent pediveliger, while <1% of both frozen larvae stages survived. Those larvae that survived were unable to develop to competent pediveliger or post-larvae. Settlement was achieved in ~9% of control larvae at 21 days post-fertilisation with most individuals developing eye spots. Significant differences were observed in neurogenesis between frozen trochophore larvae and controls. Conversely, frozen D-stage larvae did not differ greatly to controls, and differed slightly to trochophore larvae. Characterisation of shell morphology revealed abnormalities to larvae

on both frozen treatments. Frozen trochophore larvae showed the greatest shell abnormalities, which suggests that cryo-damage to the shell gland had occurred. Organogenesis was delayed in larvae within both frozen treatments with no larvae within frozen treatments developing an eye spot. However, larvae in controls successfully made the transition to settlement. This delay in organogenesis and overall developmental characteristics were indicative of cryo-injuries sustained at a cellular level. The relevance of this work ultimately fills existing gaps in larval development of *Perna canaliculus* in normal and cryopreserved larvae. Characterisation of both viable and abnormal larvae through development is of benefit in reducing commercial hatchery costs and understanding the biology of *Perna canaliculus* larvae.

CHAPTER ONE: General Introduction

1.1 INTRODUCTION AND LITERATURE REVIEW

1.1.1 *Mussel biology & ecology*

Mussels belong to the Class Bivalvia and are mostly benthic substrate dwellers which attach to substrates with byssus threads, and filter phytoplankton, zooplankton, or detritus from the water column (Vakily, 1989). The byssus threads are excreted from the foot and are made of a tanned protein (Gosling, 2003). The morphology of mussels generally consists of a set of two valves hinged together at the anterior by means of a ligament (Gosling, 2003). This area is also referred to as the umbo. The shell gland and mantle are responsible for shell secretion in most mussels (Gosling, 2003). Mussels are generally dioecious and produce large numbers of pelagic planktotrophic larvae that spend up to several weeks in the water column (Widdows, 1991). One of the most important factors for controlling mussel reproduction is seasonal temperatures and the availability of food (Verween, Vincx, & Degraer, 2009). Feeding in mussels is through the gills using exhalant and inhalant siphons to filter food through ciliary tracts (Vakily, 1989; Gosling, 2003). There is a range of mussel species throughout the world ranging in distribution from intertidal and subtidal habitats (Saier, 2002), to deep sea vents (Turnipseed, Knick, Lipcius, Dreyer, & Van Dover, 2003). The genus *Perna* includes various mussel species and differs from the genus *Mytilus* in their geographic distributions and some morphological features such as the shape and colour of the shell and tissue morphology (Siddall, 1980; Wood, Apte, MacAvoy, & Gardner, 2007). There are three species of the *Perna* genus worldwide. *Perna canaliculus* (Gmelin

1791) is endemic to New Zealand, *Perna perna* (Linnaeus 1758) which is found throughout South America and Africa, and *Perna viridis* (Linnaeus 1758) distributed within the Indo-Pacific region (Alfaro et al., 2011). Culturing of *Perna canaliculus* is well established within the New Zealand mussel aquaculture industry (Vakily, 1989).

Perna canaliculus (Gmelin 1791) is a common endemic mytilid bivalve found in intertidal and sub-tidal areas of New Zealand and is one of several mussel species found throughout New Zealand (Buchanan, 1999). Other mussel species around New Zealand include *Mytilus edulis aoteanus* (Powell 1958), *Xenostrobus pulex* (Lamarck 1819), and *Modiolarca impacta* (Herman 1783), which are all widely distributed around the New Zealand coast (Redfearn, Chanley, & Chanley, 1986). *Perna canaliculus* has distinct green shell margins and striated vertical bands which give it a unique appearance compared to other mussels found in New Zealand, such as the Blue mussel *Mytilus edulis aoteanus*. This green margin gives rise to the name Greenshell Mussel™, which is its commercial name. However, when found in the wild, this mussel species is referred to as the green-lipped mussel. Its distribution ranges widely throughout the islands, but is more commonly found in the more northern warmer climates (Powell, 1979). Some mussel beds can be very dense with up to 100 individuals m⁻² in more northern regions (Flaws, 1975; Hickman, 1991). These mussels inhabit rocky reefs, wharf piles, and soft muddy bottom habitats (Morton & Miller, 1973). The distribution of this species is suggested to be determined by environmental parameters, such as salinity, and temperature.

Temperature tolerances for this species range from 5.3°C in the far south to 27°C in the north, and salinity tolerances can be between 30 to 35 PSU (MacDonald, 1963; Flaws, 1975; & Hickmann, 1991).

Perna canaliculus is a dioecious broadcast spawner which relies on gamete dispersal through ocean currents (Jenkins, 1985). Gametogenesis has been observed in adult mussels through to release of oocytes (Fig. 1.1) and sperm (Fig. 1.2) and subsequent fertilisation and larval development (Booth, 1977; Buchanan Hickman, Waite, Illingworth, Meredyth-Young, & Payne, 1991; Buchanan & Babcock, 1997; Buchanan, 1999; Buchanan, 2001). Oocytes are approximately ~60 µm in diameter (Buchanan, 1999) (Fig. 1.3). However, detailed studies on the reproductive cycle of wild populations throughout New Zealand are lacking. A study by Alfaro, Jeffs, & Hooker (2001) investigated the reproductive behaviour of the adult green-lipped mussel at Ninety Mile Beach, Northern New Zealand, and found they were dioecious with a 1:1 sex ratio through all sizes. Alfaro et al. (2001) also discovered that the natural spawning season was from June-December, and some mussels contained ripe gametes all year which supplies mussel spat through the entire year at Ninety Mile Beach. This happens several times a season with evidence of gametogenesis occurring through the winter and spawning occurring either in late winter or spring (Hickman et al., 1991; Alfaro et al., 2001; Alfaro, Jeff, & Hooker, 2003). However, there is some evidence that suggests spatio-temporal variations in the reproductive cycle of *Perna canaliculus* exist throughout New Zealand (Hickman et al., 1991; Alfaro et al., 2001; Alfaro et al., 2003). A study by

Kennedy (1977) has also suggested that the coincidence of spawning of *Mytilus edulis aoteanus*, *Perna canaliculus*, *Xenostrobus. pulex*, and *Aulacomya ater maoriana*, which overlap spatially on New Zealand shores, raises the possibility of interspecific competition among the larvae for settlement space.



Figure 1.1. Female green-lipped mussel (*Perna canaliculus*) releasing orange oocytes.

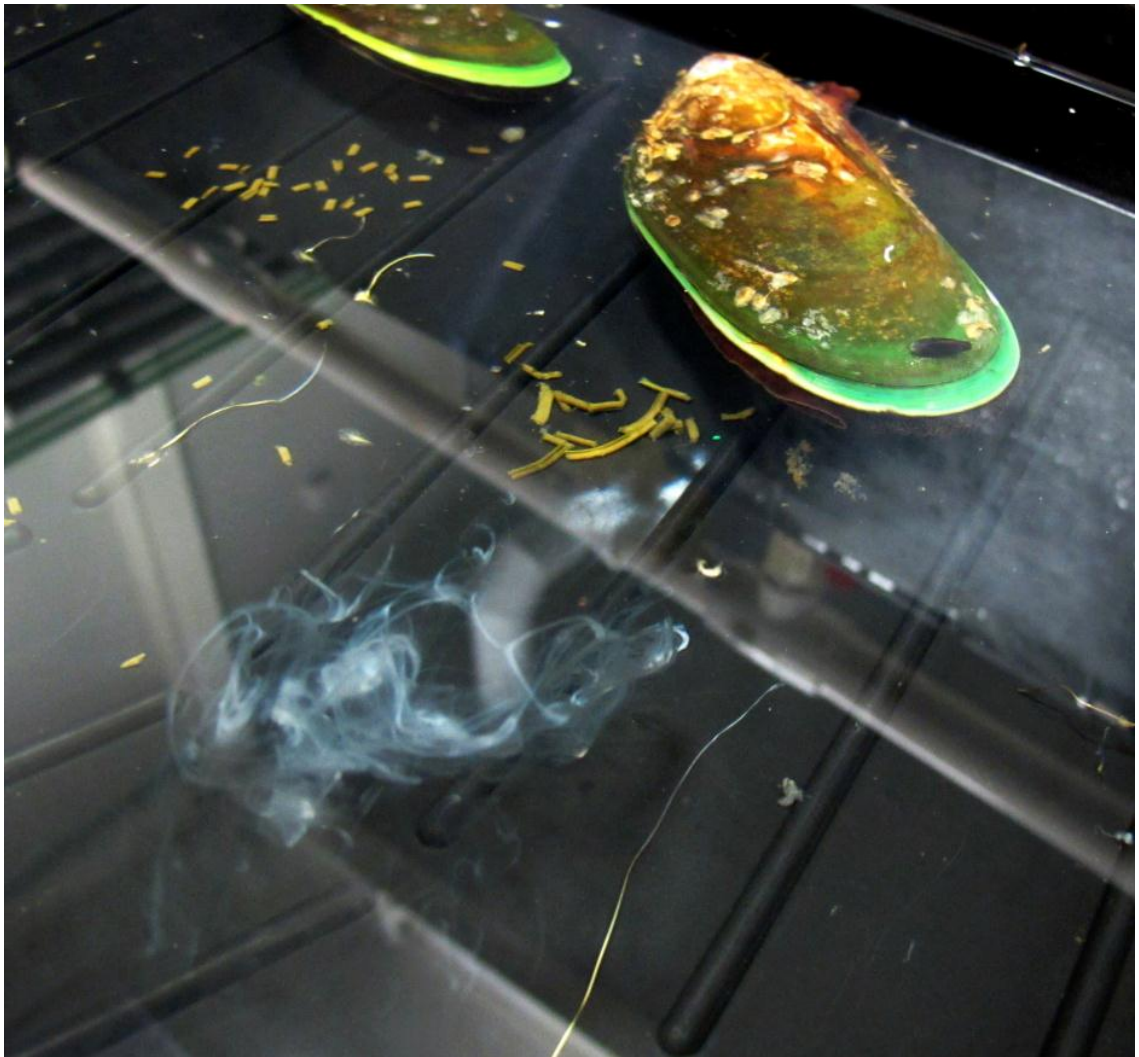


Figure 1.2. Male green-lipped mussel (*Perna canaliculus*) releasing white clouds of sperm.

Fertilised oocytes develop into a zygote, which develops unequal holoblastic spiral cleavage to form an embryo (Buchanan, 1999) (Fig 1.4). This is followed closely by a ciliated trochophore stage, which finally develops into the shelled veliger. Larvae spend a large amount of time feeding on phytoplankton in a suspended environment using their velum for both swimming and capturing microalgae. Larvae then undergo metamorphosis and make the transition from free-swimming veliger larvae to settled larvae. This settlement phase is defined

by Buchanan (1999) as the moment when larvae discontinue swimming. However, Young (2009) defined it as the firm attachment to a substrate. In this thesis settled larvae are defined by the stage at which they secrete mucous and attach to a substrate. Settled spat subsequently grow into juveniles and then adults (Buchanan, 1999). A detailed summary of this larval stage is described in chapter 2–2.21.

Detailed studies on early embryogenesis and subsequent larval development up to settlement is lacking for *Perna canaliculus*.

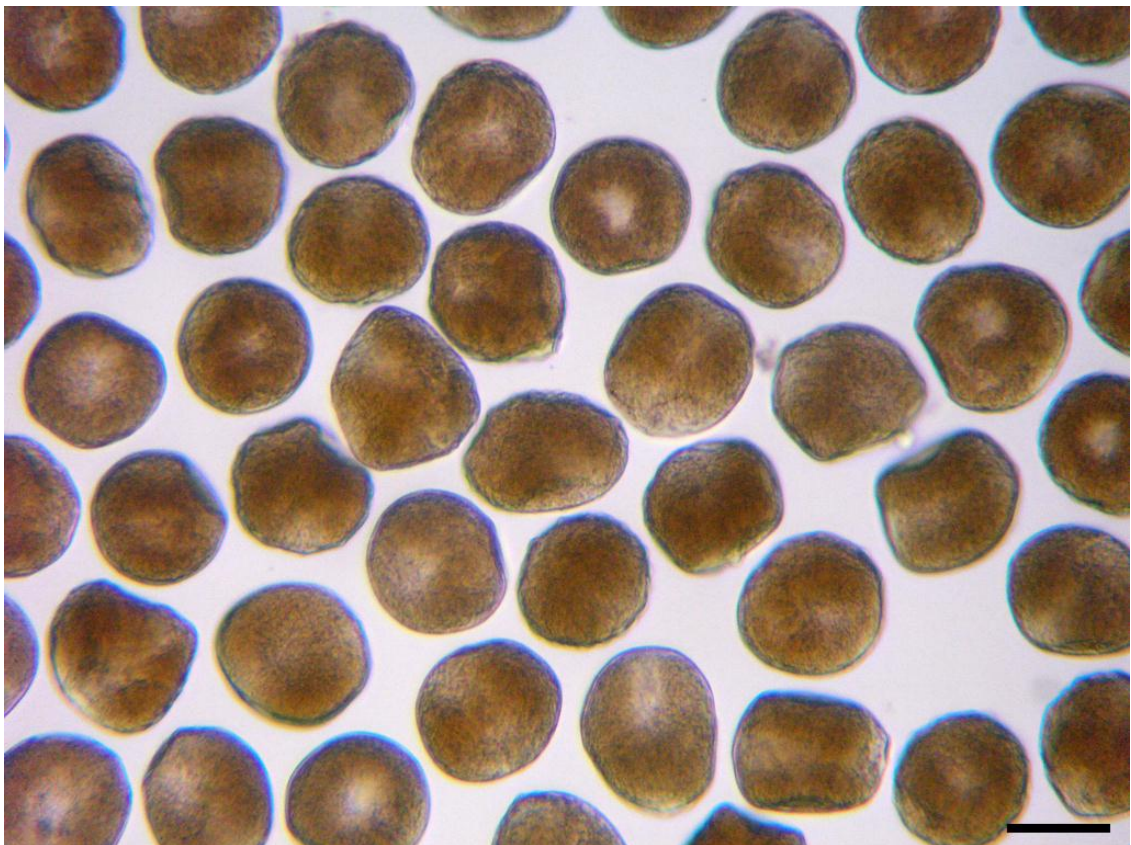


Figure 1.3. Unfertilised oocytes of *Perna canaliculus*. Scale bar = 40 μm .

Bayne (1964) was the first to describe the process of primary and secondary settlement in the blue mussel *Mytilus edulis* larvae, which includes initial attachment to filamentous substrates (primary settlement) before detaching and finding another suitable substrate (secondary settlement) to grow into adult mussels. For *Perna canaliculus*, the same principle applies with primary and secondary settlement taking place within the field or laboratory (Buchanan & Babcock, 1997; Buchanan, 1999; Alfaro & Jeffs, 2002; Young, 2009).

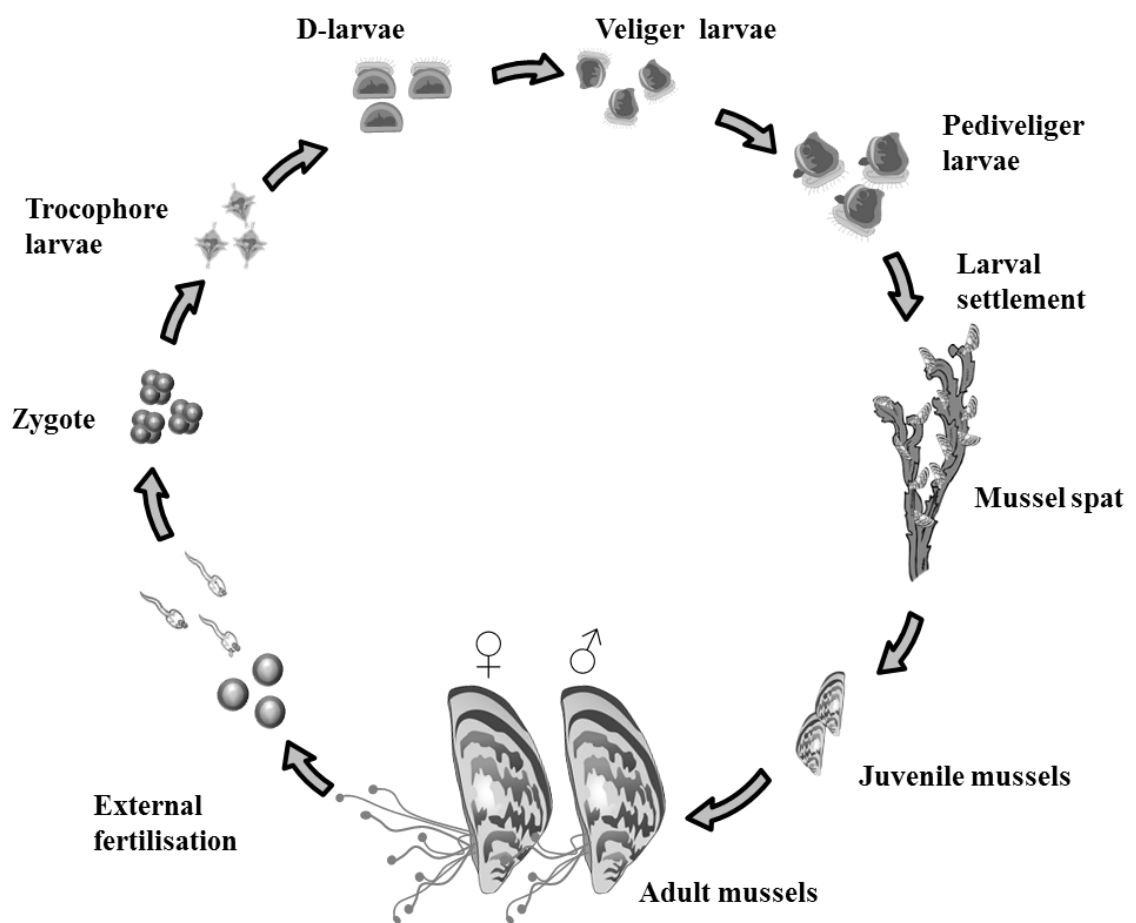


Figure 1.4. Life cycle of mussel adapted from Young et al. (2010).

A study by Buchanan (2004) on *Perna canaliculus* for Auckland's west coast beaches showed that juvenile mussels were distributed on algal substrates in relation to mussel size and degree of branching of the filamentous macroalgae. High primary settlement (< 0.5 mm) was shown to occur on finely-branched macroalgae, such as *Laurencia thyrsoifera*, *Champia laingii*, *Corallina officinalis*, and the hydroid, *Amphisbetia bispinosa*. However, moderately-branched macroalgae (*Gigartina albeata*, *Gigartina cranwellae*, *Pterocladia lucida*) had moderate numbers of primary settlers, "dispersers" (0.5–5.5 mm) and "stable" (> 5 mm) mussels. Also, coarsely-branched macroalgae (*Melanthalia abscissa*, *Pachymenia himantophora*) and the rocky shore had a high number of dispersers, a moderate number of stable mussels, and a few primary settlers (Alfaro et al., 2011).

More recent studies on the effects of neuroactive compounds on the settlement of *Perna canaliculus* have begun to expand our understanding on the mechanisms involved with this settlement behaviour (Young, 2009; Young, Alfaro, & Robertson, 2011). Chemical settlement inducers tested included hydrogen peroxide, acetylcholine, atropine, potassium chloride, epinephrine, L-DOPA, and cyclic adenosine monophosphate, all of which induced larval settlement with minimal toxic effects. Biological factors such as bacterial biofilms and biofilm exudates have also been shown to induce settlement in *Perna canaliculus* (Ganesan, Alfaro, Brooks, & Higgins, 2010).

This information in biology and ecology for *Perna canaliculus* is important for understanding the endogenous and exogenous processes involved in *Perna*

canaliculus development so that wild spat which is attached to macroalgae can be sustainably harvested to supply spat to mussel aquaculture farms around New Zealand.

1.1.2 Global & national aquaculture review

The New Zealand aquaculture industry has grown significantly over the last 40 years and is estimated to have revenue in excess of \$400 million, with a target of reaching \$1 billion in sales by 2025 as a government's goal to increase the seafood sector (Ministry for Primary Industries, 2012). The New Zealand seafood export values within the aquaculture sector were valued at \$307 million in the year 2011. In a global perspective, a limited global supply of fish from wild fisheries and increasing demand for seafood, particularly premium seafood, is set to grow substantially. By 2025, over half of all seafood consumed globally will be farm-produced, which will surpass wild capture production (Ministry for Primary Industries, 2012).

The US economy for the green-lipped mussels in the market dropped as a result of New Zealand suppliers dropping prices to maintain market share during the financial crisis. These prices have begun to rebound, which is expected to drive increased returns (Ministry for Primary Industries, 2012). The New Zealand green-lipped mussel is a commonly farmed aquaculture species with the industry producing \$226.3 million in the year of 2011. This is New

Zealand's single largest aquaculture product on the market today and is a highly important economic species (Ministry for Primary Industries, 2012). Green-lipped mussels exports make up 73.7% of total aquaculture exports from New Zealand. Currently, New Zealand only contributes a small amount in the world fisheries markets with 0.2% of aquaculture production in 2008 (Ministry for Primary Industries, 2012). The volume of green-lipped mussels exported increased by 3,969 tonnes (11.6%) to 38,097 tonnes in the year 2011. While export earnings increased by \$54.9M (32.1%) to \$226.3M in the period of 2011 (Ministry for Primary Industries, 2012). Over this time, export earnings have increased at a greater rate than export volumes which indicates export prices are increasing.

Key markets for green-lipped mussels are the United States (29.0% by value), Australia (8.4%), Korea (8.1%), and Spain (6.8%). The main driver of the increase in export earnings for green-lipped mussels was the United States as export earnings were up \$12.8M (24.2%) during the year to December 2011. Green-lipped mussel export earnings were also up from the previous 12 months for Korea (up \$5.1M), Germany (up \$4.1M) and Spain (up \$1.2M). The total volume of aquaculture species exported increased by 3.8% to 45,031 tonnes, and the total aquaculture export earnings increased by 12.0% to \$307.4 million during the year ending December 2011 (Ministry of Fisheries, 2011).

The number of authorised mussel farms in New Zealand is 1018, with the bulk of these farms based in the top of the South Island (Golden and Tasman Bays,

and the Marlborough Sounds) and the Coromandel (Firth of Thames) (Ministry of Fisheries, 2010). Around 69% of total green-lipped mussels in New Zealand are farmed in the Marlborough Sounds (New Zealand Aquaculture, 2012). The mussel industry is almost 100% reliant on seed or spat collected from the wild, most of which comes from Ninety Mile Beach, North Island, New Zealand, and is sent to commercial farms to be seeded onto ropes (Alfaro et al., 2011). The origin of this spat is virtually unknown regarding the sources of drift seaweed and other materials that constitute the settlement substrate for mussel spat harvested at Ninety Mile Beach (Alfaro et al., 2011). About 100,000 tonnes yr⁻¹ of spat is attached to seaweed and this equates to around 80% supplied to farms mainly in the Marlborough Sounds (Jefferies, 2000). The remaining 20% of spat is caught on mussel “spat catching ropes” directly from the water column (Alfaro et al., 2011). Farmers in the Marlborough Sounds and Golden Bay suspend these spat catching ropes in areas that are known to produce high quantities of planktonic larvae that are competent to settle (Young, 2009; Alfaro et al., 2011). However, Hay & Grant (2004) concluded that spat washed up or collected from spat farms has been scarce and unreliable over the years. Further ongoing threats to a continuous supply of spat include toxic microalgae, parasites and viruses, invasive species, oil spills, climate change, and depletion of broodstock populations (Alfaro et al., 2011). This emphasises the importance of having an alternative supply of mussel spat from large scale hatchery rearing. Overall, the improving economic climate suggests substantial further growth within the mussel aquaculture industry and thus the need to improve on hatchery rearing of *Perna canaliculus*.

1.1.3 Hatchery rearing of *Perna canaliculus*

Hatchery reared larvae of *Perna canaliculus* are currently being produced in Nelson, New Zealand, by Cawthron Institute (an independently owned research centre) and SpatNZ in collaboration with Sanford Ltd, Sealord Group, and Wakatu Incorporation. At both of these facilities, the adult mussels are conditioned and induced to spawn, and the gametes collected and fertilised. These embryos then develop into swimming veligers and are fed mixed diets of microalgae and reared until such time when they are competent enough to settle (18–28 days post fertilisation) onto mussel ropes.

Larval viability varies across each batch and is thought to be due to seasonal variation in broodstock conditioning, and other various environmental factors. Findings by Ragg et al. (2010) observed mean veliger survival rates of 22–49% for *Perna canaliculus* under simulated commercial culture conditions. Similar performance has been routinely observed in semi-commercial trials conducted at the Cawthron Institute, as well as occasional mortality cascades, where rapid deterioration in the tank environment can result in 100% mortality (NLC Ragg, personal communication). Other factors that are not presently being controlled under hatchery quality parameters are egg quality and bacterial loading. Variation in larval viability is proving to be a bottleneck in hatchery rearing of *Perna canaliculus*; consequently on-going applied research at the Cawthron Institute is directed towards the refinement of larval husbandry and the development of bulk culture systems for selective breeding (NLC Ragg, personal communication).

Supplementing this seasonal variation in larval viability, cryopreservation (freezing) is being trialed on *Perna canaliculus* larvae with the aim of utilizing well-conditioned broodstock. Subsequent thawing and rearing of these larvae on demand is widely used in animal husbandry of many farmed species (Paredes, 2012). Recently, researchers at the Cawthron Institute have adopted this approach by cryopreserving *Perna canaliculus* oocytes (Adams et al., 2009), sperm (Smith et al., 2012a,b), & trochophores (Paredes, 2012) with mixed results. The best success has been cryopreserving trochophore larvae (16–20 hours post-fertilisation) with 2.8% able to develop to competent pediveligers at 18 days old (Paredes, 2012). The cause of this low survivability is suggested to be affiliated with cryo-injuries during the thawing or cooling process. However, no studies have investigated the effects of these damages on subsequent larval development for this species or in cryopreserved D-stage larvae (2 days old). Paredes (2012) suggested the need to study the effects of cryopreservation on shell formation, organogenesis, and feeding during larval rearing would be of considerable value. This study therefore aims to address the effects of cryopreservation on subsequent larval development by cryopreserving trochophore and D-stage larvae, and to also describe normal larval development of *Perna canaliculus*.

Therefore the aims of this thesis are:

Aim 1: To describe *Perna canaliculus* embryonic and larval development from fertilisation through to post-settlement.

The objectives are:

- To describe early embryogenesis and shell morphology of larvae through scanning electron microscopy, and light microscopy.
- To describe organogenesis processes through histology and light microscopy.
- To describe neurogenesis from fertilisation to post-settlement through histology and immunochemistry.

Aim 2: To describe the effects of cryopreservation on overall larval development of *Perna canaliculus* from cryopreserved trochophore and D-stage larvae through to post-settlement.

The objectives are:

- To describe shell morphology of larvae through scanning electron microscopy, and light microscopy.
- To describe organogenesis processes through histology and light microscopy.
- To describe neurogenesis from D-stage to post-settlement through histology and immunochemistry.

CHAPTER TWO: Larval Development

2.1 ABSTRACT

The complex neuronal and ontogenetic development of bivalve larvae has been investigated extensively. However, few studies have taken an integrated and multidisciplinary approach to understand morphological, physiological and behavioural aspects of larval development. A comprehensive study on general embryogenesis, larval organogenesis, shell morphology, and the central and peripheral nervous system was performed on the New Zealand green-lipped mussel, *Perna canaliculus* under normal hatchery rearing conditions, over a 21-day rearing period. During this rearing process, larval samples were obtained at regular daily intervals to characterise the state of development and to record population dynamic parameters that are associated with these developmental characteristics. Light microscopy analyses revealed that embryogenesis progresses to a gastrula stage at 18 hours post-fertilisation, with the appearance of a blastopore, apical sense organ, and enclosing vegetal pole. D-stage larvae exhibited limited organogenesis with an alimentary and nervous system developing. Analysis of shell morphology on D-stage larvae indicate that they have a flat hinged pitted punctuate prodissoconch I shell followed closely by commarginal growth lines within the prodissoconch II shell. At the umbo stage, there is further organogenesis development with a protruding beating velum, a well-developed posterior and adductor muscle, velum retractor muscles, and further dissoconch II secretion of the shell with a more rounded umbonate appearance. Neurogenesis had significantly progressed with paired cerebral, pedal, and visceral ganglia observed. A fibre was seen extending

from the pedal ganglia to the anterior-adductor muscle in competent pediveliger larvae. Rapid metamorphosis occurs around the pediveliger stage with the development of a gill rudiment, eye spot, functioning foot, and the first appearance of a dissoconch layer. The nervous system becomes more refined in the pediveliger stage with innervations extending throughout muscle regions and between ganglia.

During the 21-day rearing period, the survival was generally linear, with lower survivability at the pediveliger and post-settlement stage. Feeding consumption also varied over this time period with a typical high feeding activity up to 15 days post-fertilisation and prior to metamorphosis. Shell length was positively linear with little deviation except near the settlement stage where variations in shell growth were apparent. A low density of larvae progressed onto the post-settlement stage and attached to substrates, showing competent settlement.

2.2 INTRODUCTION AND LITERATURE REVIEW

2.2.1 General bivalve larval development

The embryonic, larval and post-larval development of bivalves has been studied extensively to assist with aquaculture production on species of economic interest like the mussel (Bayne, 1964; Buchanan, 1997; Buchanan, 1999; Alfaro, 2005) or oyster (Gwo, 1995; Elston, 1999; Ellis, 2010). This research has been aimed at better understanding embryonic and larval development of planktotrophic or non-planktotrophic larvae. There are approximately 8000 species of living bivalves (Boss, 1982). All of these species have a biphasic life cycle, and most rely on a planktonic, transitory development stage for their dispersal (Zardus & Martel, 2006). The Class Bivalvia is the second largest class within the Phylum Mollusca, and includes a combination of marine and freshwater clams, mussels, scallops, and oysters (Ponder, & Lindberg, 2008; Ellis, 2010).

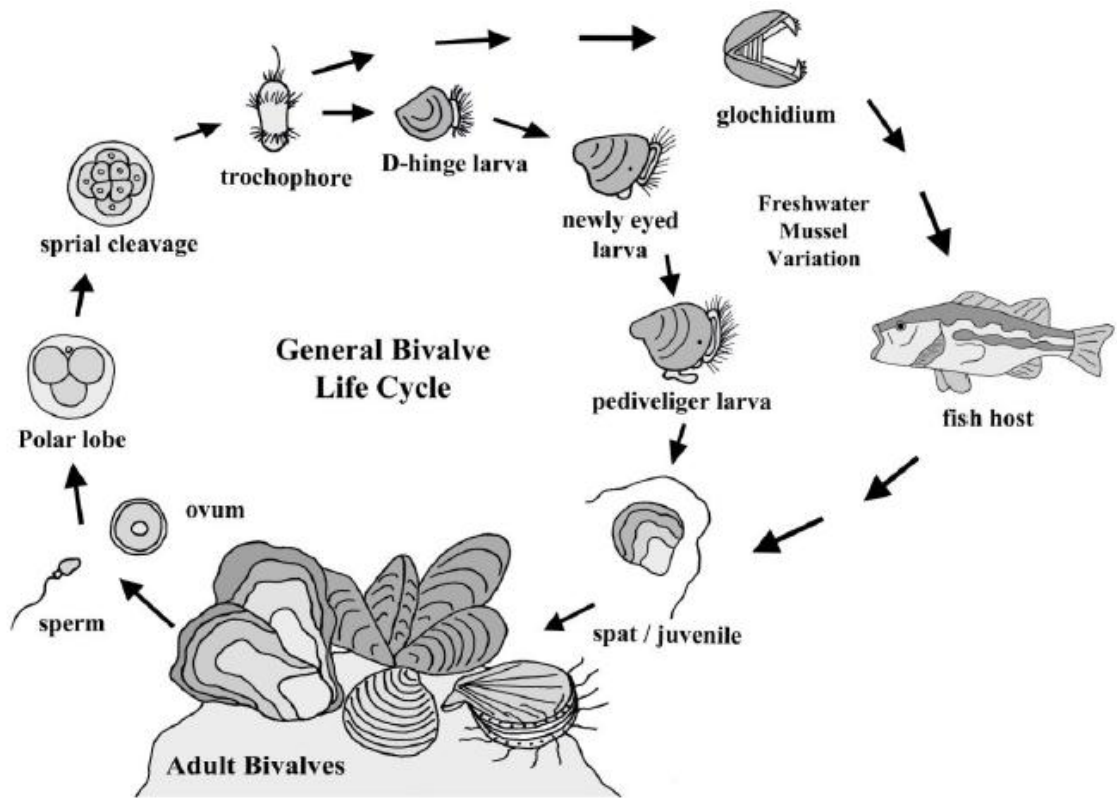


Figure 2.1. General bivalve and freshwater bivalve life cycle (Ellis, 2010).

The life cycle of bivalves in saltwater and freshwater environments normally starts with an embryonic stage, followed by a veliger larva and subsequent juvenile and adult (Fig. 2.1). Freshwater bivalves of the Superfamily Unionacea have a different life history involving veliger larvae (glochidia) undergoing a brief period as obligate ectoparasites on the fins, gills, and other external parts of fish hosts (Hagg & Warren, 1997). Reproduction among bivalve species is sexual, and most species are dioecious with some being hermaphroditic (containing both sex organs), such as scallops (Thorson, 1936; Allen, 1961; Gosling, 2003). The gametes are released by synchronised broadcast spawning, and dispersal of the eggs (oocytes) and sperm relies mostly on favourable currents and

hydrodynamic forces. Successful fertilisation depends on the quantity of gametes released, abundance of conditioned adults, and external environmental factors. The egg size varies among species and has been shown to be a predictor of developmental mode (Jaekle, 1995). Planktotrophic eggs are generally small (40–85 μm) while lecithotrophic eggs are large (90–300 μm) and are invested with an egg yolk (Gosling, 2003). Sperm penetration of the egg is facilitated by the release of a substance which lyses the vitelline membrane around the egg (Gosling, 2003). In most bivalve species, a fertilisation membrane forms at syngamy as a block to polyspermy, and a thick jelly coat is produced (Zardus et al., 2006). The appearance of polar bodies during cleavage is the first indication of successful fertilisation (Silberfeld & Gros, 2006; Costa, Darriba & Matinez-Patino, 2008). The basal pole of the oocyte develops into the blastoporal (vegetative) pole of the embryo, and the apical pole becomes the apical (animal) pole where the polar bodies are generated (Nielsen, 2004). The embryos subsequently go through a series of spiral cleavages where the cells divide to create micromeres. Embryogenesis then proceeds through the blastula, gastrula, and trochophore stages, which use lipids and other energy reserves prior to developing a velum feeding apparatus, mouth and stomach (Zardus et al., 2006). At the blastula stage cilia are visible, and a bundle of cilia develops at the animal pole, which is deemed the apical tuft that emerges from cells of the apical plate (Gosling, 2003). A combination of the apical tuft and apical plate forms the apical sense organ, sometimes referred to as the apical organ (Gosling, 2003). Many studies have described the apical sense organ as a sensory organ for detecting light,

chemicals, and orientation as it is the first part of the larva to come into contact with the external environment during the swimming phase (Nielsen, 2004). Gastrulation then occurs where invagination with the epiboly produces a laterally position blastopore which will later become the larval mouth. On the opposing side, a vegetal pole appears which will itself go through shell field invagination, typically at the late gastrula stage or trochophore. Cilia, once functional, will rotate the embryos within the fertilisation membrane and withdraw from it to become a trochophore where organogenesis will take place with the first secretion of periostracum, which composes the outer most layer of the shell (Zardus et al., 2006).

The veliger larva is free swimming and planktotrophic, distinguished by the presence of a functioning velum as a feeding and swimming apparatus and an encompassing hinged shell which is regularly seen in the subclasses Pteriomorphia and Heterodonta (Zardus et al., 2006). The rates at which bivalve larvae grow are influenced by genetic factors, exogenous and endogenous nutrition, and culture conditions (Doroudi & Southgate, 2003). Typically, the veliger stage lasts for 3–4 weeks until the larvae are competent enough to settle.

The early veliger stage includes the point when the larva first begins to feed on suspended phytoplankton and undergoes organogenesis processes. The alimentary system forms early on with a complete crystalline style, and an adductor muscle develops which helps regulate valve gaping (Zardus et al., 2006). At this early veliger stage, velum retractors are developed, which

composes of four pairs extending to the velum and three pairs of retractors attached to the posterior body wall (Cragg, 1985). This aids valve gaping motion and retraction of the velum inside the valves. The margins of the velum are composed of ciliary bands that encompass the velum and are used to provide thrust for vertical swimming and to collect particles suspended in the column for ingestion (Zardus et al., 2006).

The end of the larval stage is normally described as the onset of primary settlement, where the larvae undergo metamorphosis during the late pediveliger stage and attach with byssal threads semi-permanently to a substrate, as in mussels, or cement themselves, as in oysters (Zardus et al., 2006). Typical changes include the development of gills, an eye spot, an extended foot, partial re-absorbance of the velum, and the secretion of the adult dissoconch layer. The eye spot normally develops around the pediveliger stage at the base of the gill primordial (Zardus et al., 2006). This developmental process is followed closely by the velum being re-absorbed into the larva and the attachment onto a substrate with mucoid filaments or byssal threads to begin benthic life. To assist with orientation, statocysts develop late in the larval stage and are located on either side of the pedal ganglion (Zardus et al., 2006). Once partially re-absorbed, the velum will detach from the larvae, and reorientation of the foot and mouth occurs in most late-staged veligers. The larvae are now referred to as spat or juveniles and will develop into adults capable of producing gametes.

2.2.2 Bivalve larval shell morphology

Using scanning electron microscopy (SEM) and light microscopy, the shell morphology of a range of bivalve species has been extensively described from shell formation from the late trochophore stage through to juveniles. SEM provides an in-depth visual approach that can determine prodissoconch layers, commarginal growth rings, and surface shell terrains that would not normally be visible with a compound microscope. This approach has been adopted to describe and document external morphology for many major bivalve larval species including clams (Stephenson & Chanley, 1979; Moueza, Gros, & Frenkiel, 1999), oysters (Wassnig & Southgate, 2012), scallops (Moueza, Gros, & Frenkiel, 2006), and mussels (Redfean, Chanley & Chanley, 1986; Arellano & Young, 2009). The purpose of describing larval shell development is to provide some basic knowledge for aquaculture or general larval identification for assessing wild populations.

The first formation of a larval shell appears with the initiation of the ectodermal cells in the early embryo within the shell field (Kniprath, 1981; Weiss, Tuross, Addadi, & Weiner, 2002). Invagination of the shell field cells then occurs to form a shell gland. The remaining surface cells then produce the outermost organic layer known as the periostracum (Weiss et al., 2002). This outer shell secretion process will continue through the entire life of the animal, from larval stage to adult.

Bivalve species with a planktotrophic larval stage secrete a prodissoconch shell layer first, which is commonly known as the prodissoconch I (PI). This is closely followed by the prodissoconch II (PII) layer (Ockelmann, 1965). The shell morphology of this early stage is laterally compressed and is commonly described as a D-hinge or flat hinge, and the larva is consequently called D-larva (Zardus et al., 2006). Prodissococonch secretion is different among taxa. Ockelmann (1965) described planktotrophic larvae as having a relatively small PI (70–150 μm in length) and a large PII (200–600 μm in length). In contrast, species with non-planktotrophic larvae have been shown to develop a relatively large PI (135–500 μm in length) and the PII appears to be reduced or absent.

The PI is often characterised by the presence of a centralised pitted region surrounded by stellate radial formations extending out towards the transition zone of the PI & II (Foighil, 1986). The PI appears early on during the transition from trochophore to D-stage larva and is secreted by the shell gland and mantle epithelium (Carriker & Palmer, 1979; Waller, 1981). The size of the PI has been shown to correlate with the size of the egg (Ockelmann, 1965; Waller, 1981; Goodsell & Eversole, 1992). When the D-shaped hinge larva begins to feed, a PII shell layer develops, which is secreted by the veliger's mantle edge. This is composed of closely concentrated commarginal growth annulations which are differentiated by the pitted surface of the PI (Ockelmann, 1965; Carriker et al., 1979). During secretion of the PII, the ligament and hinge teeth develop and become useful in taxonomic determinations (Zardus et al., 2006). The larva continues to secrete shell growth in the PII region until such time when it has

progressed enough to be competent to metamorphose and settle on to a substrate and begin benthic life (Chanley & Andrews, 1971). At this time, a well-developed umbo is present along with a foot, and is often called a pediveliger larva. After this transition to the settlement and attachment phase, the velum is re-absorbed and the mantle secretes another shell layer known as the dissoconch (D) which consists of commarginal lines between the transition zone of the PII and dissoconch layer (Chanley et al., 1971; Carriker et al., 1979). At this time, the animal are now referred to as post-larvae, spat or juveniles and no longer live in a suspended aquatic environment.

2.2.3 *Bivalve larval nervous system*

The immunochemistry of bivalve larvae can be investigated with the aid of a confocal microscope, which facilitates the identification of physiological changes and neuronal development of larvae (Ellis, 2010; Todt & Wanninger, 2010). Confocal microscopy has been extensively used to create 3D imagery of marine zygotes and larvae using a series of stacked Z-images (Fallis, Stein, Lynn, & Misamore, 2010; Kristof & Klusmann-Kolb, 2010). Confocal microscopy allows for very thorough analysis of an organism, and often reveals complex systems, such as the central nervous system, with specific neuronal fluorescent labelling such as FMRFamide and catecholamine immunoreactivity, that cannot be seen with a regular compound microscope. A simpler and more direct approach to examining the nervous system of bivalve larvae is through histological

sectioning using specific stains to highlight ganglia, connective fibres, and commissures. Such tissues have been observed successfully in sections of various bivalve larvae, such as scallops (Bower & Meyer, 1990), oysters (Hickman, & Gruffydd., 1971; Ellis, 2010) and mussels (Bayne, 1971). However, histological studies on the nervous system of mussel larvae are lacking.

Earlier studies on the larval nervous system development of bivalves were described by Erdmann (1935) on the oyster *Ostrea edulis*. Results from that study suggest that the pediveliger nervous system is highly complex (Fig. 2.2). Unfortunately, that study did not include histological sections which would have revealed peripheral innervations, but schematic diagrams of the location of ganglions still remain very accurate. Erdmann (1935) described the pre-metamorphic larvae, including an apical sensory organ that was located between the two velar lobes, with cerebral ganglia positioned directly posterior of the apical sensory organ. He later described the larvae as possessing paired pedal and visceral ganglia with pleural-visceral connectives on the left and right sides. Commissures also were observed to join each of the paired cerebral, pedal and visceral ganglia (Erdmann, 1935).

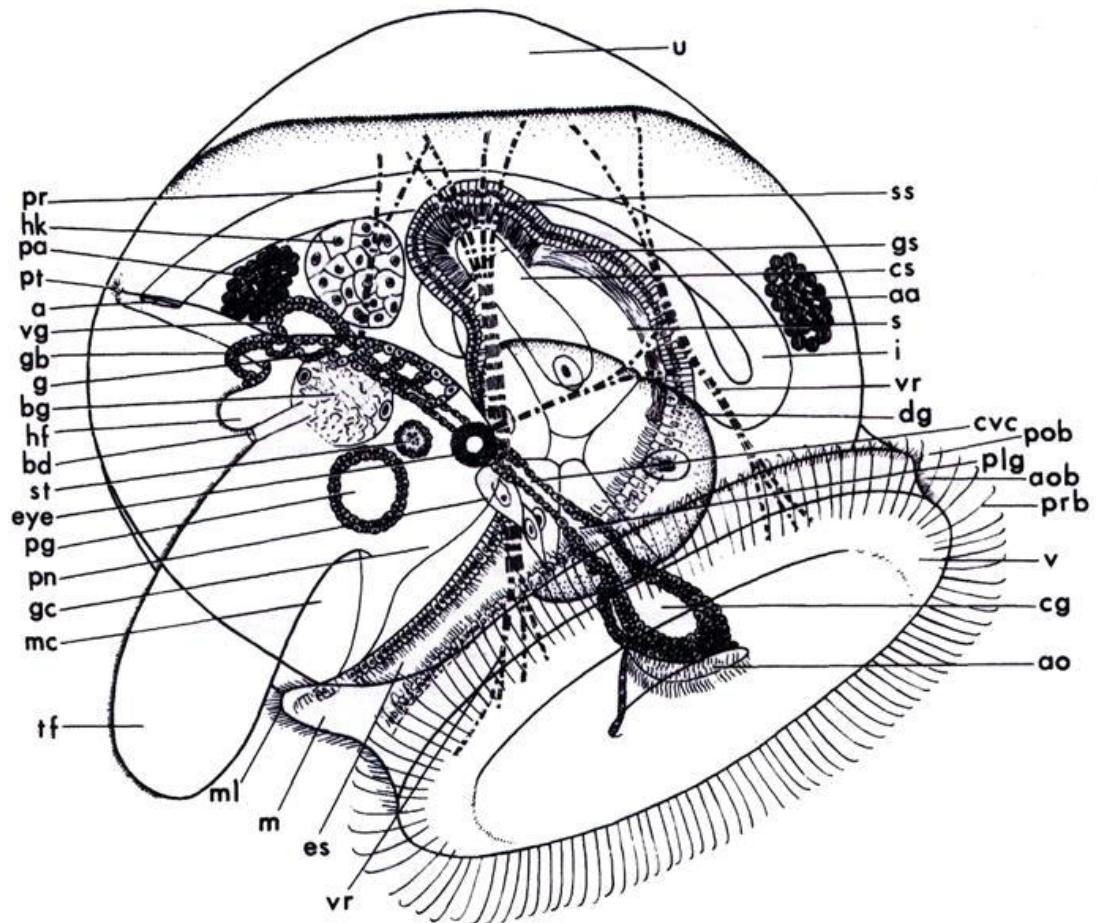


Figure 2.2. Erdmann (1935) diagram as revised by Waller (1981) of the pediveliger stage of oyster *Ostrea edulis*. a = anus; aa = anterior adductor; ao = apical organ; aob = adoral ciliary band; bd = byssal gland duct; bg = byssal gland; cg = cerebral ganglion; cs = crystalline style; cvc = cerebro-pleural-visceral connective; dg = digestive gland; es = esophagus; eye = eye; g = gill primordium; gb = gill bridge; gc = gill cavity; gs = gastric shield; hf = heel of foot; hk = primordium of heart and kidney; i = intestine; m = mouth; mc = mantle cavity; ml = mouth lobe; pa = posterior adductor; pg = pedal ganglion; plg = pleural ganglion; pn = protonephridium; pob = postoral ciliary band; pr = pedal retractor; prb = preoral ciliary band; pt = postanal ciliary tuft; s = stomach; ss = style sac; st = statocyst; tf = toe of foot; u = umbo, v = velum; vg = visceral ganglion; vr = velar retractor.

Many studies have focused on the adult nervous system of molluscs, with special attention directed at gastropods, but only recently a few studies have focused on the nervous system of bivalve larvae from embryogenesis through to post-settlement. Of particular interest is serotonergic (5-HT),

FMRFamidergic, and catecholaminergic (epinephrine, norepinephrine, and dopamine) neurons of the molluscan nervous system, which have been extensively investigated for gastropods (Croll, & Voronezhskaya, 1995; Dickinson, Croll, & Voronezhskaya, 2000; Croll, 2001; Faller, Staubach, & Kolb, 2008) and bivalves (Croll, Jackson, & Voronezhskaya, 1997; Voronezhskaya, 1997; Voronezhskaya, Nezlin, Odintsova; Flyachinskaya, 2000; Voronezhskaya, Nezlin, Odintsova, Plummer & Croll, 2008; Dyachuk, Wanninger & Voronezhskaya, 2012). These neurotransmitters are thought to be responsible for successful transition to settlement and metamorphosis (Young, 2009; Ellis, 2010). The FMRFamide neuropeptide was characterised by Price & Greenberg (1977) from an amino acid sequence. FMRFamide, an important molluscan neuropeptide, was first isolated from the Sunray Venus clam *Macrocallista nimbosa*, and was soon discovered to display activity in mollusc cardiac muscle (Frontali, Williams, & Welsh, 1967). A decade later, Price & Greenberg (1977) characterised the peptide through amino acid sequence analysis. This peptide is not only found in *Macrocallista nimbosa* ganglion extracts, but also is found across major classes of molluscs including Bivalvia, Gastropoda, Cephalopoda, Polyplacophora, and Scaphopoda (Lopez-Vera, Aguilar, & Heimer de la Cotera, 2008).

An early study by Bayne (1971) looking at histological sections of pediveliger *Mytilus edulis* revealed three pairs of ganglia and four related sense organs. However, no nervous connectives between these ganglia were identified. The cerebral ganglion lies dorsal to the apical plate, and pedal ganglia were

observed at the base of the foot, with visceral ganglia posterior of the adductor muscle. Another study on the ventral nervous system of *Mytilus galloprovincialis* trochophore by Raineri (1995) observed a series of ganglia which became organized along the two axons of the pedal ganglia, posterior pole, visceral, parietal, and pleural ganglia further anteriorly. In the veliger stage, the foot with the pedal ganglion progresses towards the fused viscera-parietal ganglia that develops into the most posterior pair of ganglia. Croll & Dickinson (2004) also suggest that the extensive larval nervous system exists widely within both gastropod and bivalve molluscs, and it comprises of an apical sensory organ, early developing posterior cells containing FMRFamide-related peptides, and numerous catecholamine-containing peripheral cells, which are found around the velum, mouth, and foot region.

A more recent study by Voronezhskaya et al. (2008) was the first detailed description of larval neuronal development in any bivalve mollusc. Voronezhskaya et al. (2008) looked at the neuronal development in larval mussel (*Mytilus trossulus*) and found that neurogenesis started at the trochophore stage with the appearance of singular FMRFamide-like and serotonin immunoreactive sensory cells. At the early veliger stage (2 days old), an apical neuropil was observed along with the first pedal cell. At the mid-veliger stage (3 days old), a fully developed set of central ganglia had developed like the pedal, cerebral, and visceral ganglia. Progressing towards the late veliger (4–5 days old) and pediveliger (22 days old) stages, interconnecting connectives and commissures were seen extending into each

ganglion. This arrangement of ganglions is commonly seen among the nervous system of many molluscs (Croll et al., 2004).

Understanding the nervous system of bivalve larvae is important for establishing connections between the structure and function of specific sites while determining the important role that these neuronal systems play in settlement, metamorphosis, and behavioural responses. Many larval neurons have been shown to disappear after metamorphosis, as well as other structures like the velum or retractor muscles which are normally highly innervated (Croll et al., 2004).

2.2.4 Larval development of *Perna canaliculus*

The general biology of *Perna canaliculus* has been recorded from gametogenesis of sessile adult mussels through to release of sperm, oocytes, and subsequent fertilisation and larval development (Booth, 1977; Buchanan Hickman, Waite, Illingworth, Meredyth-Young, & Payne, 1991; Buchanan & Babcock, 1997; Buchanan, 1999; Buchanan, 2001) (Chapter 1-Fig. 1.4). A study on *Perna canaliculus* larvae composed of settlement preferences or behavioural responses to chemical cues (Alfaro, Copp, Appleton, Kelly & Jeffs, 2006), as well as descriptive stages of development including organogenesis, general embryonic, shell morphology observations (Redfearn, Chanley & Chanley, 1986; Buchanan, 1999), and wild population dynamics (Alfaro, 2006). A study on primary and secondary settlement of *Perna canaliculus* larvae has

been performed by Buchanan (1999). He described the reproductive strategy of *Perna canaliculus*, including the production of numerous small ova of about 60 µm in diameter. Redfearn et al. (1986) reported similar findings with eggs at 56–62 µm in diameter, which were orange in colour with an off-centre vacuole in the yolk mass that was enclosed in a thick vitelline membrane. Sperm were about 54 µm in total length with an ovate sperm head 3.9 µm long, which tapered anteriorly to a slender acrosome at 4.2 µm long. The flagellum was measured at 46 µm in length (Redfearn et al., 1986). Each egg carries little maternal energetic investment and pelagic larvae must feed to acquire the energy and material necessary for growth and development. Buchannan's (1999) studies revealed that within a few hours post-fertilisation, the zygote develops an unequal holoblastic spiral cleavage, to form an embryo (Buchanan, 1999). This is followed closely by a ciliated trochophore stage which finally develops into the shelled veliger. The veliger is D in shape, with a flat and straight hinge and is often referred to as a D-stage larva (Buchanan, 1999). This D-stage is reached between 24–48 hours post-fertilisation (hpf), as described by Redfearn et al. (1986). At this stage the larvae begin to feed on phytoplankton with the aid of a velum to capture microalgae from the water column. This velum also is used for vertical migration in the aquatic environment. From the D-stage, larvae then develop a raised hinge (the umbo), taking on a typically clam-like appearance (Buchanan, 1999). Late in the larval period, they undergo metamorphosis and develop a pedal organ (foot) that is used to explore substrates (Buchanan, 1997; Young, 2009). They also develop gills and an eye spot on both valves which is a precursor to settlement. After

primary settlement, larvae are known as pediveligers (Buchanan, 1999), and it is believed larvae often will settle on filamentous algae for a short period of time, and may undergo a secondary settlement phase (Alfaro, 2006). This movement is accomplished through detachment and secretion of a mucous thread that acts like a sea anchor or drag line which increases the hydrodynamic drag and mobility (Buchanan, 1999). This allows re-suspension in the water column by sea currents and the larvae can travel some distance before settling as juveniles to begin its benthic life. This travelling stage has been described for a similar species *Mytilus edulis* by Bayne (1964) on primary and secondary settlement stages and for many other bivalve larvae.

A previous study on shell morphology of *Perna canaliculus* larvae was performed by Redfearn et al. (1986) using both a scanning electron microscope (SEM) and compound microscope. From this, he described external shell morphology of four New Zealand mussel species, *Mytilus edulis aoteanus*, *Perna canaliculus*, *Xenosirobus pulex*, and *Modiolarca impacta*. External features and the internal hinge of these species were described as sharing similar characteristic traits typically found within Mytilids. *Mytilus edulis aoteanus* and *Perna canaliculus* umbo staged larvae appear very similar and ovoid in the anterioposterior direction and later more rounded with shell heights approximately equal to lengths, with umbos broadly rounded. The shoulders of *Perna canaliculus* larvae appear higher and more angular than those of *Mytilus edulis aoteanus* (Redfearn et al., 1986). However, no mention was made of the formation of dissoconch layers from D-stage to post-settlement, and no detailed

description of embryogenesis prior to developing a shell was described by Redfearn, et al. (1986) or Buchanan (1999). Ericson (2010) briefly distinguished the PI & II on *Perna canaliculus* in an SEM study looking at the effects of ocean acidification on fertilisation and early development in polar and temperate marine invertebrates, but did not elaborate on shell morphology characteristics during larval development. Petrone, Ragg, Girvan, and McQuillan (2009) also conducted an SEM study on *Perna canaliculus* larvae adhesive secretion properties onto glass and teflon substrates, but did not mention shell morphology.

At present, no neurogenesis studies have been performed on *Perna canaliculus* at the larval stage. However, characterisation of the neurons in the visceral ganglion of the adult green-lipped mussel (*Perna canaliculus*) has been performed using antibodies raised against neuropeptides and neurotransmitters to highlight the neurons responsible for reproduction and spawning (Mahmud, Mladenov, Sheard and & Chakraborty, 2008). Mahmud et al. (2008) found that Anti-ELH and anti-APGWamide showed very strong immunoreactivity in small type neurons, and that Anti-5-HT and anti-DA immunoreactivity was mostly found in the large type neurons. Anti-APGWamide immunoreactive small cells were seen scattered between larger cells near the periphery of the visceral ganglia. Many small cells were found to show immunoreactivity but only at the periphery of the cell body and the immuno-positive fibres were distributed widely throughout the visceral ganglia. A few immunoreactive neurons were found near the commissure of the visceral ganglia. Nerve fibres and neurons

were discovered in the visceral ganglion and this suggests the presence of ovulation and reproduction hormones (Mahmud et al., 2008). While these neurons like the visceral ganglion and nerve fibres are associated with the nervous system of adult *Perna canaliculus*, other neuronal components in the nervous system have not been described for this species.

2.2.5 Significance of research on *Perna canaliculus* larvae

Perna canaliculus is an important species due mostly to its huge commercial value and ecological significance. Within an academic perspective, *Perna canaliculus* larvae are readily accessible for study, and with an extensive amount of reproductive history already being established, this species is an ideal candidate for the investigation of larval development. This species alone shares common larval development characteristics with other important commercial species, such as mussels within the genus *Mytilus* and oysters *Crassostrea* spp., which have been extensively studied. The identification and characterisation of all aspects of *Perna canaliculus* larval development will be an important step for future integrated studies of academic and commercial importance.

2.3 AIM & OBJECTIVES

The aim of this chapter is to describe *Perna canaliculus* embryonic and larval development from fertilisation through to post-settlement.

The objectives are:

- To describe early embryogenesis and shell morphology of larvae from fertilisation to post-settlement.
- To describe organogenesis processes from fertilisation to post-settlement.
- To describe neurogenesis from fertilisation to post-settlement.

2.4 METHODS AND MATERIALS

2.4.1 General larval rearing

Adult green-lipped mussels (*Perna canaliculus*) were obtained from mussel farms in the Marlborough sounds, New Zealand, and were held at the Glenhaven Aquaculture Centre Ltd, Cawthron Institute in Nelson to allow for reproductive conditioning. Prior to spawning, these broodstock were cleaned to remove fouling organisms. On September 2011, these broodstock were held in 16°C filtered 1 µm seawater (31 ppt seawater) for 2 hours and then thermal shocked with a cold rinse of 8°C and 16°C filtered seawater (FSW) every 30 mins. Adult mussels that did not spawn after the first thermal cycle were

subjected to further thermal shock treatment until spawning occurred. Once an individual began to spawn freely, they were removed from the spawning tray and put into separate 1 L plastic containers to collect sperm and oocytes. These were kept at 5°C to allow for optimum viability. Sperm and oocytes were collected from 11 males and 26 females, over a 4-hour period and pooled for later fertilisation. Sperm concentration was determined using a Neubauer haemocytometer. Approximately 13 million oocytes per tank were fertilised at a concentration of 200 sperm per oocyte and 1000 oocytes mL⁻¹ for a contact time of 15 mins in 13 L of FSW with gentle agitation every few minutes. Then, the gametes were transferred to 4 static rearing tanks containing 100 L of FSW maintained at an average temperature of 15.49 ± 2.29°C. The tanks also contained 1 mg L⁻¹ of ethylenediaminetetraacetic acid (EDTA) to remove any heavy metals like zinc or lead not removed through filtration (Fig. 2.4).

Once the larvae had progressed to the D-stage, they were transferred to 4 specialised rearing tanks called a Cawthron Ultra Dense Larvae Rearing System (CUDLRS) with a holding capacity of 2.5 L. Each tank received a mixture of 2-day old microalgae at a ratio of 5:1, *Chaetoceros calcitrans*, *Isochrysis galbana* at 40 cells μL⁻¹ with FSW via a glass dropper (5 mm diameter) at a constant rate of 80 mL min⁻¹. Tanks were maintained at an average temperature of 19.06 ± 1.71°C with constant homogenous aeration via a glass tube. Excess water and microalgae overflowed out of the tank through a 45 μm mesh to contain larvae within the tank. Larvae were reared at a density of 500,000 per tank. A 50 cm length of coir rope soaked in microalgae

Chaetoceros calcitrans and *Isochrysis galbana* for 2–3 hours was placed into each CUDLRS when larvae were beginning to develop an eye spot and gill rudiment. This was undertaken to determine if larvae were viable and healthy enough to attach to a surface as they would normally have under given larval rearing conditions.

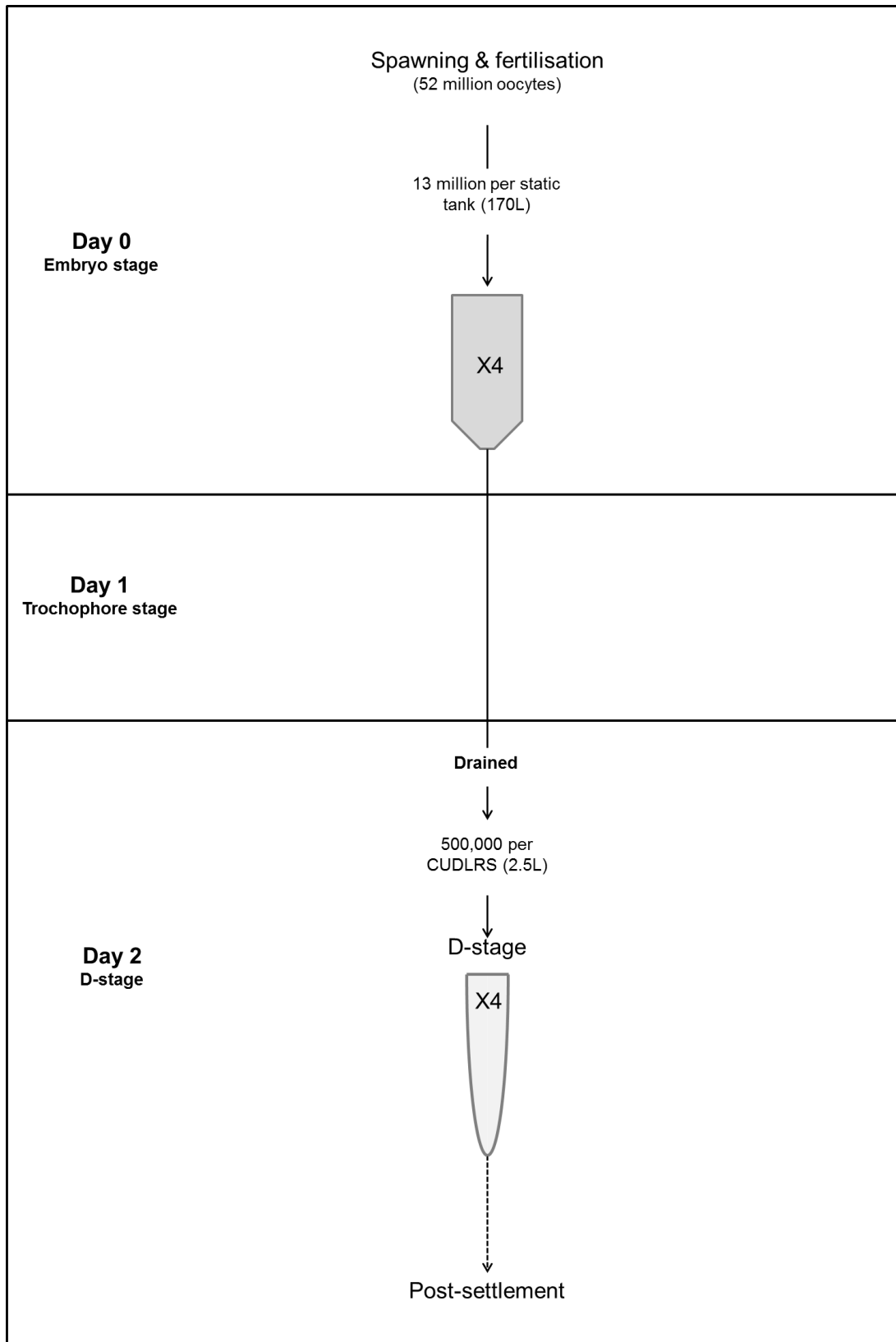


Figure 2.4. Experimental design showing larval rearing from fertilisation to post-settlement.

2.4.2 *Survivability*

On days 4, 7, 9, 11, 14, 16, 18 and 21, the survivability for each CUDLRS was determined by draining the tanks onto a 45 µm screen and gently washing them into a 1L beaker with FSW. Three replicate volumes (200 µL) were taken while constantly homogenising the beaker, and the average survival rate was calculated by observing gapping valves and ciliary action. Daily sampling for histology, SEM, and confocal microscopy were taken into consideration when working out the overall remaining population density.

2.4.3 *Shell length*

Every day, a water subsample (200–500 µL) was taken from each CUDLRS to view the larvae. Larval photographs were obtained using an Olympus CK2 inverted microscope with a mounted Olympus C-7070 7.1 mp camera with 20× objective. A customised particle recognition macro was used to isolate individual larvae using ImageJ software to measure the longest measurement across the ovoid (ferret shell length) to determine shell length relationships through larval development.

2.4.4 Feeding consumption

Larval feeding consumption of mixed (*Isochrysis galbana* and *Chaetoceros calcitrans*) microalgal diets were determined daily for each replicate CUDLRS using a hand held fluorometer (Cyclops-7 chlorophyll A fluorometer with a 30 mL black polyethylene sample chamber). The fluorometer output was recorded in millivolts (mV) readings. The consumption rate per tank was estimated daily using Equation 1, where: ΔmV is the mV difference between the inflow (mV_{in}) and outflow (mV_{out}) readings of the CUDLRS and mV_{blank} is the background mV reading of FSW prior to entering the header tank where the diet was introduced.

Equation 1:

$$\% \text{ Consumption} = \Delta mV / (mV_{in} - mV_{blank}) * 100.$$

2.4.5 Light microscopy

Visual assessments of mussel larval development were taken every day using an Olympus CK2 inverted microscope with a mounted Olympus C-7070 7.1 mp camera with 20x objective. Morphological and physiological changes were observed to assess the progression of organogenesis and the onset of settlement cues, such as eye spot and gill rudiment development. Behavioural observations, such as velum movement also were taken to assess the viability of larvae and to observe any abnormalities.

2.4.6 Scanning electron microscopy

Approximately 500 mussel embryos and veliger larvae were taken from the static tank system for the first 3-days, and then every day to post-settlement from CUDLRS. Embryos and larvae were first pipetted out of the tanks using a known volume and placed onto a 43 μm mesh. These embryo and larvae were gently siphoned out using a disposable eye dropper and placed into a 1.5 mL eppendorph tube. Embryos and larvae were then gradually relaxed using 7.5% magnesium chloride until larvae were immobile and concentrated on the bottom of the tube. Excess saltwater was removed from the eppendorph tube and larvae fixed in 4% paraformaldehyde in phosphate buffered saline (PBS, 100 mM sodium phosphate and 140 mM sodium chloride; pH 7.4) for 24 hours at room temperature, washed in PBS, and then placed in 70% ethanol for storage at 4°C. Embryos and larvae were centrifuged at 2.0 rpm for 30 seconds to concentrate larvae at the bottom of the tube. Embryos and larvae then went through a dehydration process of ascending series of 90%, and 2 series of 100% ethanol for 15 min intervals. They were then gently placed onto stubs and allowed to air dry for 48 hours. Specimens were then sputter-coated with gold before observation with a Hitachi SU-70 Shottky field emission SEM microscope. Images were modified by filling the background in black and contrast and brightness intervals adjusted with Adobe Photoshop CS5.

2.4.7 Histology

Approximately 2000 larvae were sampled from each CUDLRS each day. These larvae were fixed in Davidson's fixative for 24 hours and then stored in 70% ethanol. Larvae were later decalcified in 10% EDTA for 2–3 hours at room temperature. Decalcification was monitored by dropping a few larvae on a slide and placing a coverslip to observe any shards of shell appearing. The larvae were then embedded in heated agar (4.5%) at 50°C and allowed to cool to room temperature. Larvae were then dehydrated in a series of 80%, 90%, and three series of 100%, ethanol, cleared in two series of xylol and then infiltrated in paraffin wax. Once infiltration was completed, the larvae were mounted into a cassette with paraffin wax to create a mounting block. Larvae in these blocks were kept at 4°C until sectioning was performed. Sections of 5 µm were cut using a Leica microtome for larvae from each treatment. The sections were placed into a water bath at 42°C while carefully placing an adhesive polylysine slide underneath to allow the sections to bind to the slide. Slides were allowed to dry in a vertical rack and then excess wax was removed by placing the slides in an 80°C oven for 10–15 mins until excess wax had melted off. The slides were then dipped in two solutions of xylol to remove excess wax and rehydrated through two series of 100%, 90%, 80%, 70%, 50%, 30% ethanol, followed by distilled water. Slides were stained with regressive harris's haematoxylin and 1% eosin, rinsed with deionised water, and then dipped in ascending series of 75%, 95%, and two series of 100% ethanol. Sections were cleared in three series of xylol and then allowed to dry for 10–15 mins at room temperature. Slides were then mounted with DPX mountant and allowed to set for 24 hours.

Images were taken using a Leica DM2000 microscope with 20× and 40× objective.

2.4.8 Confocal microscopy

Larvae were obtained from each CUDLRS by taking approximately 500 larvae per tank each day into 1.5 mL eppendorph tubes. Larvae were gradually anesthetized in 7.5% magnesium chloride in FSW until valves relaxed open and the velum fully extended. Once relaxed, larvae were fixed in 10% formalin for 24 hours and then stored in 70% ethanol at 4°C. Larvae were then gently centrifuged at 2.0 rpm for 30 seconds to concentrate larvae at the bottom and excess ethanol was removed. Following a modified procedure from Voronezhskaya et al. (2008), larvae were transferred to a BD Falcon Low Evaporation 96 well plate and rinse three times in PBS for 15 mins. Shells of D-stage to post-settlement were then decalcified in 5% EDTA in PBS for 6 hours until almost complete decalcification, and rinsed in PBS for 15 mins. Then the samples were blocked in PBS overnight containing 10% normal goat serum, 0.25% bovine serum albumin, 1% Triton X-100 (TX), and 0.03% sodium azide overnight in 4 degrees on a gentle agitator. Larvae were single labelled with FMRFamide AB (diluted 1:500 in PBS with 1.0% normal goat serum and 1.0% TX) for 3 days at 4°C with gentle agitation. The larvae were then washed (3 × 1h) in PBS and incubated for 4 days in goat anti-rabbit IgG (Alexa 488) diluted 1:50 in PBS at 4°C with agitation. After incubation in the second antibody,

larvae were rinsed several times more in PBS and then transferred to a μ -slide 8 well ibitreat chamber with AF1-Citifluor mountant. In order to determine the presence of FMRFamide immunoreactivity, a control without a primary AB was used to distinguish between positive and negative neuropeptide cell responses.

All of the larvae were examined under a Zeiss LSM 710 inverted confocal microscope with 20 \times objectives and appropriate wavelength filter settings. Three-dimensional (3D) rotatable images were created using ZEN 2009 Light edition and converted into Z-stacked LSM files. Single projections from optimal images were exported as TIFF images. These were then adjusted for contrast and brightness with Adobe Photoshop CS5. The number and optical section size of each image are given in each figure caption.

2.4.9 Statistical analyses

Minitab 16 Statistical software was used to analyse experimental results. Significance levels were set to $p < 0.001$ for all statistical tests. Survivability data were analysed by performing a repeated measures ANOVA using arcsine transformed data to meet parametric assumptions. Shell length was analysed using a repeated measures ANOVA with Tukeys tests and a regression analysis. Feeding consumption was analysed using a Kruskal-Wallace test.

2.5 RESULTS

2.5.1 Survivability analysis

Survivability in the CULRS showed a significant linear decrease over 20 days (ANOVA; $F_{8,24} = 107.90$, $p < 0.001$). Larval survivability had a steep decline from day 2 to 7, and then a gentler decline for the remaining rearing period (Fig. 2.5). The relationship was strong ($R^2 = 0.8390$).

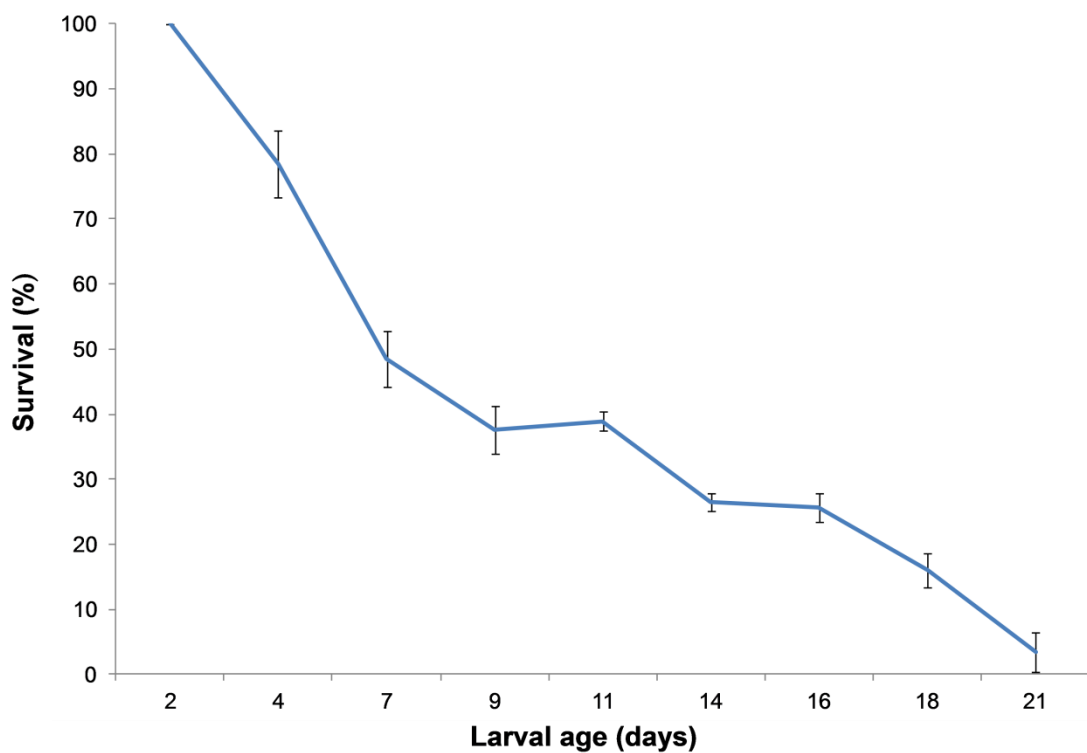


Figure 2.5. Average percent survivability (\pm SD) of mussel larvae over 21 day rearing period.

2.5.2 Shell length analysis

A relationship between shell length (μm) and larval age (days) was strongly correlated ($R^2 = 0.8650$) and showed a positive linearity between shell length and age of larvae ($7.57\mu\text{m}$ per day) (ANOVA; $F_{14,39} = 31.27$, $p < 0.001$). The variation in shell growth was considerably high from day 14–18 due to low numbers of larvae and the variation in rapid shell growth experienced during pre-settlement (Fig. 2.6).

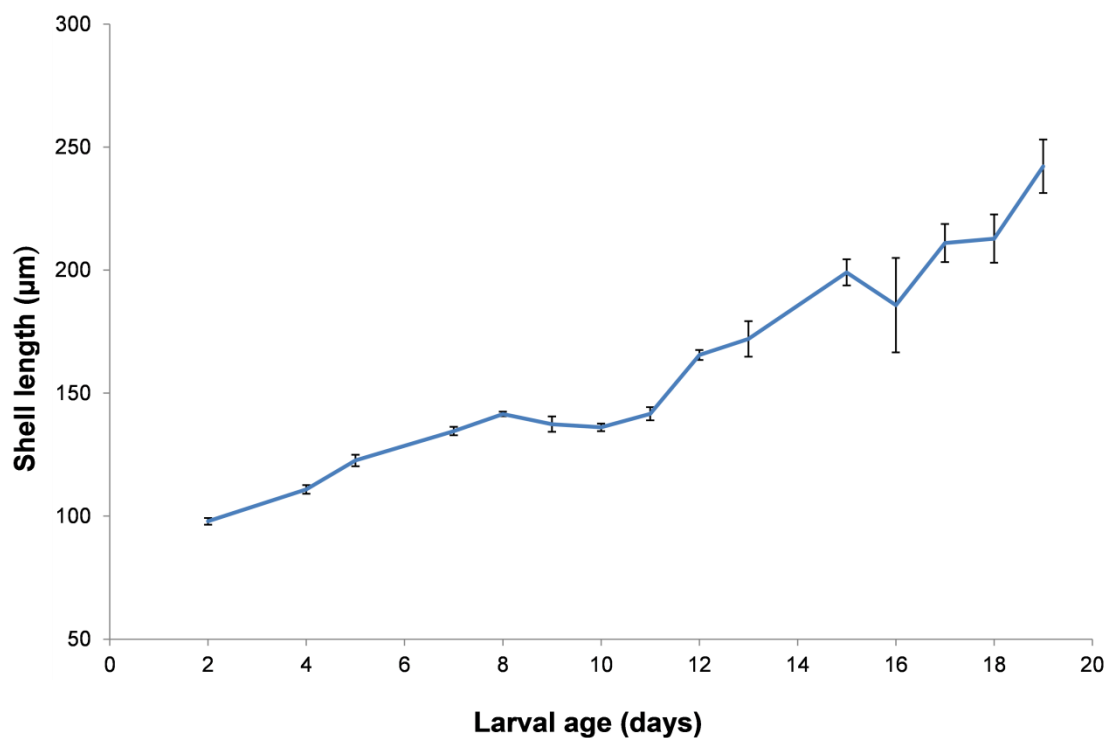


Figure 2.6. Average shell length (μm) ($\pm\text{SD}$) of mussel larvae over 21 day rearing period.

2.5.3 Feeding consumption analysis

Feeding consumption increased a substantial amount when larvae were 6 days old ($32.1 \pm 2.10\%$ SD) and dropped considerably over a 24 hour period (Fig. 2.7). Larvae then began to consume more food than on any other previous day, and were consuming the most at 15 days old ($41.4 \pm 3.92\%$ SD). Kruskal-Wallice results revealed significant differences among feeding consumption over day 15 compared to day 21. Feeding consumption also increased greatly between day 7 and day 14. Feeding consumption over the 20 days of feeding was statistically significant (ANOVA; $F_{20,63} = 3.44$, $p < 0.001$).

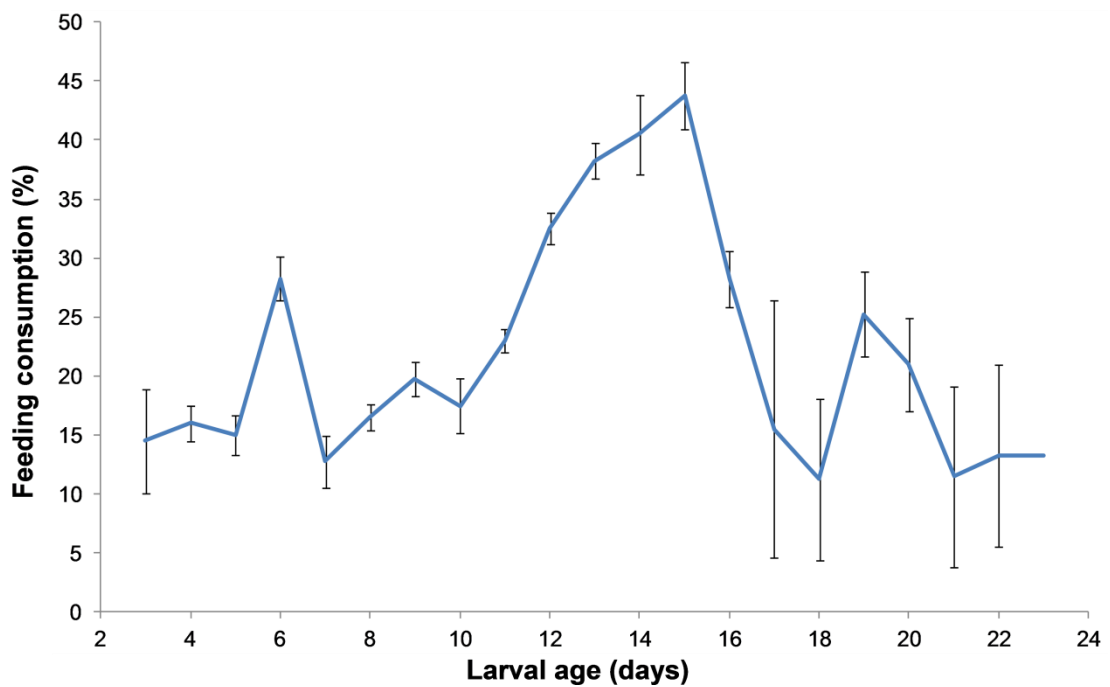


Figure 2.7. Average percent feeding consumption (\pm SD) of mussel larvae over 21 day rearing period.

2.5.4 Embryogenesis

Unfertilised eggs of *Perna canaliculus* appeared brown and spherical with a mean diameter of $61.0 \pm 8.55 \mu\text{m}$ (n=20 oocytes) (Fig. 2.8). Table 1 shows the different stages of embryonic and larval development and the time when these occurred. The ciliated gastrula stage T0 + 18h with a mean diameter of $64.0 \pm 7.88 \mu\text{m}$ (n=7 embryos) was differentiated by a large depression in its vegetal pole with cilia present around the margins of the vegetal pole. An apical sense organ made up of several fibres was seen protruding out of the larvae (Fig. 2.9B). The ciliated gastrula stage T0 + 18h showed a blastopore on the opposing side of the vegetal pole and an apical sense organ is seen protruding out of the gastrula (Fig. 2.9C). Late gastrula between T0 + 18h and T0 + 19h showed an enclosing vegetal pole within the presence of a shell field developing (white arrows) with cleavage of one of the macromeres (Fig. 2.9D).



Figure 2.8. Figs. A-F. *Perna canaliculus*. Light images of unfertilised egg to umbonate larva. **A.** Unfertilised egg. **B.** Ciliated gastrula stage T0 + 18h. **C.** D-stage larva (2 days old). **D.** Early umbo stage (9 days old). **E.** Late umbo stage (13 days old). **F.** Umbonate larva (17 days old). Abbreviations: AAM, anterior adductor muscle; Ci, cilia; DD, digestive diverticulum; E, esophagus; F, foot; GR, gill rudiment; M, mouth; S, stomach; SS, style sac; U, umbo; Ve, velum; Vr, velum retractor muscle; VP, vegetal pole. Scale bars = 20 µm.

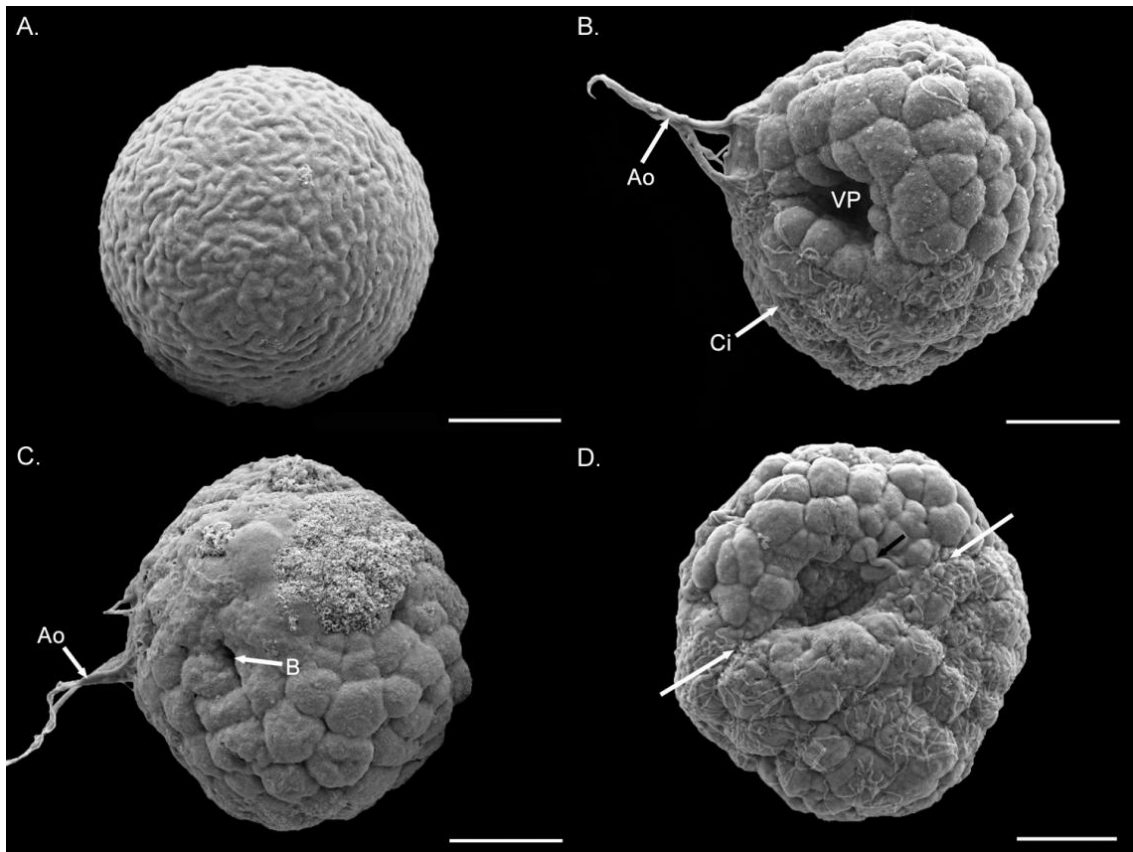


Figure 2.9. Figs. A–D. Embryogenesis of *Perna canaliculus*. SEM images of unfertilised egg to late gastrula stage. **A.** Unfertilised egg. **B.** Ciliated gastrula stage T0 + 18h. **C.** Posterior end of ciliated gastrula stage T0 + 18h. **D.** Late gastrula between T0 + 18h and T0 + 19h. Abbreviations: Ao, apical sense organ; B, blastopore, Ci, cilia; VP, vegetal pole. White arrows = Shell field invagination. Black arrow = Cleavage. Scale bars = 10 μm for figures.

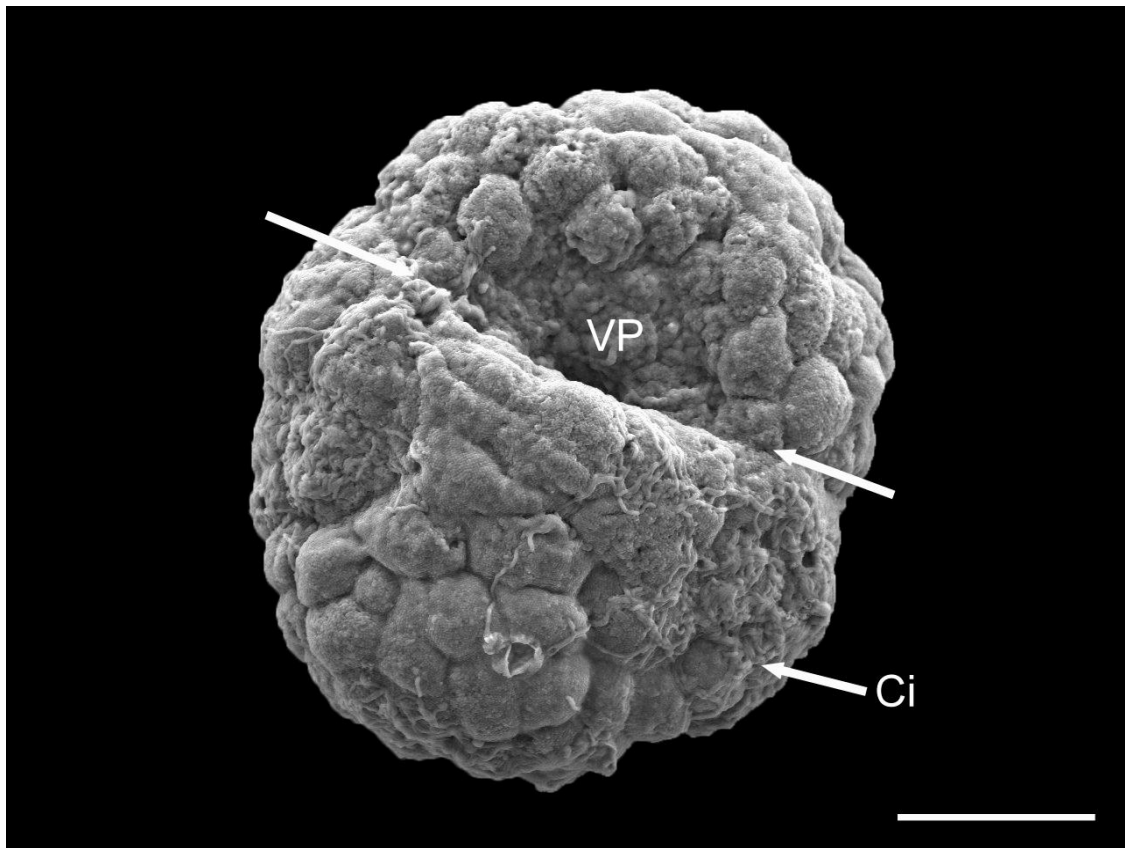


Figure 2.10. Late gastrula between T0 + 18h and T0 + 19h with cilia (Ci) showing a enclosing vegetal pole (VP) with the presence of a shell field developing (white arrows). Scale bar = 10 μm .

2.5.5 Shell morphology

D-stage larva (2 days old) with an average shell length of $97.9 \pm 9.12 \mu\text{m}$ (n=12 larva) showed a PI layer with a prominent pitted punctate pattern and a stellate radial region extending from this margin to the edge of the mantle and hinge (Fig. 2.11A). D-stage larva (4 days old) with an average shell length of $110.9 \pm 22.91 \mu\text{m}$ (n=15 larva) showed a PII layer with commarginal growth rings formed (Fig. 2.11B). Another day 4 larva with higher magnification showed an extended velum consisting of many singular cilia within the region of the mouth

comprising of many more cilia, and a prodissoconch transition zone clearly visible (Fig. 2.12). Early umbo stage (10 days old) with an average shell length of $136.1 \pm 51.3 \mu\text{m}$ (n=24 larva) displayed a developing umbo and further secretion of the PII protruding outwards towards the mantle edge (Fig. 2.11C). Late umbo stage (11 days old) with an average shell length of $141.6 \pm 22.9 \mu\text{m}$ (n=3 larva) had a velum present and the shell taking on an umbonate appearance (Fig. 2.11D). Umbonate larva (16 days old) with an average shell length of $185.7 \pm 100.6 \mu\text{m}$ (n=12 larva) displayed a well-developed umbo and rounded shell appearance (Fig. 2.11E). Post larva stage (20 days old) with an average shell length of $242.2 \pm 54.19 \mu\text{m}$ (n=7 larva) had the presence of a dissoconch layer forming at the mantles edge indicating the onset of settlement transition (Fig. 2.11F, & 2.13).

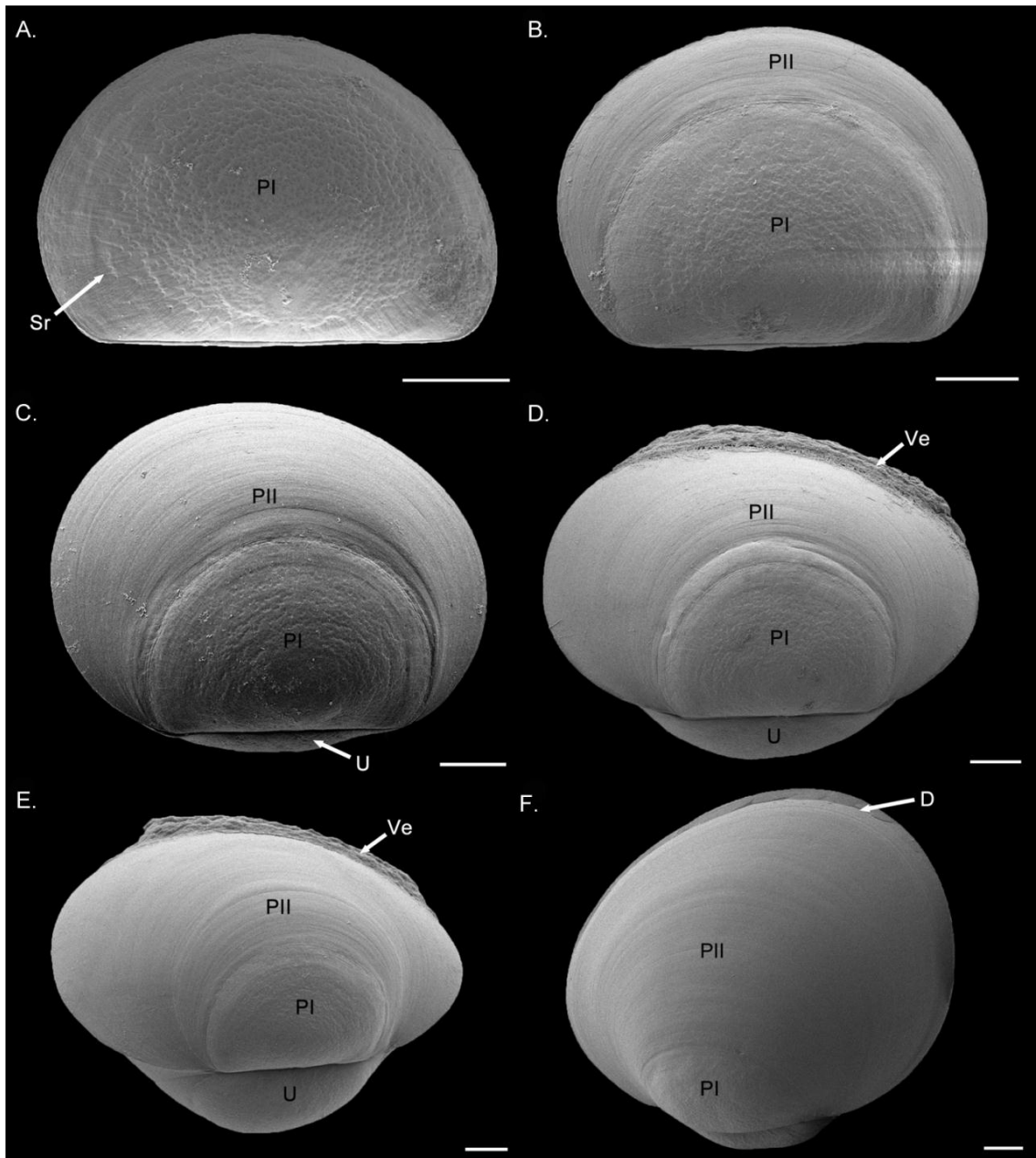


Figure 2.11. Figs A–F. Shell development of *Perna canaliculus*. **A.** D-stage larva (2 days old). **B.** D-stage larva (4 days old). **C.** Early umbo stage (10 days old). **D.** Late umbo stage (11 days old). **E.** Umbonate larva (16 days old). **F.** Post larva stage (20 days old). Abbreviations: Ao, Apical sense organ; B, Blastopore; Ci, Cilia; D, Dissoconch; PI, prodissoconch I; PII, prodissoconch II; Sr, stellate-radial region; U, umbo; Ve, velum; Vp, vegetal pole. White arrows = Shell field invagination. Black arrow = Cleavage. Scale bar = 20 μ m.

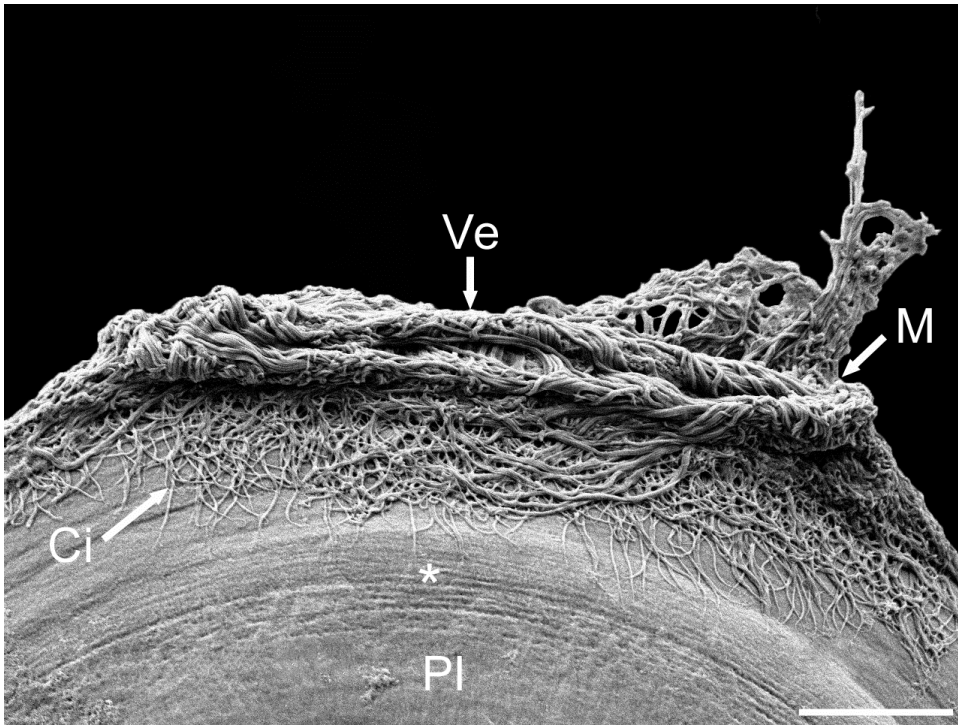


Figure 2.12. D-stage larva at 4 days post-fertilisation. Abbreviations: Ci, cilia; M, mouth, PI, prodossoconch I, Ve, velum. * = Transition zone. Scale bar = 10 μ m.

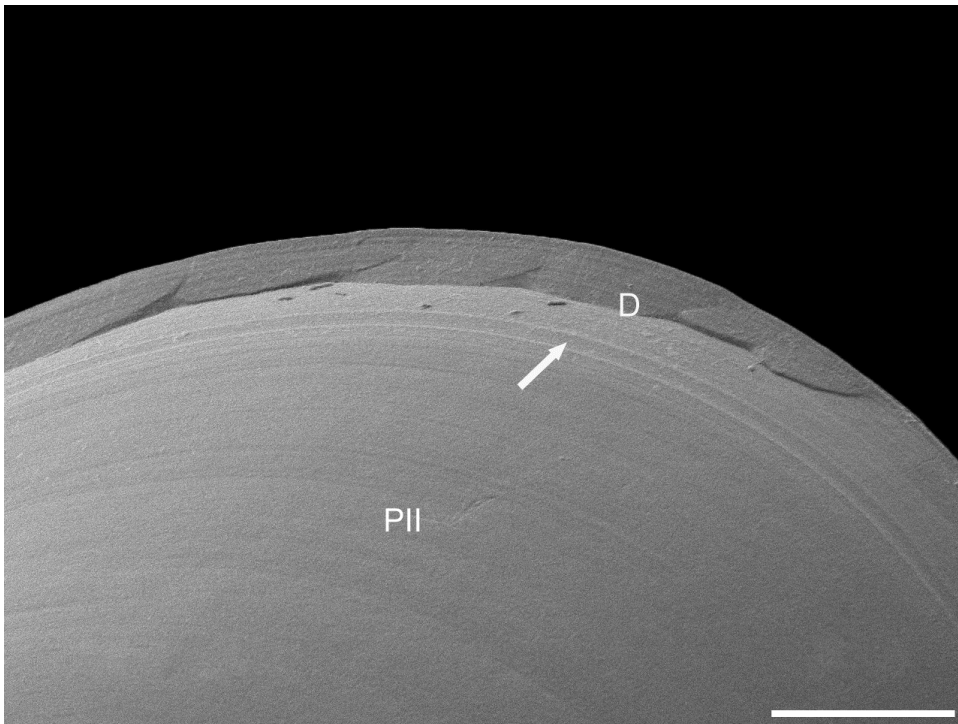


Figure 2.13. Post-larva at 20 days post-fertilisation. Abbreviations; D, dissoconch; PII, prodossoconch II. White arrow = transition zone. Scale bar = 10 μ m.

Table 1. Different embryonic and larval stages of *Perna canaliculus* in hours (h) and days (d).

Time post-fertilisation	Stage
–	Blastula
18 h	Early Gastrula
18–19 h	Late Gastrula
–	Early Trochophore
–	Late Trochophore
2 d	D-shaped larva
7 d	Early umbo larva
11 d	Late umbo larva
16 d	Umbonate larva
18 d	Pediveliger
21 d	Post-larva

2.5.6 Organogenesis

Histological sectioning and light microscopy revealed only a limited amount of organogenesis had occurred at the early D-stage. This stage of organogenesis is to be expected as this is the earliest stage of larval development. At day 2, the larva have gone through the first stages of organogenesis and developed into a D-stage larva with a straight hinge and the beginnings of a stomach becoming visible (Fig. 2.8C). A velum is seen extending outwards of the valves and was observed beating repeatedly for locomotion and feeding. At day 3 the larvae are developing an alimentary system complete with an esophagus, digestive diverticulum, and apical ganglion seen in a sagittal section (Fig. 2.14). The digestive diverticulum consists of pockets of digestive tubules or vacuoles and is differentiated from the stomach which appears oval shaped and merged as one complete system.

The early umbo stage shows progression in organogenesis and a complete alimentary system has developed with a style sac dorsal of the stomach and ventral of the hinge (Fig. 2.8D). A well-developed velum is present and a mouth opening seen (Fig. 2.8D). Algae are also observed in the stomach by the intense brown colouration. A posterior adductor muscle has developed posteriorly to the digestive diverticulum and anterior of the mantle edge, and an intestine developing (Fig. 2.15). A frontal section reveals the apical ganglion is present at the ventral end and a velum retractor muscle is seen extending dorsally from the velum down the left hand side (Fig. 2.16).

At the late umbo stage, the larvae have a well-developed umbo with velum retractor muscles seen extending outwards from the umbo region to the velum lobe and velum. The stomach and digestive diverticulum appear larger in shape when microalgae are contained within (Fig. 2.8E). The stomach and digestive diverticulum are larger in size and the remnants of the anterior adductor muscle are lightly stained pink with a velum retractor muscle lying posteriorly (Fig. 2.17). Another sagittal section of a slightly older larva shows a velum retractor muscle lying posterior to the mouth and velum, with a long esophagus extending from the stomach towards the velum (Fig. 2.18). Light micrographs reveal a series of velum retractor muscles extending ventrally from the hinge to the velum, thought to be velum retractor muscles. The anterior adductor muscle also can be seen (Fig. 2.8E).

Light micrographs of an umbonate larva stage shows that larva have undergone the first stages of metamorphosis with the development of a foot and a gill

rudiment extending posteriorly from the stomach towards the mantle edge of the valve, and an eye spot has developed at the base of the gill rudiment (Fig. 2.8F). Larvae then began developing an eye spot at 17 dpf and showed typical settling behaviour where they had secreted a mucous thread to stick to the side of the tanks. At the pediveliger stage (18 dpf), the majority of larvae had developed an eye spot and began extending their foot out of the shell and touching the substratum. The beginning of velum re-absorption also was seen in some larvae (Fig. 2.21). A transverse section revealed a pedal ganglion at the base of a well-developed foot (Fig. 2.20).

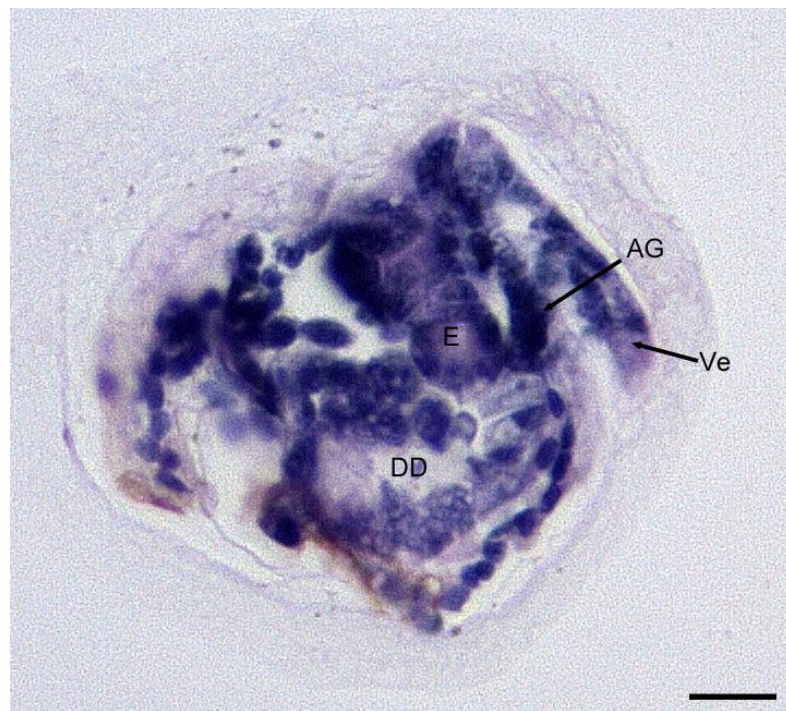


Figure 2.14. Sagittal section of a D-larva (3 days post-fertilisation). Abbreviations: AG, apical ganglion; DD, digestive diverticulum; E, esophagus; Ve, velum. Scale bar = 20 μ m.

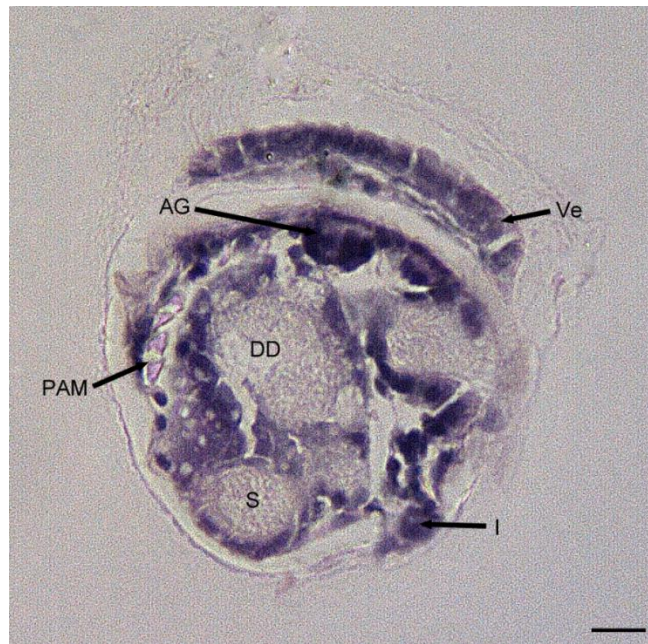


Figure 2.15. Sagittal section of an early umbo larva (7 day post-fertilisation). Abbreviations: AG, apical ganglion; DD, digestive diverticulum; I, intestine; PAM, posterior adductor muscle. Scale bar = 20 μ m.

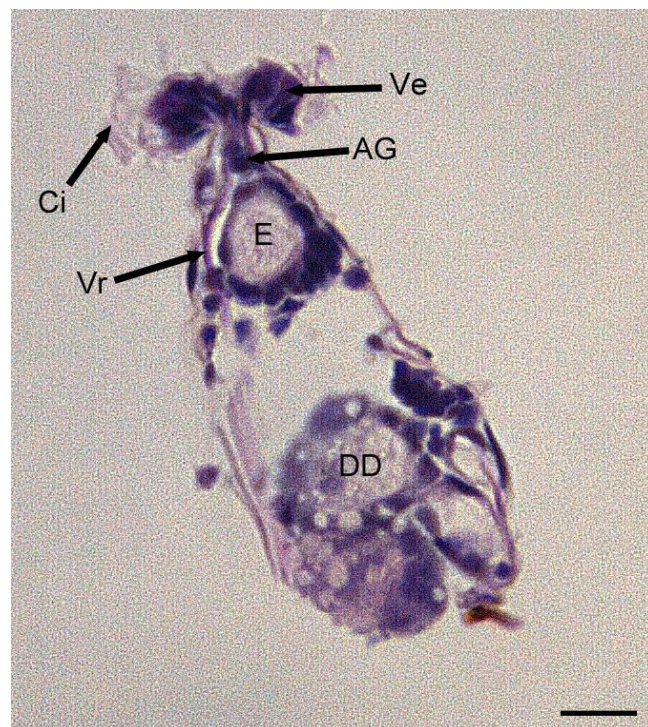


Figure 2.16. Frontal section of an early umbo larva (7 days post-fertilisation). Abbreviations: AG, apical ganglion; Ci, cilia; DD, digestive diverticulum; E, esophagus; Ve, velum; Vr, velum retractor muscle. Scale bar = 20 μ m.

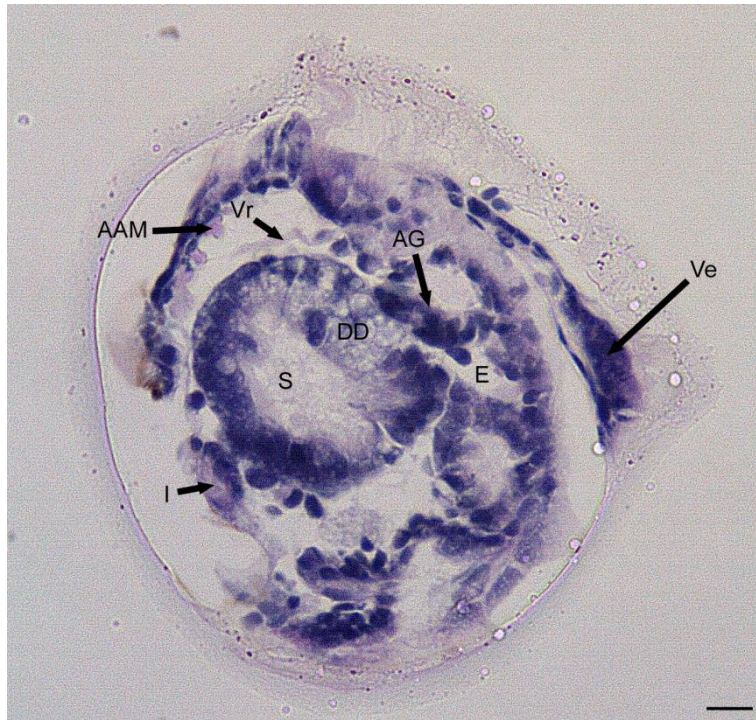


Figure 2.17. Sagittal section of late umbo larva (11 days post-fertilisation). Abbreviations: AG, apical ganglion; AAM, anterior adductor muscle; DD, digestive diverticulum; E, esophagus; S, stomach; Ve, velum; Vr, velum retractor muscle. Scale bar = 20 μ m.

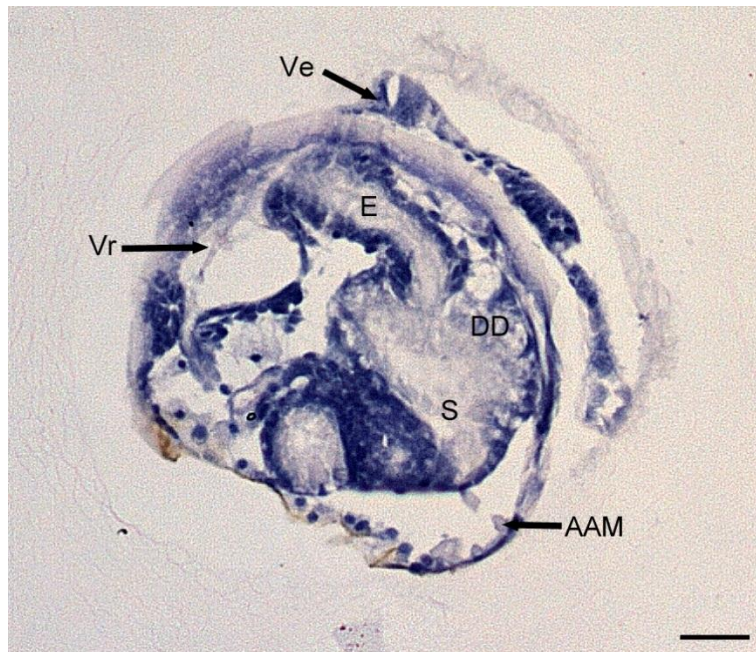


Figure 2.18. Sagittal section of late umbo larva (13 days post-fertilisation). Abbreviations: AG, apical ganglion; AAM, anterior adductor muscle; DD, digestive diverticulum; E, esophagus; S, stomach; Ve, velum; Vr, velum retractor muscle. Scale bar = 20 μ m.

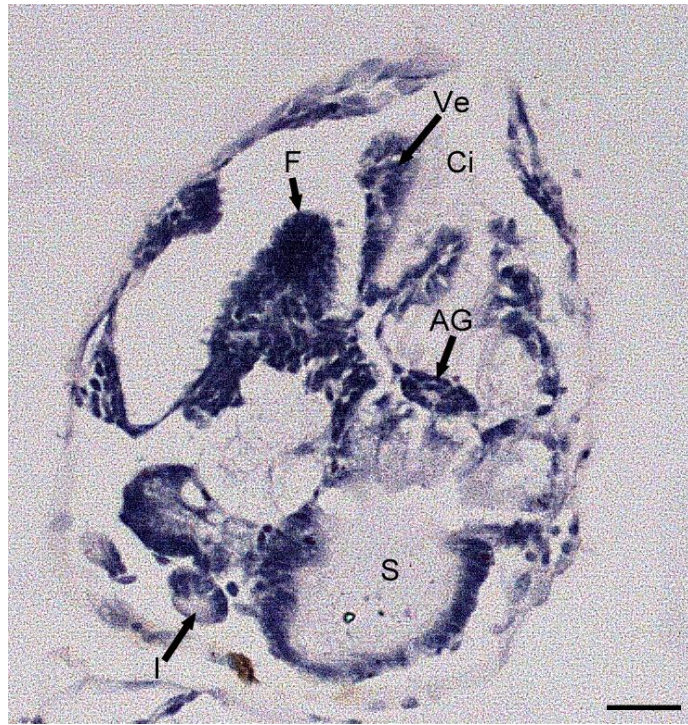


Figure 2.19. Transverse section of late umbo larva (15 days post-fertilisation). Abbreviations: AG, apical ganglion; Ci, cilia; F, foot; MC, mantle cavity, stomach; Ve, velum; Vr, velum retractor muscle. Scale bar = 20 μ m.

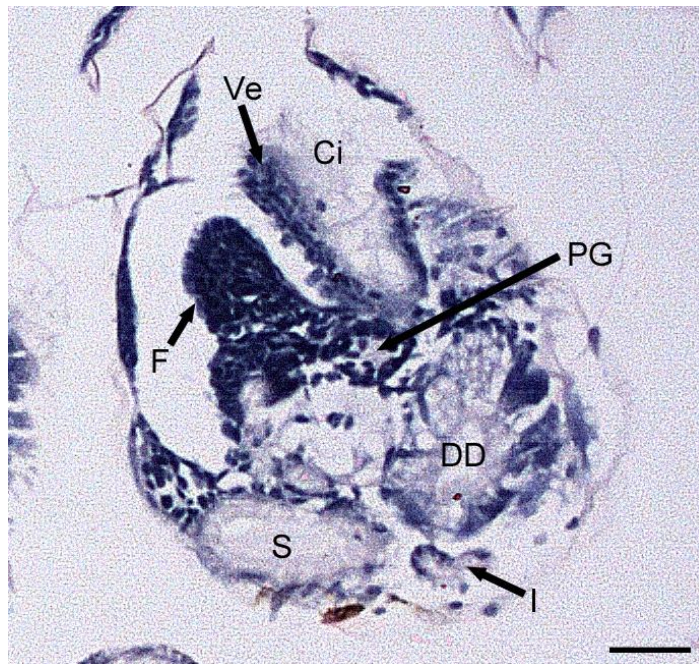


Figure 2.20. Transverse section of pediveliger (18 days post-fertilisation). Abbreviations: Ci, cilia; F, foot; S, stomach; Ve, velum. Scale bar = 20 μ m.



Figure 2.21. Larva of pediveliger (18 days post-fertilisation) with prominent foot. Unlabelled arrows shows velum cells breaking down and being reabsorbed. Abbreviations: E, esophagus; F, foot; I, intestine; Pf, pseudofaeces; S, stomach; SS, style sac; Ve, velum. Note: eye spot is out of focus. Scale bar = 20 μ m.

2.5.7 Neurogenesis

Solitary FMRFamide-ergic cells were present in trochophore larva (18 hpf). However, these could not be identified due to a weak immunopositive response which suggests that the nervous system is yet to fully develop (Fig. 2.22). At the early D-stage (2 dpf), the larva possess very little FMRFamide-like

immunoreactive cells and location of these sites suggests it may be the origin of the apical/cerebral ganglion (Fig. 2.23). A sagittal section of a D-larva (3 dpf) revealed an area of intense staining thought to be the apical ganglion (Fig. 2.14). Larva at the D-stage (5 dpf) showed the beginning of a peripheral system with thin fibres running from the anterior-adductor muscle through to the cerebral ganglion. However, the mantle nerve was brightly stained and the stomach consisted of two unknown immunoreactive sites (Fig. 2.24). Sections of early umbo larva in the sagittal and frontal planes of view showed that a distinct apical ganglion had formed (Fig. 2.15 & 2.16). Progressing further, early umbo larva (10 dpf) had developed a complete nervous system with weak peripheral innervations running throughout the larva (Fig. 2.25). A mantle nerve completely encompassing the mantle region was observed. Dorsal to the velum, the ventral osphradial nerve runs dorsally from the cerebral ganglion and connects to the fibre that runs from the anterior adductor muscle to the pedal ganglion. The pluro-visceral connective projects onto the pedal ganglion and travelling posteriorly separates into two connective fibres that connect to the visceral ganglion. There appears to be two weakly stained connectives running from the pedal ganglion to the visceral ganglion. Late umbo (14 dpf) show innervations running throughout the anterior adductor muscle, which join to a single fibre which runs posteriorly to the pedal ganglion. No fibres within the anterior adductor muscle are observed extending to the ventral osphradial nerve. The ventral osphradial nerve progressed anterior of the anterior adductor muscle and travelled dorsally terminating before the umbo. The pedal ganglion itself composes of two heavily immunoreactive neuronal sites and this

suggests the pedal ganglion is composed of two neuronal sites with interconnecting fibres (Fig. 2.26). The intestine had some weak innervations running along the intestinal tract. Larvae at the pediveliger (18 dpf) had progressed to the settlement stage where morphological changes occurred with the development of a gill rudiment and foot (Fig. 2.27). However, there are no innervations associated with these two distinct changes in organogenesis and a sagittal section showed a well-developed pedal ganglion near the base of the foot (Fig. 2.20). The cerebral ganglion appears more intensely stained, indicating further neurogenesis development. The anterior adductor muscle is highly innervated with a series of network fibres extending throughout the muscle and interconnecting with several neuronal sites. The ventral osphradial nerve now connects to the mantle nerve anterior to the anterior adductor muscle. The posterior adductor muscle also is innervated with fibres that extend posteriorly to two unknown neurons that are connected to the mantle nerve that encompasses the entire mantle region.

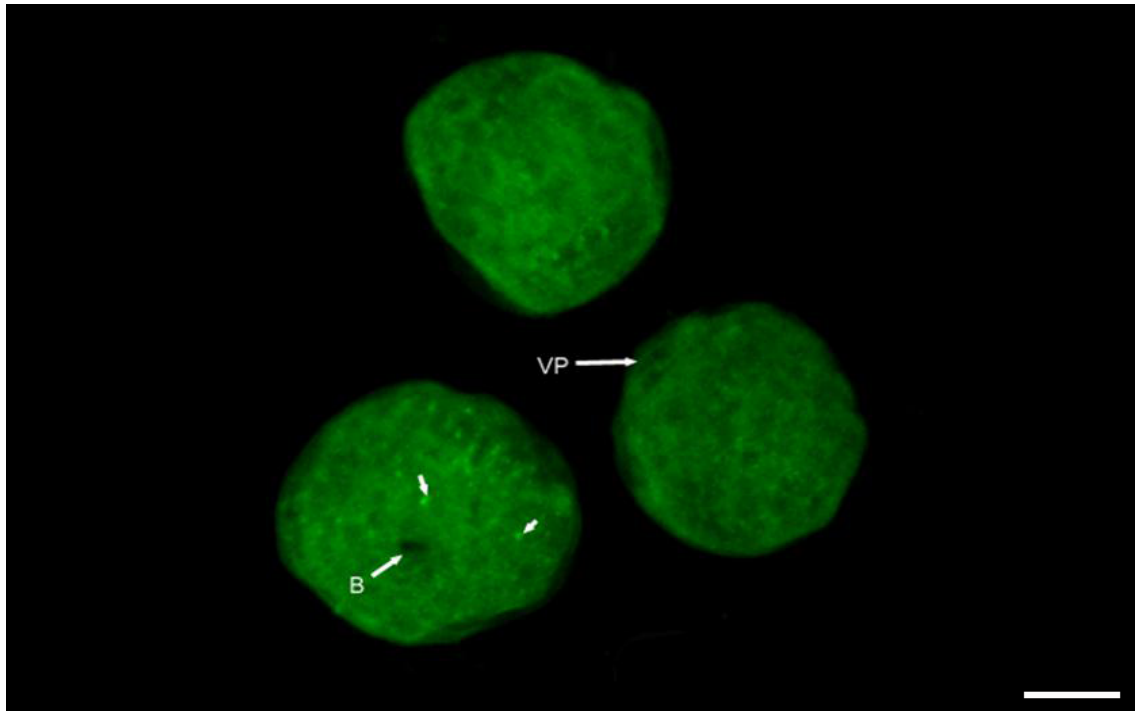


Figure 2.22. FMRFamide-like green immunoreactivity in trochophore larvae (18 hours post-fertilisation) ($22 \times 0.97\mu\text{m}$). Abbreviations: B, blastopore; VP, vegetal pole. Scale bar = $20\mu\text{m}$.

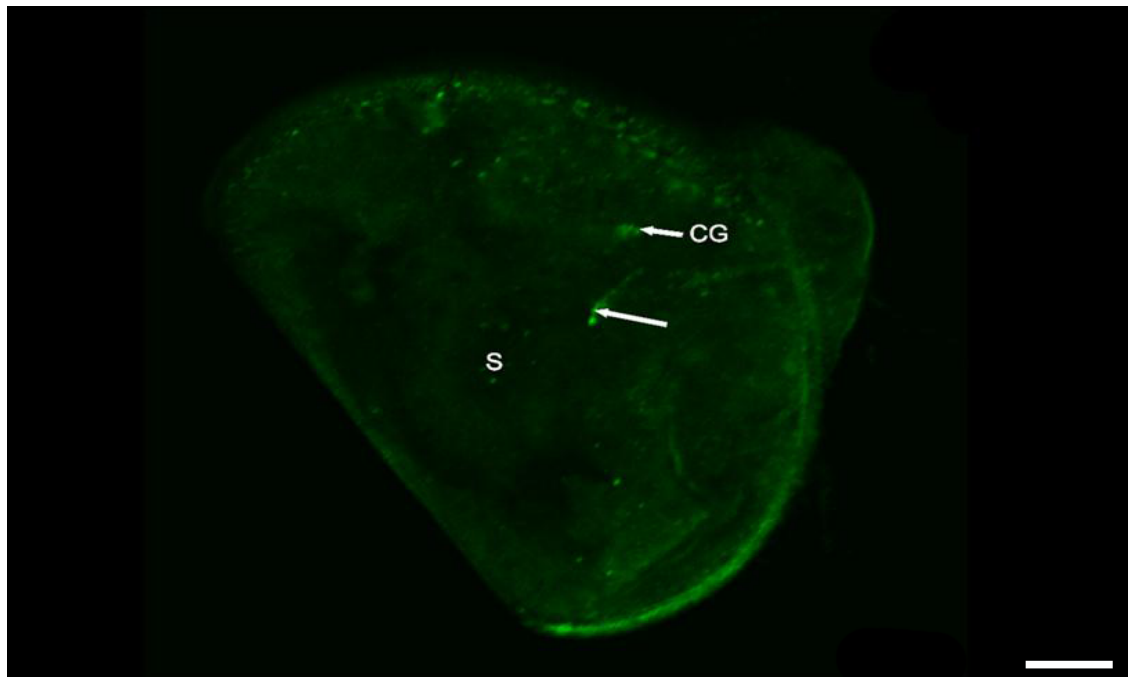


Figure 2.23. FMRFamide-like green immunoreactivity in a D-stage larva (day 2). ($29 \times 0.97\mu\text{m}$). Abbreviations: CG, cerebral ganglion; S, stomach. White arrow = unknown immunoreactive site. Scale bar = $20\mu\text{m}$.

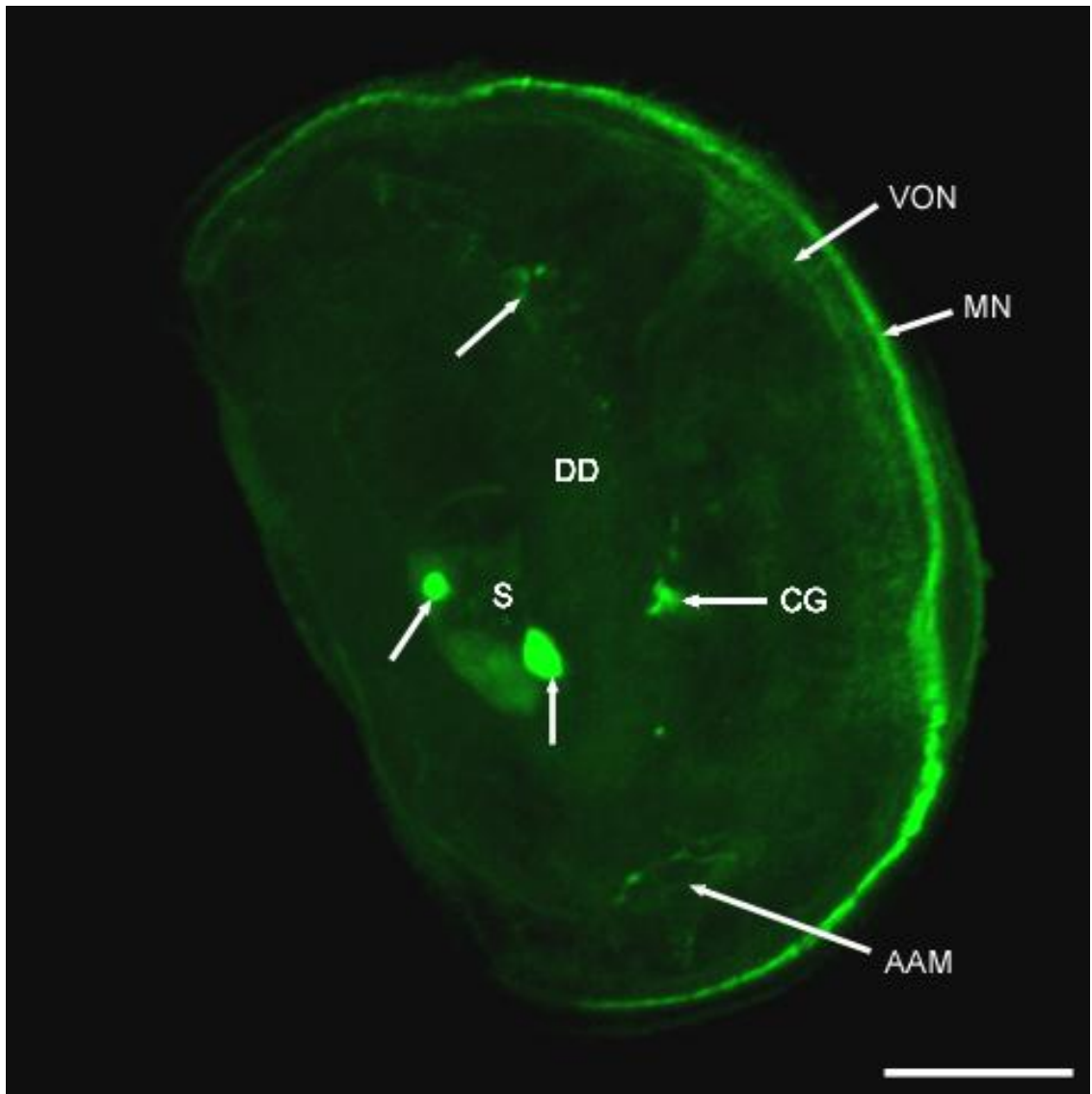


Figure 2.24. FMRFamide-like green immunoreactivity in a D-stage larva (day 5) ($12 \times 0.97\mu\text{m}$). Abbreviations: AAM, anterior adductor muscle; CG, cerebral ganglion; DD, digestive diverticulum; MN, mantle nerve; S, stomach; VON, ventral osphradial nerve. White unlabelled arrow = unknown immunoreactive site. Scale bar = $20\mu\text{m}$.

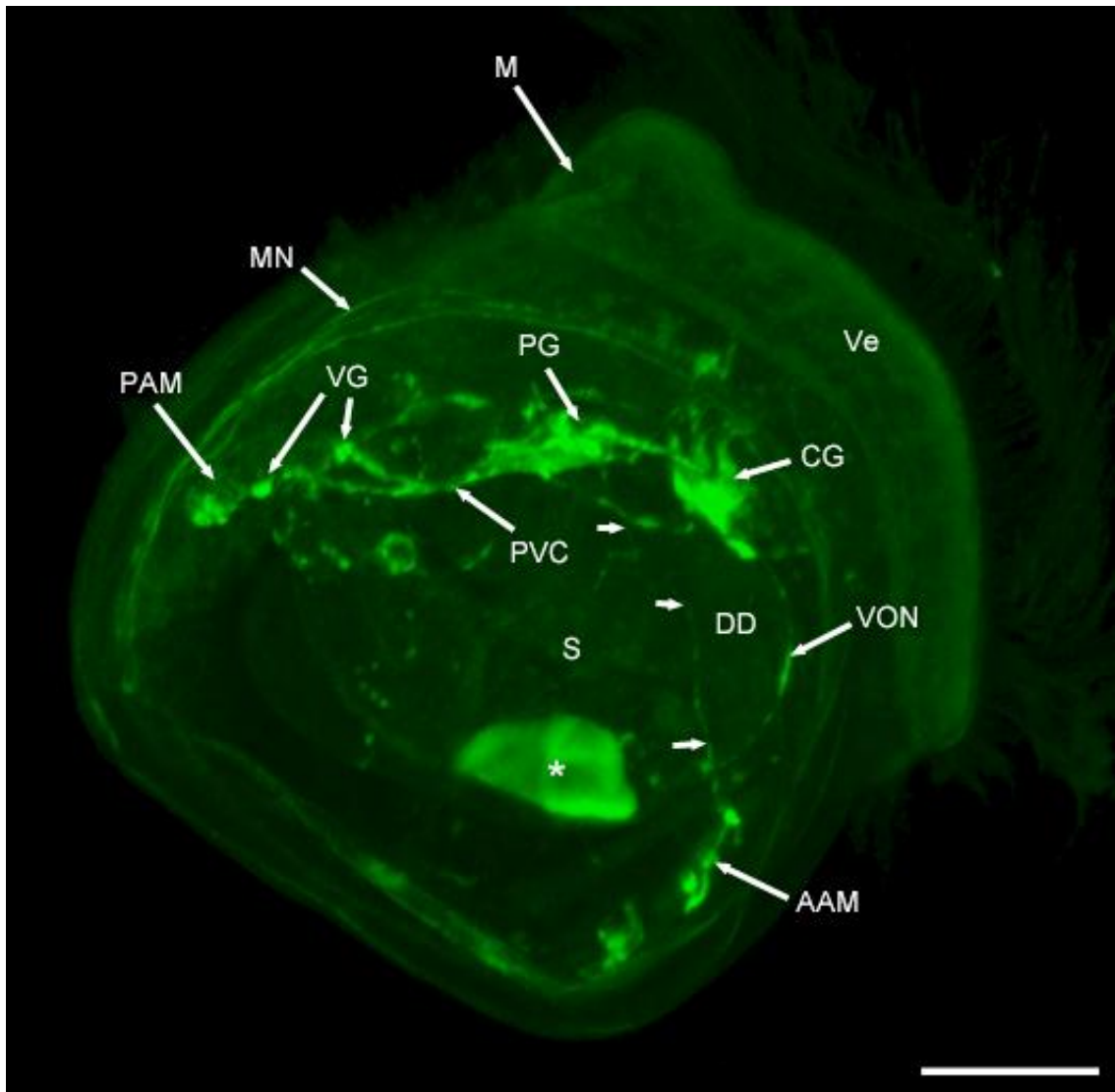


Figure 2.25. FMRFamide-like green immunoreactivity in an early umbo larva (day 10) ($30 \times 1.07\mu\text{m}$). Abbreviations: AAM, anterior adductor muscle; CG, cerebral ganglion; DD, digestive diverticulum; Mouth, Mouth; MN, mantle nerve; PAM, posterior adductor muscle; PG, pedal ganglion; PVC, pleuro-visceral connective; S, stomach; VG, visceral ganglion; VON, ventral osphradial nerve. White unlabelled arrows; innervation from AAM to PG. * = autofluorescence. Scale bar = $20\mu\text{m}$.

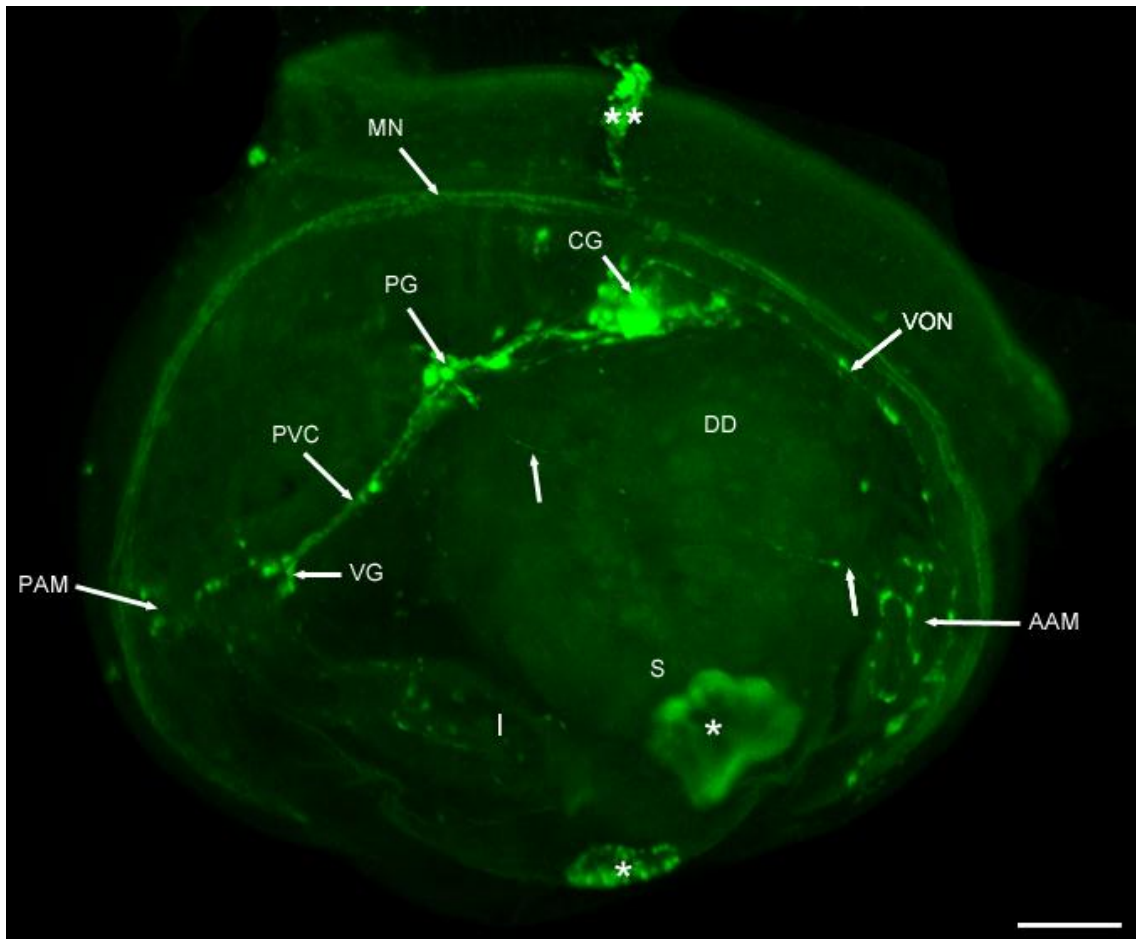


Figure 2.26. FMRamide-like green immunoreactivity in a late umbo larva (day 14) (52 x 0.97). Abbreviations: AAM, anterior adductor muscle; CG, cerebral ganglion; DD, digestive diverticulum; I, intestine; MN, mantle nerve; PAM, posterior adductor muscle; PG, pedal ganglion; PVC, pleuro-visceral connective; S, stomach; VG, visceral ganglion; VON, ventral osphradial nerve. White unlabelled arrows; innervation from AAM to PG. * = autofluorescence. ** = artefacts. Scale bar = 20µm.

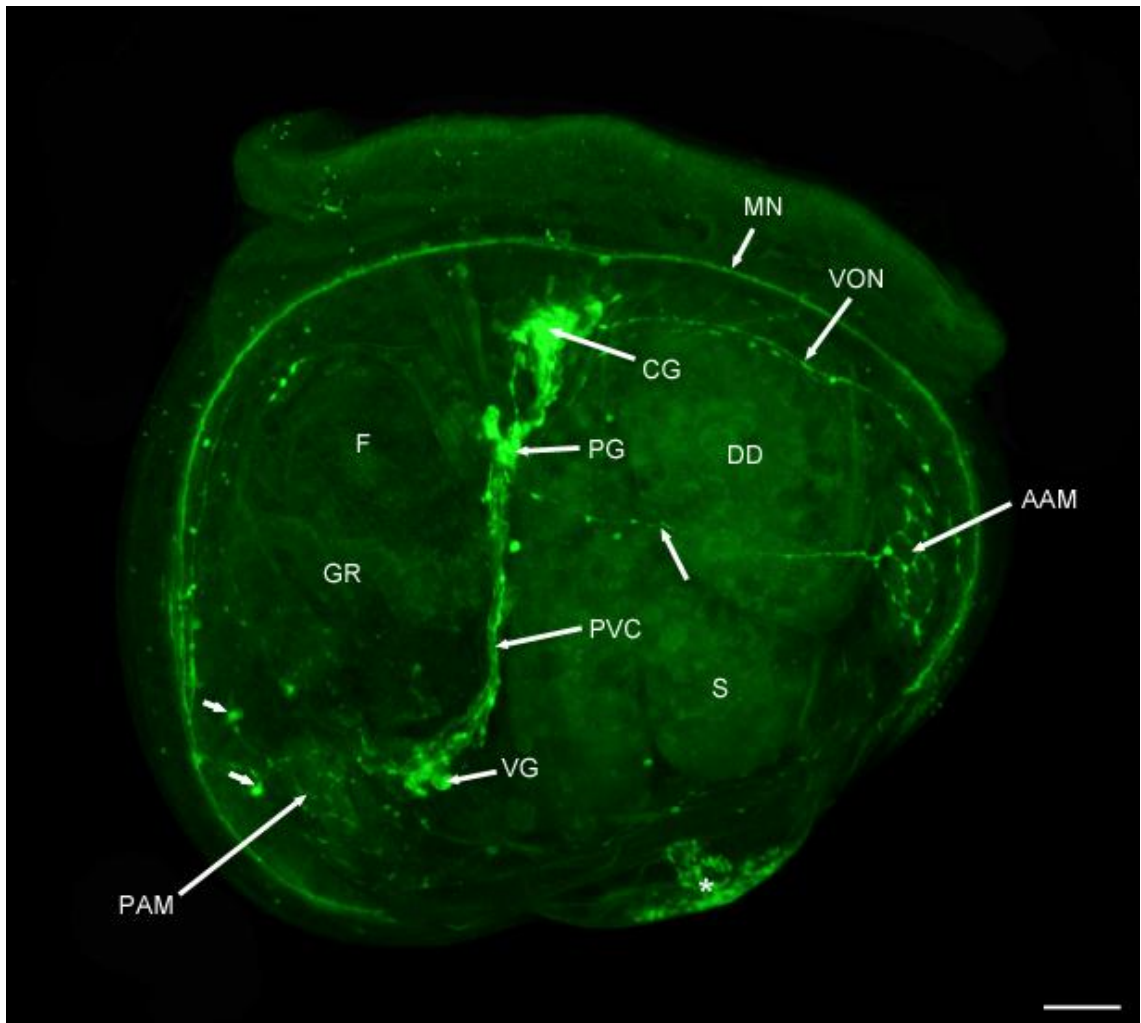


Figure 2.27. FMRFamide-like green immunoreactivity in a pediveliger larva (day 18) ($54 \times 1.07 \mu\text{m}$). Abbreviations: AAM, anterior adductor muscle; CG, cerebral ganglion; DD, digestive diverticulum; F, foot; G, gill rudiment; MN, mantle nerve; PAM, posterior adductor muscle; PG, pedal ganglion; PVC, pleuro-visceral connective; S, stomach; VG, visceral ganglion; VON, ventral osphradial nerve. White short arrows; unknown neurons. White long unlabelled arrow; innervation from AAM to PG. * = autofluorescence. Scale bar = $20\mu\text{m}$.

2.6 DISCUSSION

A number of studies have focused on various aspects of bivalve larval development, ranging from survival, clearance rates, shell growth, settlement, organogenesis, neurogenesis, and metamorphosis within a hatchery reared environment (Ockelmann, 1965; Zardus et al., 2006; Ellis, 2010; Ragg, King, Watts, & Morrish, 2010; Todt & Wanninger, 2010). Recently, advancements have been made in assessing neurogenesis processes that are fundamentally important during bivalve larval development (Flyachinskya, 2000; Voronezhskaya, Nezhlin, Odintsova, Plummer & Croll, 2008; Dyachuk, Wanninger & Voronezhskaya, 2012).

Studies on organogenesis, embryogenesis, neurogenesis, shell morphology, shell growth, and clearance rates are lacking for *Perna canaliculus* larvae (but see, Redfearn, Chanley & Chanley, 1986; Buchanan, 1999; Ragg et al., 2010). Settlement of *Perna canaliculus* larvae under hatchery rearing conditions has been described by Buchanan (1999). More recently, a study on the effects of neuroactive compounds on the settlement of *Perna canaliculus* has begun to expand our understanding on the mechanisms involved with settlement behaviour (Young, 2009; Young et al., 2011). Understanding these aspects of larval development is fundamental to the successful cultivation of larvae under hatchery conditions and to improve the overall yield of larvae reaching settlement. This study aims at improving our understanding of larval development from early fertilisation to settlement at ~21 days post-fertilisation. Attention is directed at survival, shell morphology, feeding consumption,

embryogenesis, organogenesis, and neurogenesis of *Perna canaliculus* using a multidisciplinary approach (light microscopy, histology, immunochemistry, & SEM).

2.6.1 Survivability

The survivability of larvae over the rearing period had a linear sloping decrease, with a low proportion (<4%) reaching settlement after 21 days in the Cawthron Ultra Dense Larvae Rearing System (CUDLRS). These results were similar to findings by Ragg et al. (2010) who observed mean veliger survival rates of 22–49% for *Perna canaliculus* under simulated commercial culture conditions. Similar performance also has been routinely observed in semi-commercial trials conducted by the Cawthron Institute, as well as occasional mortality cascades, where rapid deterioration in the tank environment can result in 100% mortality (NLC Ragg, personal communication). Another study by Paredes et al. (2012) had control larvae reach ~26% survival at day 18 post-fertilisation. A potential reason for the low survivability obtained in that study around the settlement stage may be due to low lipid reserves in oocytes and within feeding larvae which are fundamental to growth and successful metamorphosis (Gallager, Mann, & Sasaki, 1986a; Gallager, & Mann, 1986b). Energy is utilised from lipids and high lipid reserves have been suggested to be affiliated with high larval survival, but abundant reserves do not necessarily guarantee good larval survival (Gallager, et al., 1986a). Seasonal gametogenesis of *Perna*

canaliculus broodstock has been shown to occur over winter and spawning (August-September) (Buchanan, 2001). This timing of gamete release coincided with the same season of our experimental trials in September, and visual observation of the broodstock gonads prior to spawning revealed good gonad condition. Buchanan (1999) used a similar rearing design and feeding diet to our experiment and he trialled several feed types. Results showed that *Perna canaliculus* larvae fed mixed diets of *Isochrysis galbana* with *Tetraselmis chuii* and *Chaetoceros* had a 66% survival rate. He also showed that survivability of larvae fed a combination of *C. calcitrans* and *I. galbana* was higher than any other mixture of microalgae trialled. Tong & Redfearn (1985) indicated that under normal rearing conditions, a very large proportion of the gametes are not viable or do not develop into healthy larvae for *Perna canaliculus*. As a consequence, a larval yield as low as 25%, although not ideal, seems to be the norm for commercial production. This low survivability can be related to environmental conditions or biological origin. Species-specific requirements for good larval survival are sometimes not well understood. Considerable variation among bivalve species like the mussel *Mytilus edulis* at low temperatures can achieve good survival rates over long periods, yet the reasons for the viability of these survival rates remains unknown (Beaumont & Budd, 1982). The use of grading tanks is a common practice in bivalve larval rearing to remove excess microalgae, waterborne parasites, and bacteria that accumulate on dead larvae. Within this study, larvae were not graded to remove dead larvae, so as to give a clear representation of the total population variability. This cascade of dead larvae increases the likelihood of hosting

protozoa and bacteria. The population increase of these microorganisms can stress the larvae and possibly reduce the feeding consumption, which in turn could contribute to high mortality rates as observed in *Mytilus edulis* (Bayne, 1978). Ragg et al. (2010) found colony-forming bacterial counts in 2-day old *Chaetoceros calcitrans* cultures to be substantially lower than in older cultures. Introducing bacteria from the same aged microalgae (2 days old) to our experimental tanks was considered a low risk to the health of *Perna canaliculus* larvae based on these previous findings.

Overall, this study highlights the high variability in survival within the larval rearing environment, and the need to develop successful measures to reduce bacterial threats and parasitism. Survival is highly dependent on various endogenous and exogenous factors, and variation among larval survival needs to be investigated further.

2.6.2 Shell morphology and growth

The shell morphology of *Perna canaliculus* displays similarities with other bivalve species with a planktotrophic larval phase, such as oysters, (Wassnig et al., 2012) other mussels, (Martel, Hynes, & Nicks, 1995) and various clams (Moueza et al., 1999). Results from this study show a shell length growth of 7.57µm per day and a strong positive correlation between shell length and days. These results are similar to those of Redfearn et al. (1986) who showed shell length growth of 6–9 µm per day. In our study, shell growth was generally

positively linear with some high variation occurring among larvae from 14 dpf onwards. This was due to low numbers and massive morphological changes that seem to occur within the population at this transition phase. Feeding ratios and availability of food type play a vital role in shell growth. Ragg et al. (2010) showed that varying *Chaetoceros calcitrans* and *Isochrysis galbana* ratios and culture age affected the mean shell size of *Perna canaliculus* larvae after 22 days of rearing, but not for food availability for concentrations above 20 cells μL^{-1} . Our feeding ratio of 40 cells μL^{-1} would therefore seem sufficient for shell growth over the larvae rearing period.

The appearance of shell secretion from embryogenesis was not documented here. Samples were only taken and observed from the appearance of a D-shell and onwards at 48 hpf. Redfearn et al. (1986) described that the straight-hinge stage referred to here as the D-stage was completed within 24–48 hpf. Therefore, we can assume that the first secretion of shell begins shortly after the late gastrula stage (18–19 hpf) where complete invagination within the vegetal pole is to take place. Silberfeld & Gross (2006) described the shell formation process during embryonic development of the tropical bivalve *Tivela mactroides* began at around the late gastrula (9–10 hpf) through shell- field invagination. Shell formation of a D-shell was complete at 18 hpf. It has been suggested that for this D-stage form to succeed, the invagination process needs to close completely, as described in *Mytilus galloprovincialis* (Kniprath, 1980), *Pecten maximus* (Casse, Devauchelle, & Le Pennec, 1998) or partially, as seen in *Spisula solidissima* (Eyster & Morse, 1984). This supports the theory that

Perna canaliculus is most likely dependent on successful invagination in the embryo stage for the D-shell to form.

For *Perna canaliculus*, the appearance of a shallow and flat D-shell (48 hpf) was seen with a common stellate radial region extending ventrally from the pitted punctate region towards the valve opening and hinge of the larvae. This pitted punctate zone, described by Waller (1981) on the European oyster, *Ostrea edulis* is thought to be secreted all at once, whereas formation of the stellate radial region is achieved through increments. These two regions incorporated together form PI which is secreted by the shell gland. The two prodissoconch regions PI and PII observed by Ericson (2010) were apparent in this study along with the dissoconch region which has not been described before for *Perna canaliculus*. Larvae at 4 dpf had secreted a prodissoconch II layer extending to the mantle edge from a clear transition zone from the PI. At the early umbo stage, the umbo becomes more prominent with proturbances to the shell near the hinge. There was a distinct transition zone which composes of heavy commarginal growth lines between each prodissoconch and dissoconch region and is commonly displayed in other bivalves (Moueza et al., 1999; Silberfeld, 2006). The umbonate and post-larva stage revealed further prominent proturbances to the shell near the hinge with the post-larva developing a dissoconch layer. Overall, these shell morphology characteristics are common among various mussel species like the zebra mussel, *Dreissena polymorpha* (Pallas) (Martel et al., 1995), and three species of New Zealand mussel larvae *Mytilus edulis aoteanus*, *Xenostrobus pulex*, and *Modiolarca*

impacta through subsequent larval development (Redfearn, 1986). Further research regarding when the shell begins to form in the trochophore stage would assist commercial hatcheries with identifying when larvae are going through this transition. Ultimately, avoiding handling at this period would reduce potential damage to newly secreted shell and would be of considerable value to commercial hatchery's rearing *Perna canaliculus*.

2.6.3 Feeding consumption

Larvae on average consumed different amounts of the supplied *Chaetoceros calcitrans* and *Isochrysis galbana* microalgae at 40 cells μL^{-1} throughout the 21-day rearing period. Larvae at 6 dpf, showed an unexplained increase in microalgae consumption over a 24-hour period. Consumption generally increased up to 15 dpf before declining at settlement. An increase in microalgal consumption was mostly probably due to larvae progressing in organogenesis and preparing for the metamorphosis transition by accumulating energy reserves (da Costa, Novoa, Ojea, & Martinez-Patino, 2012; Sanchez-Lazo & Martinez-Pita, 2012). Immediately after this stage, a reduction in feeding consumption occurred. This is similar to other larvae progressing towards metamorphosis, which showed a decline in feeding consumption as observed in *Ostrea edulis* (Holland & Spencer, 1973), *Crassostrea gigas* (Gerdes, 1983), and *Mytilus edulis* (Sprung, 1984) in the early stages of metamorphosis. These studies suggest that this transition from veliger to metamorphosis requires using

stored biochemical reserves. This consumption rate decline was similar to our study with larvae at the umbonate stage consuming low volumes of algae before making the transition to pediveliger and then post-larva.

In contrast to our study, Ragg et al. (2010) used the same CUDLRS design to rear *Perna canaliculus* larvae being fed *Chaetoceros calcitrans*, and a mix of both *Chaetoceros calcitrans* and *Isochrysis galbana* with results showing that there was a steady increase in clearance rates among veliger larvae. However, Ragg et al. (2010) did observe that around the pediveliger stage, large amounts of mucus secreted by pediveliger larvae bound up large amounts of algae, which artificially increased the apparent clearance rate. This could explain the small increase in apparent algae consumption observed in our study once larvae had progressed to competent pediveliger larvae, but does not explain the dramatic reduction in feeding consumption prior to this transition. The dramatic reduction in feeding consumption could be based on a cascade effect from an accumulation of dead larvae remaining in the tanks, as dead larvae were not removed through the rearing period. This would ultimately increase favourable conditions for ciliates or protozoans to thrive on dead larvae. Indeed, a study by Bayne (1978) showed that exponential increases in the population of parasites caused larvae to restrict feeding due to stress and unfavourable conditions, which ultimately negatively affected growth and survival.

2.6.4 Embryogenesis

Unfertilised oocytes of *Perna canaliculus* eggs appeared spherical in shape and with an average size of ~60 µm, similar to a study by Buchanan (1999). Following fertilisation, embryos progressed to a ciliated gastrula stage at 18–19 hpf. Common morphological features included a small blastopore, apical sense organ, and large vegetal pole within the shell field. This shell field at 19 hpf was observed at an early invagination process due to cleavage within the margins of the vegetal pole. This invagination period is similar to the shell field invagination of *Mytilus edulis* at 24 hpf (Humphreys, 1969). External morphology was identical to other planktotrophic bivalve species, such as the tropical clams *Anomalocardia brasiliana* (Moueza et al., 1999), and *Tivela mactroides* (Silberfeld, 2006). *Anomalocardia brasiliana* had a large blastopore at the early gastrula stage, while *Tivela mactroides* had a large vegetal pole where the shell field would later develop. This large vegetal pole was present in *Perna canaliculus* gastrula.

However, the observations of *Perna canaliculus* at the late gastrula stage (18–19 hpf) were considerably different to other bivalve species. For example, the gastrula stage was reached much earlier for tropical clams *Anomalocardia brasiliana* and *Tivela mactroides*. *Anomalocardia brasiliana* had an earlier gastrula stage of 6 hpf (Moueza et al., 1999), and *Tivela mactroides* between 4–5 hpf (Silberfeld, 2006) in contrast to *Perna canaliculus* gastrula at 18–19 hpf. Warmer tropical bivalves like the pearl oysters in tropic climates generally have a shorter embryo stage as opposed to colder climates (Wassnig et al., 2012).

Few studies exist involving biomineralisation of the shell for *Perna canaliculus* trochophores, but from this study we can estimate that this occurs between 20-48 hpf as with larvae of other species, such as the abalone *Haliotis tuberculata*, which formed a prototroch I at 19 hpf (Gaume et al., 2011). In contrast, a study by Jardillier et al. (2008) on the same species revealed the protoconch I occurred at 30 hpf. This time lag in shell mineralisation as suggested by Gaume et al. (2011) could be due to using a 2.0°C increase in seawater temperature. In the present study, rearing temperatures of *Perna canaliculus* post-larvae varied considerably by 2.0°C and could be an underlying cause of possible slow or sporadic development. This is highly plausible as temperature has always been suggested as a regulating factor of larval development rate in marine invertebrates (Scheltema, 1967).

In this study, there were some inconsistencies with water quality during the embryonic period due to high suspended water solids within the water supply. The treatment of FSW with EDTA was used to reduce the adverse effects of heavy metal ions (zinc, lead) which is common practice and has been proven to increase veliger yield of *Perna canaliculus* by as much as 20% (Buchanan 1999). There appeared to be some cell shrinkage due to storage in alcohol in the unfertilised oocyte and embryonic stages. However, this analysis was still a clear representation of specific morphology within the gastrula stage. This cell shrinkage is commonly seen in critical point or air drying techniques (Bozzola & Russel, 1999).

The findings of this study are of two development stages (unfertilised oocytes and embryogenesis at the gastrula stage), and more intensive sampling of the first 24–48 hpf will reveal other stages of embryogenesis and shell mineralisation prior to developing a D-shell. Whether the rate of embryonic development is normally represented here or affected by temperature or other external environmental conditions is yet to be established.

2.6.5 Organogenesis

Histological sections and light micrographs revealed similar organogenetic development of veligers to other bivalve species, such as the oyster *Crassostrea virginica* (Ellis, 2010), the European oyster *Ostrea edulis* (Waller, 1981), the scallop *Patinopecten yessoensis* (Bower & Meyer, 1990), and the mussel *Mytilus edulis* (Bayne, 1971). The digestive diverticulum appeared early within the D-stage larvae and was distinguished from the stomach by large digestive tubules that encompass the digestive diverticulum and a style sac that is observed at the dorsal end of the stomach near the hinge. These large digestive tubules containing digestive cells are seen in various bivalve larvae and the algae is broken down in vacuoles and taken up by these digestive cells (Gosling, 2003). At the early umbo stage, there was a well-developed alimentary system consisting of the stomach and digestive diverticulum, similar to a study by Bayne (1971) on the mussel *Mytilus edulis* and the oyster *Crassostrea virginica* (Ellis, 2010). The presence of algae suggests normal

uptake, and a style sac dorsal of this was apparent. The velum was very pronounced and the mouth positioned ventral and an interconnecting esophagus travelling down towards the digestive diverticulum and stomach. This connection between the esophagus, digestive diverticulum and stomach was seen in histological sections of *Mytilus edulis* (Bayne, 1971). Velum retractor muscles that are responsible for the contractility of the velum were observed within this study and were similar to findings by Cragg (1985) who also observed these retractor muscles in the early veliger larvae of *Pecten maximus*. Histological sections at the early umbo showed an intestine which is used to excrete unwanted wastes. Prior to excreting digested and broken down algae, the waste is suggested to contain digestive enzymes which could be utilised by the stomach for extra-cellular digestion (Gosling, 2003).

The late umbo stage had progressed further in organogenesis with distinct retractor muscles seen in histological and light microscopy extending outwards from the umbo region to the velum lobe and velum. The stomach and digestive diverticulum appeared larger in shape containing microalgae. The anterior adductor muscle was similar to histological sections of the scallop *Patinopecten yessoensis* with striated muscle fibres (Bower & Meyer, 1990). Another sagittal section of a slightly older larva shows a velum retractor muscle lying posterior of the mouth and velum, with a long esophagus extending from the stomach towards the velum similar to the scallop *Patinopecten yessoensis* (Bower et al., 1990). Light micrographs through the translucent larvae shells reveal a series of retractor muscles extending ventrally from the hinge to the velum, thought to

be velum retractor muscles, and the anterior adductor muscle distinguished by its rod shape muscle. The presence of many retractor muscles could also consist of pedal retractor muscles as described in the early veliger of *Pecten maximus* (Cragg, 1985).

Organogenesis proceeded with metamorphosis at the late umbonate and pediveliger stage with the development of a functioning foot, gill rudiment, and an eye spot on both valves. All of these characteristics have been observed by Buchanan (1999) during the metamorphosis and pediveliger stage of *Perna canaliculus*. This dramatic change is observed in various planktotrophic larvae that undergo metamorphosis including clams (Stephenson & Chanley, 1979; Moueza, Gros, & Frenkiel, 1999), oysters (Wassnig & Southgate, 2012), scallops (Moueza, Gros, & Frenkiel, 2006), and mussels (Redfearn, Chanley & Chanley, 1986; Arellano & Young, 2009). Metamorphosis and settlement is said to be triggered by catecholamines as suggested in *Mytilus edulis* (Croll, 1997). Chemical cues like GABA (γ-aminobutyric acid) also have been shown to induce settlement and/or metamorphosis in larvae of mussel *Mytilus galloprovincialis* and *Aulacomya maoriana*, the clams *Venerupis pullastra* and *Ruditapes philippinarum*, and the oyster *Ostrea edulis* (Garcia-Lavandeira et al., 2005).

The digestive diverticulum in *Perna canaliculus* pediveliger is large in shape and anteriorly takes most of the visceral mass as seen in the larvae of *Mytilus edulis* (Bayne 1971). The functional foot, characteristic of pediveligers, was situated lying posteriorly within the shell. The foot was observed to extend out of the

shell and sense the substrate in explorative type behaviour for short periods of time. The role of the foot at this stage is to test for suitable substrates and make a transition to attach as suggested by Buchanan (1999) for *Perna canaliculus*. Similar species, such as the oyster *Crassostrea virginica* (Ellis, 2010) and *Ostrea edulis* (Waller, 1981) showed similar substrate feeling behaviour at the pediveliger stage. The role of the eye spot which rose from the base of the gill rudiment in *Perna canaliculus* is unknown, but Buchanan (1999) suggested it as an indication of larvae being competent to settle, and was observed in an earlier study on several New Zealand bivalve larvae (Booth, 1977). This eye spot also was observed in the mussel *Mytilus edulis* (Bayne, 1964).

The rate of overall larval organogenesis can be affected by the nutritional gain from mixed diets. A study by Strathmann (1993) looking at the rate of development in *Crassostrea gigas* larvae found that optimum microalgal cell concentration affected the size of larval structures, such as velum size, shell length, and eye spot development. Interestingly, a reduction in microalgal concentration induced greater growth in the velum which was proportionally bigger than the shell. This was due to a possible consequence of limited food available. Our ratio of *Chaetoceros calcitrans* and *Isochrysis galbana* was 5:1 at 40 cells μL^{-1} , and has been suggested to meet optimum nutritional requirements for successful larval development of *Perna canaliculus* under simulated rearing conditions (Buchanan, 1999; Ragg et al., 2010). A study by Brown (1991) reinforces the importance of the mixed diet *Chaetoceros*

calcitrans and *Isochrysis galbana* which appears to complement each other in that carbohydrate fractions from *Chaetoceros calcitrans* were lacking the sugar arabinose, and that *Isochrysis galbana* had an abundant source of this sugar. Also, low fucose and rhamnose levels in *Isochrysis galbana* can be buffered by the presence of these sugars in the *Chaetoceros calcitrans*. Conservatively, we can assume that the diet requirement of *Perna canaliculus* has been optimised and that the rate and success of larval development is best suited with acceptable trade-offs, such as growth and metamorphosis.

2.6.6 Neurogenesis

This study is the first to describe the larval neuronal development of *Perna canaliculus*. To distinguish the nervous system components of this species, comparisons were made to recent immunochemical and histological studies on the nervous system of other bivalve larvae, such as the mussel, *Mytilus trossulus* and the oysters, *Crassostrea gigas* and *Crassostrea virginica* that show similar larval development to *Perna canaliculus* (Voronezhskaya et al., 2008; Ellis, 2010; Dyachuk et al., 2012). These three comparative species are free-swimming, non-feeding trochophore larvae, which then develop into planktotrophic veliger larvae that subsequently metamorphose into settled juveniles, much like *Perna canaliculus* larvae. Only at a later developmental stage of post-settlement do the bivalve larvae show unique species-specific morphological features useful for species identification. Histological sections

revealing certain ganglia were compared to other histological studies on larvae of the oyster *Crassostrea virginica* (Ellis, 2010), *Ostrea edulis* (Hickman et al., 1971), various other oysters (Elston, 1999), and the scallop *Patinopecten yessoensis* (Bower et al., 1990). Results revealed FMRFamideergic fibres and cell bodies from early D-stage larva and then paired ganglia in veliger larvae through to post-settlement. Histological results revealed some ganglions, such as the apical ganglion and the pedal ganglion, but did not clearly identify other important ganglions and connective fibres seen with FMRFamide immunostaining. This was similar in the D-stage oyster *Crassostrea virginica* where histological sections did not show the presence of ganglia, commissures, and connectives which suggested further neurogenesis was to take place (Ellis, 2010).

FMRFamideergic cells first appeared at the D-stage in the cerebral ganglion area which later became the most immunoreactive site in the nervous system of *Perna canaliculus* larvae. Interestingly, there was no presence of FMRFamideergic cells within trochophore larvae at 18 hpf. In contrast, Voronezhskaya et al. (2008) showed the first FMRFamide like immunoreactive cell to appear 27 hours after fertilisation into the trochophore stage of *Mytilus trossulus*. However, a study on the trochophore of *Mytilus edulis* by Flyachinskaya (2000) showed the first presence of FMRFamide sites to occur at 14–15 hpf within the transfer of the conchostoma stage to the trochophore stage before the turning of the shell gland. The mantle nerve in *Perna canaliculus*, which encompasses the mantle region and extends dorsally and

dissipates at the flat hinge has been described by Ellis (2010) in the larvae of the oyster *Crassostrea virginica*. The presence of weak innervations in the anterior adductor muscle and the ventral osphradial nerve at D-larva (5 dpf) are the first visible fibre connectives observed and these became more pronounced during larval development.

At the early umbo stage (10 dpf), a complete nervous system developed with the presence of the cerebral ganglion encompassed by cell bodies and fibres extending dorsally towards the pedal ganglion and subsequently onto paired visceral ganglia via the pluro-visceral connective. The existence of paired connective loops between the cerebral ganglia and pedal ganglion, and also between the pedal ganglia and visceral ganglia completes a nervous system. Rotatable z-stacked images could not reveal if the pedal and cerebral ganglia were paired, but paired connectives running between these ganglia suggests otherwise. Paired sets of ganglia for the cerebral, visceral, and pedal has been observed in the pediveliger of *Ostrea edulis* (Erdmann, 1935), *Crassostrea virginica* (Ellis, 2010), and in the late veliger of *Mytilus trossulus* (Voronezhskaya et al., 2008). The first appearance of a complete fibre connective is seen running from the pedal ganglia to the anterior adductor muscle that diverges into two fibres within the muscle that connects to individual cell bodies. This fibre connective was observed in larva of the oyster *Crassostrea gigas* and mussel *Mytilus trossulus* (Dyachuk et al., 2012). The ventral osphradial nerve appears to extend dorsally over the fibre between the anterior adductor muscle and pedal ganglion running around the margin of the

digestive diverticulum and terminates in the stomach. The mantle nerve for the first time shows two distinct nerves running along both shell valves.

The late umbo stage (14 dpf) reveals more fibre like innervations forming in the anterior adductor muscle and a weak fibre extends posteriorly from this muscle and connects to the pedal ganglia. At this stage there are paired visceral, pedal, and cerebral ganglia, though the cerebral ganglion shows intense staining to conclude if they are indeed paired. The distance between these ganglia begins to increase as the larvae undergo further organogenesis.

FMRF-amidergic immunoreactive innervations at the pediveliger stage (18 dpf) running from the anterior adductor muscle to the pedal ganglion show almost identical symmetrical neurogenesis with the findings of Dyachuk et al. (2012) on the mussel, *Mytilus trossulus* and the oyster, *Crassostrea gigas* nervous elements of the pediveliger. The innervations within the anterior adductor muscle are still not well understood and the presence of FMRFamide neurons that send peripheral processes to the smooth catch muscles has been described by Dyachuk et al. (2012) that suggested FMRFamide can be released by neuronal excitation to act on muscle fibres. However, no FMRFamide innervations running through the velum like in *Crassostrea gigas* were apparent in *Perna canaliculus*, and consequently no innervations in the velum were seen for *Mytilus trossulus* (Voronezhskaya et al., 2008; Dyachuk et al., 2012). The location and innervations running from the cerebral ganglion to the pedal ganglion and to the visceral ganglion *via* the pleuro-visceral connective appear very similar to FMRFamide containing cells found within

Mytilus trossulus (Voronezhskaya et al., 2008; Dyachuk et al., 2012). The differentiation between the cells of the apical ganglion and cerebral ganglion location through FMRFamide staining has not been well documented for other bivalve species. Results from the present study show a large area of intense staining that will most likely incorporate both these ganglia and other cell bodies, but is commonly referred to as the cerebral ganglion in other studies (Dyachuk et al., 2012). The findings of this study at the pediveliger stage reveal a completed nervous system with peripheral innervations running throughout the larva. The foot and velum of *Perna canaliculus* showed no FMRFamide like staining, but other studies suggest this is highly innervated with catecholamines and serotonin like immunoreactivity (Croll, 1997). The nervous system composes of the cerebral ganglion which lies dorsal of the velum and is connected to the pedal ganglion by two connective loops, with the pedal ganglion composing of several cell bodies *via* parallel connective loops travelling dorsally to the visceral ganglia. This was similar to the mussel *Mytilus edulis* (Voronezhskaya et al., 2008). The posterior adductor muscle consists of thin fibres extending throughout the muscle *via* the visceral ganglia and has several connective fibres with unknown cell bodies traveling posteriorly to the mantle nerve. This innervation of FMRFamide fibres though out the posterior adductor muscle is previously seen in the oyster *Crossostrea gigas*. However, in the same study, no mention was made of these fibres innervating posterior adductor muscles of the mussel *Mytilus trossulus* (Dyachuk et al., 2012).

Overall, this study on the nervous system of *Perna canaliculus* larvae is important in establishing an understanding in which neuronal components may be responsible for neuromodulation of larval behaviours and critical processes such as settlement and metamorphosis. Chemical cues or environmental conditions affiliated with such behaviour could be investigated further using a multitude of techniques, such as aldehyde-induced fluorescence of catecholamine and serotonin-like immunoreactivity as outlined in a detailed study on *Mytilus edulis* (Croll, 1997). Further research on how these neural components are linked with such behaviour through subsequent larval development would be of considerable value to successfully improving hatchery reared *Perna canaliculus*.

In summary, this study describes the characteristics of *Perna canaliculus* larval development under hatchery reared conditions. Overall development was similar to species, such as the oyster *Crassostrea virginica* and mussel *Mytilus trossulus*. Survivability was similar to other past studies on *Perna canaliculus*, with low survival encountered at the settlement stage. Shell morphology revealed characteristics common to other planktotrophic larvae incorporating a small PI with a pitted punctuate and stellate-radial region and PII with growth annulations extending to the mantles edge. Shell length was generally linear with variability towards the pediveliger and settlement stage with findings similar to previous studies. Feeding consumption was observed to be at its highest between 7 and 14 dpf, and was thought to be associated with an increase in organogenesis. Conversely, decreasing feeding consumption occurred around

the pediveliger and settlement stage commonly seen in several bivalve species, *Ostrea edulis*, *Crassostrea gigas* and *Mytilus edulis*. Embryogenesis revealed an early and late gastrula stage with an enclosing vegetal pole, apical sense organ, blastopore, and shell field invagination at around 18-19 hpf. Organogenesis occurred from early D-stage through to metamorphosis and settlement with typical bivalve larvae organs developing over this time frame. Neurogenesis began at an early D-stage with immunoreactive cells, followed by further neurogenesis involving paired cerebral, pedal, and visceral ganglia through the veliger and pediveliger stage. While this study describes larval development using a multidisciplinary approach, further detailed research into each area from embryogenesis through to post-settlement would endeavour to improve hatchery rearing of this species.

CHAPTER THREE: Cryopreservation

3.1 ABSTRACT

Effects of cryopreservation on development of trochophore (18 hours post-fertilisation) and D-stage larvae (48 hours post-fertilisation) of *Perna canaliculus* were evaluated over a 21 day rearing period. Examination of development was undertaken through histology, scanning electron microscopy (SEM), confocal microscopy, light microscopy, and visual observations. Larvae which were cryopreserved using a standard protocol in cryoprotectant (CPA) 10% ethylene glycol (EG) and 0.4 M trehalose were compared with larvae which were not cryopreserved (controls). Results showed that there were significant differences in survivability, shell length, and feeding consumption between controls and frozen treatments, but no comparable differences among both frozen treatments after the 21-day development period. At 18 days post-fertilisation, ~23% of control larvae had progressed to competent pediveliger, while <1% of frozen larvae survived and were unable to develop to competent pediveliger or post-larva. Settlement was achieved in ~9% of controls at 21 days post fertilisation with most individuals developing eye spots. Differences in neurogenesis between frozen trochophore larvae and controls were observed, while frozen D-stage larvae did not differ greatly to controls. Characterisation of shell morphology revealed abnormalities to both frozen treatments, with frozen trochophore larvae showing the greatest shell abnormalities. Organogenesis was delayed in larvae within both frozen treatments with no larvae within frozen treatments developing an eye spot. However, controls successfully made the transition to settlement. This delay in organogenesis and overall development

was indicative of cryo-injuries sustained at a cellular level. This is the first study conducted on the effects of cryopreservation on D-stage and trochophore larvae of this species, and results indicate that D-stage larvae to have a higher resilience to cryopreservation. Further on-going research aims to optimise cryopreservation protocols to improve the long-term viability of cryopreserved *Perna canaliculus* larvae.

3.2 INTRODUCTION AND LITERATURE REVIEW

3.2.1 General bivalve cryopreservation

Cryopreservation is increasingly being used on bivalve mollusc spermatozoa, embryos and larvae as a possible alternative to overcoming seasonal constraints in broodstock conditioning and offspring production. Cryopreservation research has provided successful results on commercially important species, such as the oyster *Crassostrea gigas*, but results have been variable for other species, such as *Crassostrea virginica* (Paniagua-Chavez, 2000; Cheng et al., 2001; Paniagua-Chavez, 2001; Adams et al., 2004; Adams et al., 2008), *Pinctada fucata martensii* (Choi et al., 2003), *Mytilus galloprovincialis* (Di Matteo et al., 2009) & *Perna canaliculus* (Adams et al., 2009). Other studies have focussed on cryopreservation of spermatozoa and embryos of scallops (Xue, 1994; Espinoza, Valdivia & Dupre, 2010), mussel

larval development (Wang et al., 2011) and spermatozoa (Di Matteo, Langellotti, Masullo, & Sansone, 2009).

Cryopreservation involves short or long term storage of living cells using liquid nitrogen as a coolant (Chao & Liao, 2001). These cells must survive the cooling and thawing procedure, which often is harmful to cells (Chao et al., 2001). In order to avoid cell damage by ice formation, a cryoprotectant (CPA) is used to reduce crystallisation, also known as intracellular -ice formation (IIF) (Renard, 1991; & Lin et al., 1999). However, the effectiveness of cryoprotectants is dependent on the compound type (i.e., permeating or non-permeating), concentration, equilibration time, and temperature during loading (Lin et al., 1999). Effective CPAs used in bivalve cryopreservation range in different concentrations of ethylene glycol (EG), propylene glycol (PG), dimethyl sulphoxide (DMSO) and trehalose. A study on cryopreservation in embryos of the Pacific oyster *Crassostrea gigas* without CPA showed that the ultrastructural arrangement of the plasma membrane and organisation of organelles within the cytoplasm were disrupted (Renard, 1991). Another study on *Crassostrea gigas* also had similar results, where most of the cryopreserved larvae appeared to have a rough surface, which suggested there was a functional disruption to the plasma membrane, and as a consequence affected motility of the larvae (Usuki, Hamaguchi, & Ishioka, 2002).

Bovine serum albumin (BSA), a highly soluble protein and important circulating antioxidant, is sometimes used in the thawing or post-thawing process of some cryopreserved bivalve larvae, such as for *Perna canaliculus* sperm, oocytes,

and trochophore (Adams et al., 2009; Smith et al., 2012 a,b; Paredes et al., 2012). BSA is used in *Perna canaliculus* sperm assays as a surfactant (Serean Adams, personal communication). Albumin has been suggested to show several important physiological and pharmacological functions (Roche et al., 2008). Its role is to transport metals, fatty acids, cholesterol, bile pigments, and drugs across membranes. It is also an element in the regulation of osmotic pressure and distribution of fluid between different compartments (Roche et al., 2008). Paredes et al. (2012) suggested that including BSA in the thawing medium for *Perna canaliculus* trochophore could reduce lipid peroxidation of the membrane and/or DNA damage. Observations within this study also show thawed trochophores in the presence of BSA had less blebbing, and appeared more motile and did not stick together as much as trochophores without BSA.

Oocytes of the Pacific oyster, *Crassostrea gigas*, have successfully been frozen and thawed with high survival rates through to post-metamorphosis (Tervit et al., 2005). For oysters, EG (10%) and DMSO (15%) were found to be the most effective CPAs, resulting in good post-thaw fertilisation rates and allowing large volumes of oocytes to be cryopreserved (Lin et al., 1999; Tervit et al., 2005). Another study on trochophore larvae of *Crassostrea gigas* showed that the cells are generally more tolerant to toxicity of CPAs when compared to the morula and gastrula stages, and consequently have higher survival rates (Gwo, 1995). Cryopreservation of eastern oyster (*Crassostrea virginica*) larvae and fertilisation of oocytes with cryopreserved sperm has been successful in producing spat for commercial purposes (Paniagua-Chavez, Buchanan, Supan,

& Tiersch, 2000; Paniagua-Chavez, & Tiersch, 2001). The blue mussel *Mytilus galloprovincialis*, also has been successfully cryopreserved at the D-stage (30 hours post-fertilisation (hpf)) using a combination of chemicals as CPAs (Wang et al., 2011). The most effective CPA in that study was 5% DMSO, which resulted in the highest post-thaw survival rate of $55.3 \pm 7.8\%$. However, it was not significantly different from the 10 and 15% survivability obtained with EG.

Overall, good survival rates of cryopreserved bivalve species are obtained when the larvae are cryopreserved at later stages of development, such as early or late D-stage (Choi et al., 2003). The effects of cryopreservation on subsequent larval development are not well understood, and suggestions have been made that an alternative assessment on overall quality of larvae, not just immediately after post-thawing would be of considerable value (Wang et al., 2011; Paredes et al., 2012).

3.2.2 Cryopreservation on *Perna canaliculus*

Cryopreservation of green-lipped mussel oocytes (Adams et al., 2009), sperm (Smith et al., 2012a,b), and trochophore stage larvae (Paredes et al., 2012) has been investigated with mixed results. For trochophore larvae cryoprotectant (16–20h old), EG was found to be most effective at around 10–15% in the presence of $0.2\text{--}0.4 \text{ mol L}^{-1}$ trehalose (Paredes et al., 2012). Using this optimised cryoprotectant solution, 40–60% of trochophores were able to develop to D-larvae when normalized to controls. However, only 2.8% of the

cryopreserved trochophore developed in to competent pediveligers, while control larvae reached ~26% survival at the pediveliger stage (Paredes et al., 2012). In a different study, oocytes were cryopreserved using ethylene glycol and trehalose with high post-thaw fertilisation success achieved (Adams et al., 2009). However, again subsequent development rates were low with less than 1% survival to D-stage. It was suggested that this low yield was in response to sub-lethal chilling injury and not extracellular ice triggering intracellular ice formation (Adams, et al., 2009). For cryopreservation of *Perna canaliculus* sperm, fertilisation rates equivalent to fresh sperm could be achieved but only when higher concentrations of sperm were used (~365 × more sperm required; Smith et al., 2012a). A subsequent study indicated that viability decreased significantly following cryopreservation ($69.9 \pm 3.5\%$ for fresh sperm versus $25.3 \pm 2.9\%$ for cryopreserved sperm) and motility also was affected (Smith et al., 2012b).

Paredes et al. (2012) concluded that further research is needed to explain what happens to D-larvae from the beginning of larval rearing to the settlement point in order to increase survival. For example, the effect of cryopreservation on shell formation, organogenesis and feeding during larval rearing need to be investigated. The effects over longer development periods as opposed to immediately after post-thawing also need to be assessed. Overall, it appears that the cryopreservation protocols for *Perna canaliculus* sperm, oocytes and trochophore larvae are in need of further refinement.

3.2.3 Significance of cryopreserving *Perna canaliculus* larvae

Successful cryopreservation of *Perna canaliculus* larvae will be an important step in providing an alternative supply of viable larvae on demand when broodstock are not well conditioned due to seasonal constraints. This can help reduce the cost of conditioning broodstock and achieve a higher success of utilising viable larvae. Cryopreservation also is an alternative source of larvae if New Zealand's wild green-lipped mussel populations were to experience high mortality due to disease outbreaks, or natural disasters. The use of cryopreservation also could allow an efficient method of enhancing selective breeding lines among favourable genetic broodstock. This can ultimately provide a reference family in selective breeding so that the same family of larvae are thawed out each year which can separate seasonal or yearly effects.

3.3 AIM & OBJECTIVES

The aim of this chapter is to describe the effects of cryopreservation on subsequent larval development of *Perna canaliculus* from cryopreserved trochophore and D-stage larvae through to post-settlement.

The objectives are:

- To describe shell morphology.
- To describe organogenesis.
- To describe neurogenesis.

3.4 METHODS AND MATERIALS

3.4.1 *Experimental reagents*

For the cryopreserved treatments, we used a cryoprotectant (CPA) combination of 20% (v/v) ethylene glycol (EG) and 0.8 M trehalose (TRE) obtained from Sigma-Aldrich chemicals and prepared in Milli-Q water. Bovine serum albumin (BSA; Albumax I Lipid Rich BSA, GIBCO Invitrogen Corporation, Auckland, NZ) at 0.1% (w/v) in FSW was used during thawing and for counting.

3.4.2 *Larval incubation and collection*

Mature broodstock were spawned using thermal cycling and the resulting gametes fertilised as described in chapter 2–2.2. Fertilised oocytes were then transferred into 12 × 170 L static tanks containing 1 mg L⁻¹ EDTA at ~17°C as shown schematically in Fig 3.1.

At 16 hpf, fertilised oocytes had developed to trochophore stage. Four of the 12 static tanks were gently drained onto a 15 µm screen which was submerged in 1 µm filtered seawater (FSW) to minimise handling stress (Fig. 3.1). Trochophores were collected off the mesh by gently swirling the screen, removing with a pasteur pipette, and placing in a 50 mL falcon tube. Larvae were further concentrated by centrifugation at 0.3 RCF (1.1 rpm) for 3 min. Excess FSW was removed and larvae were then re-suspended in 26 mL and

observed under a microscope to ensure they were not visually damaged. Larvae from each tank were then divided into two treatments: cryopreserved trochophore and control trochophore (handled in the same manner as the cryopreserved treatment but not frozen). Control trochophore larvae were returned to the 170 L tanks for further incubation to D-stage (48 hpf). Cryopreserved trochophore were frozen as outlined below and then placed into four separate 170 L tanks for incubation to D-stage upon thawing.

At 48 hpf, larvae had reached the D-stage. At this time, four incubation tanks which had not previously been drained were filtered through a 45 µm mesh screen that was submerged in FSW to minimise handling stress (Fig 3.1). Larvae were collected in to 50 mL falcons and cryopreserved as outlined below. Upon thawing, larvae were introduced into a specialised rearing system called a Cawthron Ultra Density Larval Rearing System (CUDLRS). The remaining 170 L tanks were also drained at this time and their yield determined by resuspending the larvae in 1 L of FSW and performing counts on replicate sub-samples. These larvae were then also introduced to the CUDLRS.

3.4.3 Cryopreservation

Larvae were cryopreserved at trochophore and D-stage. Aliquots of 1mL containing concentrated larvae ($3-6 \times 10^5 \text{ mL}^{-1}$ trochophore larvae; $5-10 \times 10^5 \text{ mL}^{-1}$ D-larvae) were added to $13 \times 5 \text{ mL}$ glass tubes, respectively for each treatment. Then, 1 mL of CPA was added to each test tube at room

temperature (~17°C) and gentle agitation applied to each tube. Larvae with CPA were then aspirated into 0.25 mL plastic straws (IMV Technologies, France) and sealed with PVC powder at room temperature. The time of CPA larval exposure was ~20 mins. Loaded straws were then placed into a cryogenesis freezer and held at 0°C for 5 mins. The freezer was then programmed to cool at 1°C min⁻¹ to -10°C and hold for 5 mins. Straws were then seeded with a cotton bud cooled with liquid nitrogen, if ice formation within the straw had not occurred. After this holding period, straws were further cooled at 0.5°C min⁻¹ to -35°C and then plunged into liquid nitrogen and held until thawing (1–2 h). Straws were thawed in a water bath at 28.0 ± 1.0°C until the ice had melted.

To determine how many trochophore larvae had been frozen (not all larvae had been sucked into straws), at least three straws that were not frozen were each diluted in 1mL of FSW containing 0.1% BSA and then diluted a further 20 fold (50 µL into 950 µL of saltwater + 0.1% BSA). For each straw, two 25 µL aliquots were taken and larval counts were performed.

For larvae cryopreserved at D-stage, 20 thawed straws were re-suspended in a 1 L beaker, and the total number of larvae in this volume was determined by counting replicate 100 µL sub-samples.

3.4.4 Larval rearing & sampling

A total of 16 CUDLRS were prepared with 4 replicates per treatment (Frozen trochophore, frozen D-stage, controls-handled at trochophore) at a density of 500,000 larvae per CUDLRS at 2 days post-fertilisation (dpf) (Fig. 3.1). Samples taken from each CUDLRS were fixed on this day and on consecutive days for the control and frozen treatments until post-settlement as described in chapter 2–2.4. Rearing parameters, sampling regime, and analysis were the same as described in chapter 2–2.4. Larvae were reared until post-settlement with each tank receiving a mixture of 2-day old microalgae at a ratio of 5:1, *Chaetoceros calcitrans*, *Isochrysis galbana* at 40 cells μL^{-1} with FSW *via* a glass dropper (5 mm diameter) at a constant rate of 80 mL min^{-1} . Tanks were maintained at an average temperature of $19.1 \pm 1.71^\circ\text{C}$ with constant homogenous aeration *via* a glass tube. Controls from chapter 1 were also used to compare development of shell morphology (SEM & light microscopy) and neurogenic (FMRFamide-like immunochemistry) development between unfrozen and cryopreserved treatments (Fig. 3.1).

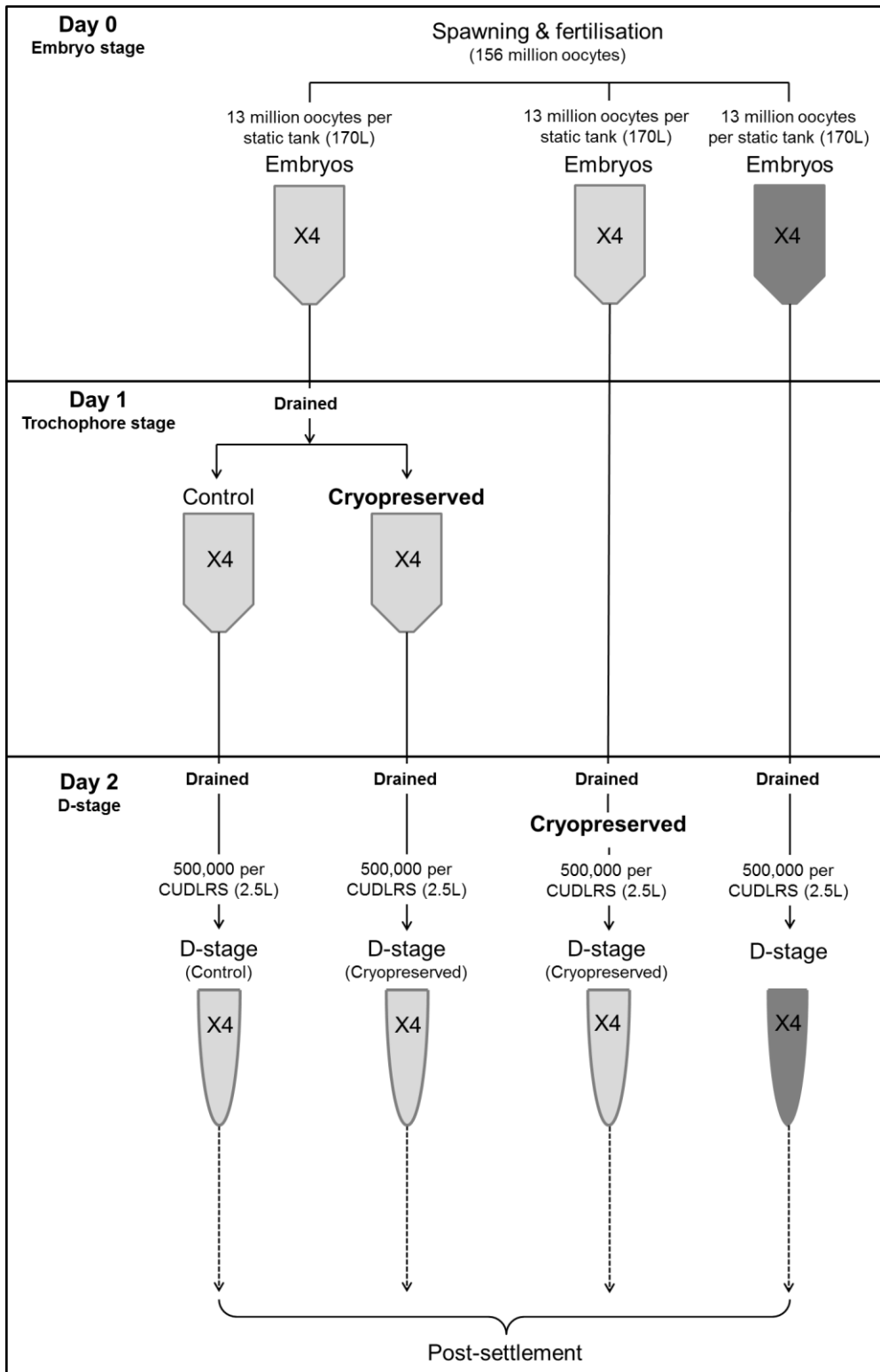


Figure 3.1. Experimental design showing larval rearing of cryopreserved and non-cryopreserved larvae. Note: Dark grey tanks (controls) for chapter 2 were used for chapter 3 for neurogenesis and shell morphology comparisons.

3.4.5 Statistical analyses

Minitab 16 Statistical software was used to analyse experimental results. Significance levels were established at $p < 0.05$ for all statistical tests. Survivability data were analysed by performing an analysis of covariance (ANCOVA) using arcsine transformed data and age as the covariate. Shell length data were analysed through an ANCOVA test and regression analysis. Feeding consumption data contained equal variance (Levene's) and inspection of the probability plot of residuals showed only small departures from linearity. Two-way analysis of variance (ANOVA) within a generalized linear model framework is robust towards such data and was therefore selected as the appropriate model for analysis.

3.5 RESULTS

3.5.1 Survivability

Survivability (%) among controls and frozen D-stage and trochophore treatments over the 21-day rearing period were significantly different (ANCOVA; $F_{2,95} = 31.14$, $p < 0.001$). Average percent survival of control larvae was significantly different to the cryopreserved trochophore and D-stage larvae (Tukey test; $p < 0.001$). However, there was no significant (Tukey test; $p > 0.005$) difference in percent survival between trochophore and D-stage larvae. At day 3, cryopreserved trochophore larvae had slightly higher percent survival

of $89.2 \pm 7.28\%$ compared to controls $83.7 \pm 6.17\%$ and cryopreserved D-stage larvae $78.1 \pm 5.22\%$ (Fig. 3.2). However, by day 7 the percent survival of cryopreserved trochophore and D-stage larvae were lower than those of control larvae, and were highly variable. This declining trend continued with few cryopreserved trochophore ($0.03 \pm 0.03\%$) and D-stage ($0.5 \pm 0.26\%$) larvae successfully making it to 18 days, and none of the larvae achieved settlement at around 21 days (Fig. 3.2). Survival rates of the control larvae at the pediveliger stage (18 days) was high ($23.0 \pm 9.6\%$) and at settlement lower ($9.1 \pm 6.14\%$) (Fig. 3.2).

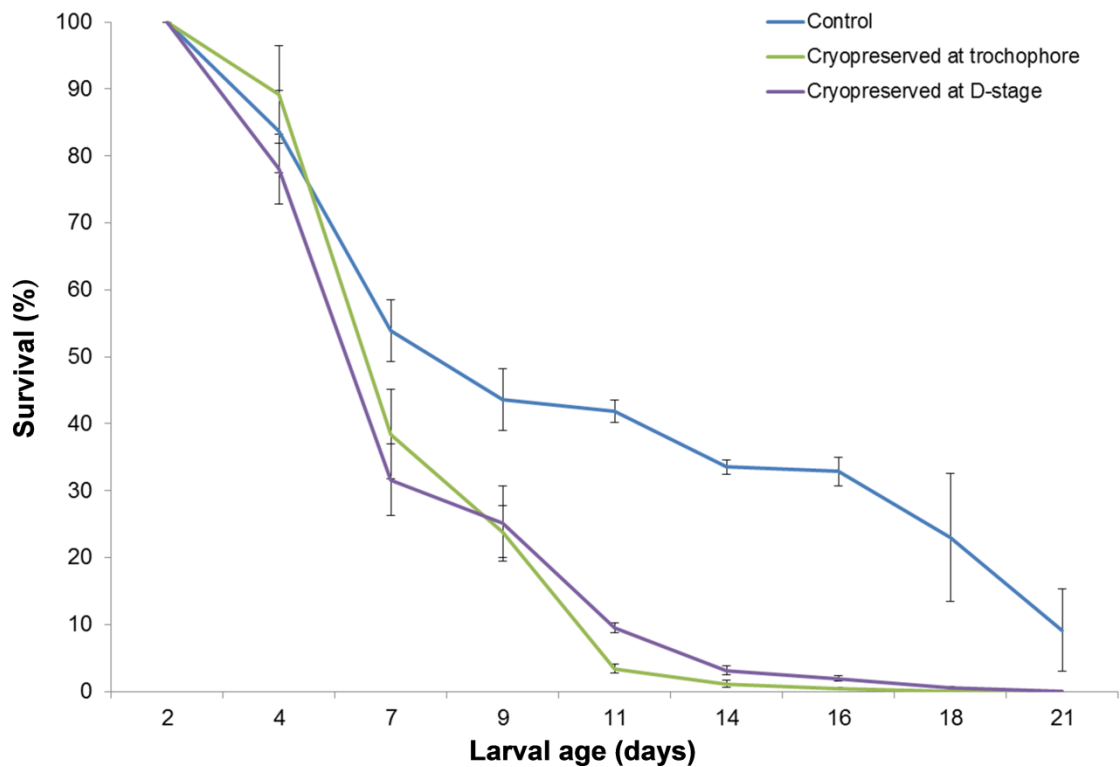


Figure 3.2. Average percent survival (\pm SD) of mussel larvae over the 21-day rearing period.

3.5.2 Shell length

Shell length (μm) measurements among controls and frozen D-stage and trochophore larvae over the 21-day rearing period were significantly different (ANCOVA; $F_{2,132} = 55.19$, $p < 0.001$). Average larval shell lengths in the control were significantly different to frozen trochophore and D-stage larvae ($p < 0.001$). However, frozen trochophore larvae were not significantly different to frozen D-stage larvae ($p > 0.05$). A regression analysis showed that controls had an average daily shell length growth of $7.54 \mu\text{m}$ with a strong relationship between days and shell length ($R^2 = 0.7900$). Trochophore larvae had an average daily shell length growth of $4.10 \mu\text{m}$ with a moderate relationship between shell length and larval age ($R^2 = 0.4100$). However, there was a large variation in shell length between 10 and 12 days due to low survivability. D-stage larvae had an average daily shell length growth of $4.32 \mu\text{m}$ with a good relationship between shell length and larval age ($R^2 = 0.6300$), but also experienced large variations in shell length between days 15 and 19 due to low survivability.

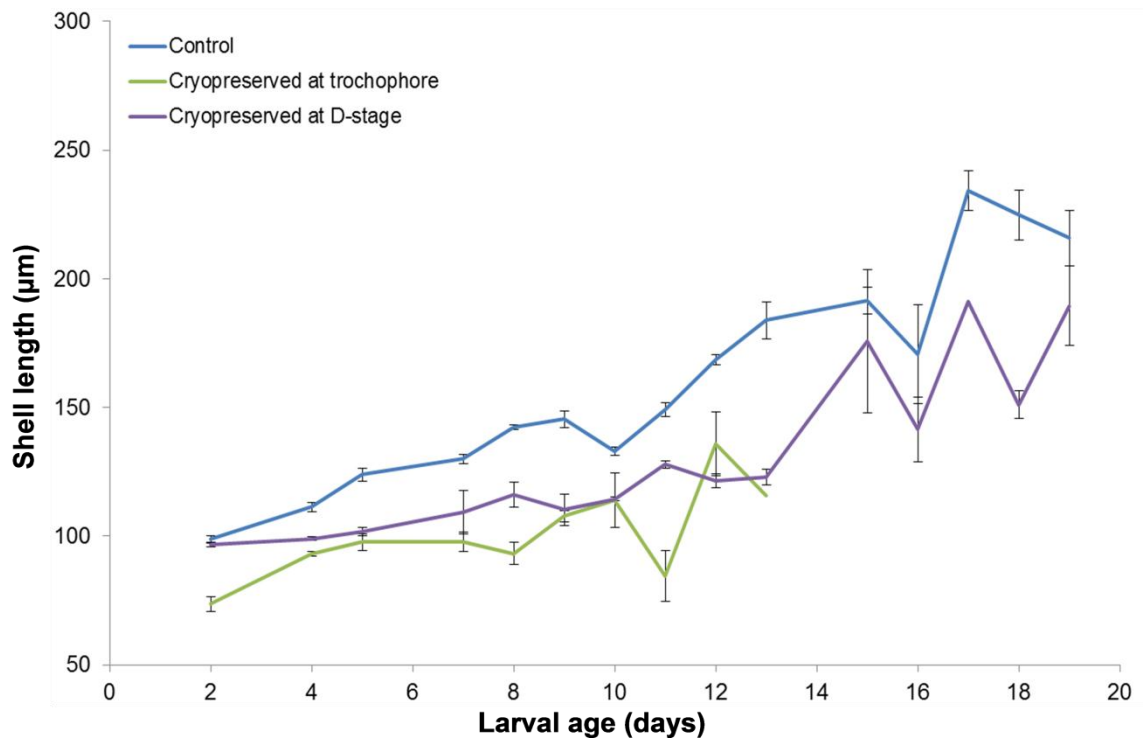


Figure 3.3. Average shell length (\pm SD) of larvae over 19 days. Note- Cryopreserved trochophore larvae had high mortalities at day 13, therefore shell length was not attainable.

3.5.3 Feeding consumption

A two-way ANOVA test revealed significant differences in feeding consumption throughout the larval rearing period (ANOVA; $F_{20,189} = 9.98$, $p < 0.001$), and among treatments (ANOVA; $F_{2,189} = 111.75$, $p < 0.001$). However, no significant differences were observed in the interaction between larval age (days) and the treatments (ANOVA; $F_{40,189} = 1.34$, $p > 0.05$).

Control larvae had an increasing feeding consumption over time with a dramatic increase on Day 6 ($33.5 \pm 2.22\%$) and between days 8 ($16.5 \pm 3.28\%$) and 15 ($50.3 \pm 1.70\%$) before rapidly declining before settlement around 21 days (Fig.

3.4). The feeding consumption of cryopreserved trochophores ($19.0 \pm 1.68\%$) and D-stage larvae ($20.0 \pm 1.73\%$) had a similar pattern, except for the significant increase between days 12 and 16 (Fig. 3.4). Overall, feeding consumption of both cryopreserved D-stage and trochophores for the remainder of the larval rearing period was considerably low ($<16.5\%$) compared to controls which had a high feeding consumption ($<50.25\%$) (Fig. 3.4).

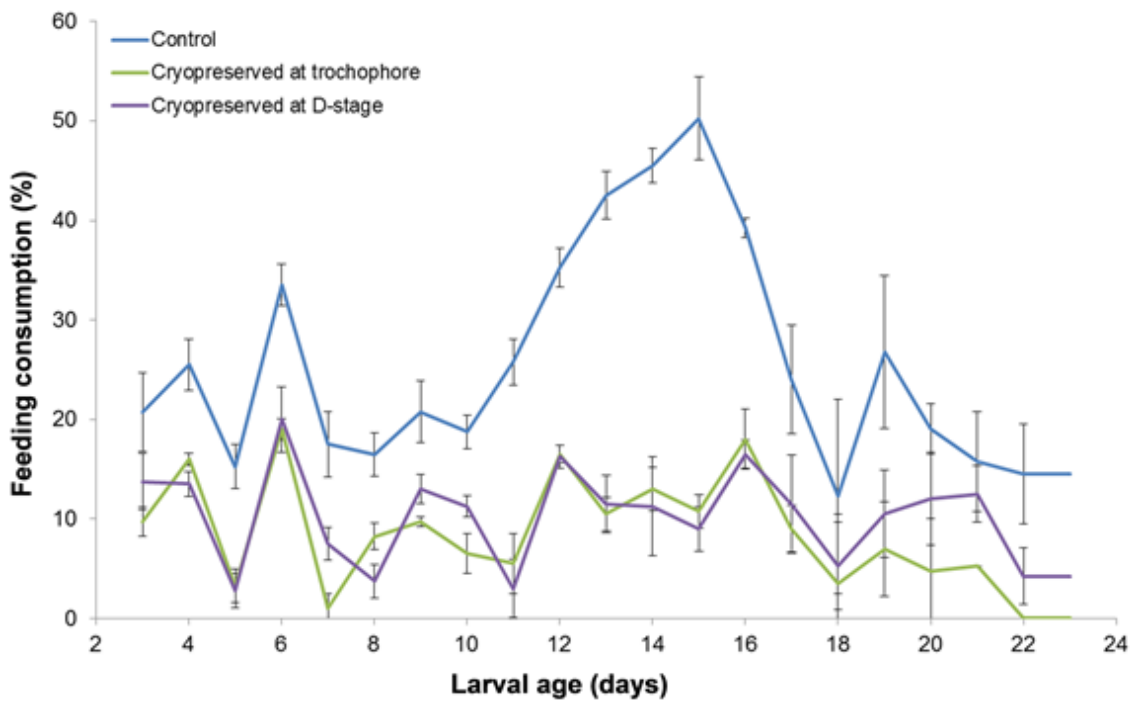


Figure 3.4. Average percent feeding consumption (\pm SD) of larvae over 23 days.

3.5.4 Shell morphology

Control larvae

D-stage larva (2 dpf) obtained from the CUDLRS had an average shell length of $98.92 \pm 1.50 \mu\text{m}$ (n=12 larva) and had a punctate pitted region showing a prodissoconch I (PI) layer with a stellate radial region extending ventrally towards the edge of the mantle (Fig. 3.5-1A). Control larvae (5 dpf) had developed a prodissoconch II (PII) layer with commarginal growth annulations extending from the transition zone of the PI and PII and had an average shell length of $123.85 \pm 1.80 \mu\text{m}$ (n=20 larva) (Fig. 3.5-1B). Non-cryopreserved larvae (11 days old) with a shell length of $149.31 \pm 2.41 \mu\text{m}$ (n=5 larva) had developed an umbonate shell appearance with a rounded umbo and further secretion of the PII layer (Fig. 3.5-1C). At 14 days old, larvae had developed a well-rounded umbo shell with further shell secretion within the PII zone (Fig. 3.5-1D). At 16 days old, larvae had developed a very umbonate shell appearance with a distinct rounded umbo and an average shell length of $170.72 \pm 41.20 \mu\text{m}$ (n=10 larva) (Fig. 3.5-1E).

Cryopreserved at D-stage

Larva cryopreserved at the D-stage (2 days old) had an average shell length of $96.63 \pm 1.54 \mu\text{m}$ (n=12 larva) and showed a punctate pitted region and a PI layer with a stellate radial region extending ventrally towards the mantle edge (Fig. 3.5-2A). Larvae at 5 days old had progressed and developed a PII layer

with typical shell growth annulations extending ventrally from the transition zone. The transition zone showed a distinct abnormal depression (Fig. 3.5-2B). The average shell length for these individuals was $101.61 \pm 3.30 \mu\text{m}$ (n=20 larva). At 8 days old, larvae showed a slow continuing shell length growth with an average shell length of $109.29 \pm 16.82 \mu\text{m}$ (n=18 larva), and some abnormalities to the PII layer (Fig. 3.10). At 11 days old, larva had an average shell length of $127.90 \pm 1.96 \mu\text{m}$ (n=3 larva) and had secreted more shell growth in the PII layer with a clear abnormal depression at the transition zone of the PI & PII layer. At 14 days old, the larvae had developed an umbo and further shell secretion in the PII region (Fig. 3.5-2D). Larvae at 15 days old showed some continuing abnormalities to the mantles edge (Fig. 3.11, 3.12). At 16 days old, larvae had developed an umbonate shell appearance with further shell secretion in the PII region and an average shell length of $141.50 \pm 25 \mu\text{m}$ (n=7 larva).

Cryopreserved at trochophore stage

Larvae cryopreserved at the trochophore stage had developed a D-shell (2 days old) with an average shell length of $73.60 \pm 5.55 \mu\text{m}$ (n=11 larva). The shell morphology of these individuals had a common punctate pitted region and a stellate radial region extending towards the mantle. There were abnormalities to the shell extending from the punctate pitted region ventrally towards the mantle edge (Fig. 3.5-3A). Cryopreserved trochophore larvae (5 days old) with

an average shell length of $97.68 \pm 6.57 \mu\text{m}$ had secreted a PII layer with commarginal growth annulations extending ventrally. Abnormalities were apparent at the hinge (Fig. 3.5-3B) and at the edge of the mantle for both the right and left valve (Fig. 3.6). At 7 days, the larvae had uneven abnormalities to the hinge area with wrinkling like appearances to the PI & PII layer and a wide depression in the transition zone (Fig. 3.7 & 3.8). At 11 days old with an average shell length of $84.51 \pm 19.94 \mu\text{m}$ (n=2 larva), larvae had secreted more shell growth in the PII region with abnormal growth annulations and apparent unsymmetrical valves (Fig. 3.5-3C & 3.9). At 14 days old, the larvae had secreted further shell in the PII region with apparent abnormalities still present around the transition zone of the PI & PII (Fig. 3.5-3D).

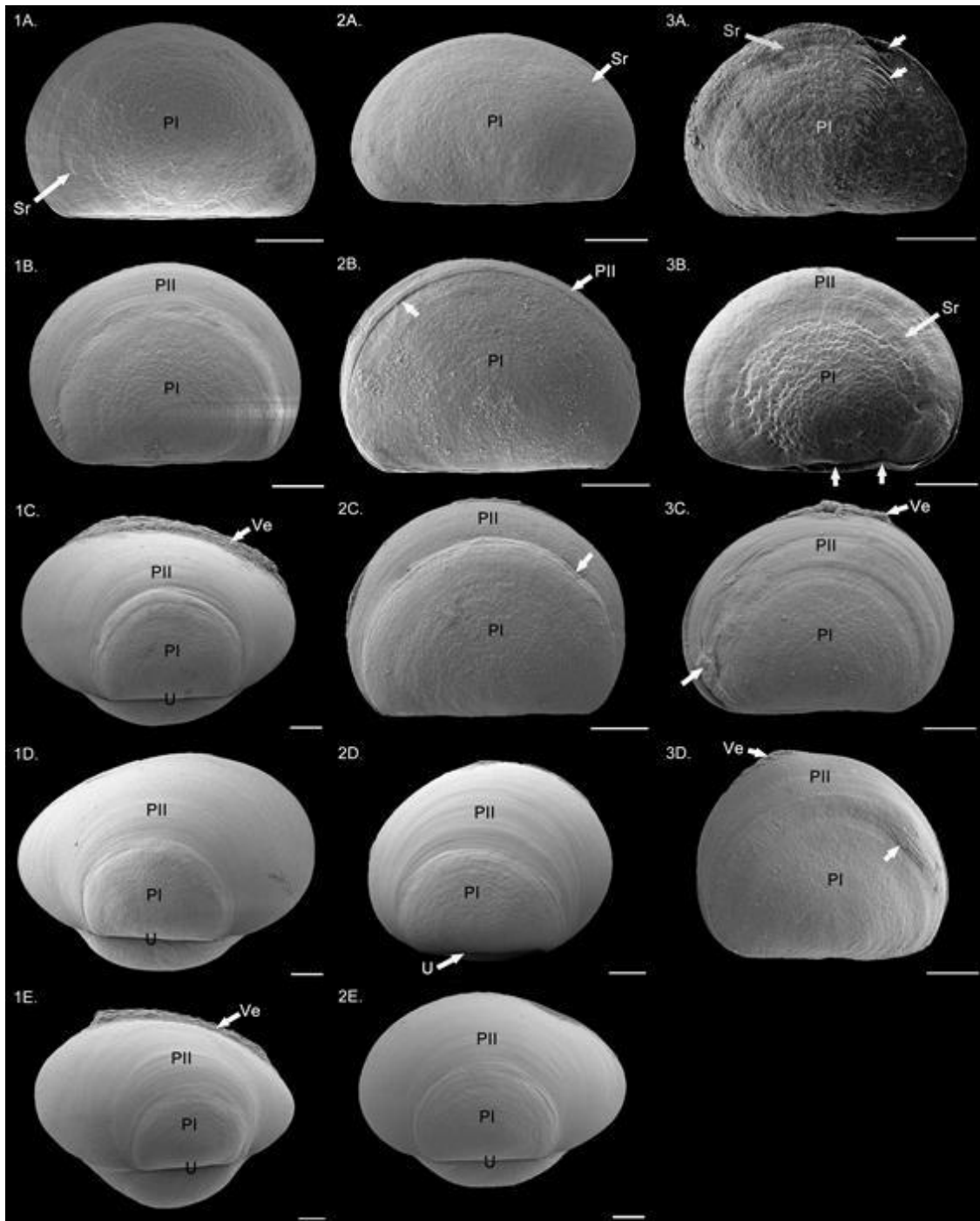


Figure 3.5. 1A-3D. *Perna canaliculus*. SEM images of D-stage to umbonate larvae. Control = 1A–1E; cryopreserved at D-stage larvae = 2A–2E; & cryopreserved at trochophore larvae = 3A–3E. A = 2 days old, B = 5 days old, C = 11 days old, D = 14 days old, E = 16 days old. Abbreviations: PI, prodissoconch I; PII, prodissoconch II; Sr, stellate-radial region; U, umbo; Ve, velum. White unlabelled arrows = abnormalities. Scale bars = 20 μ m.

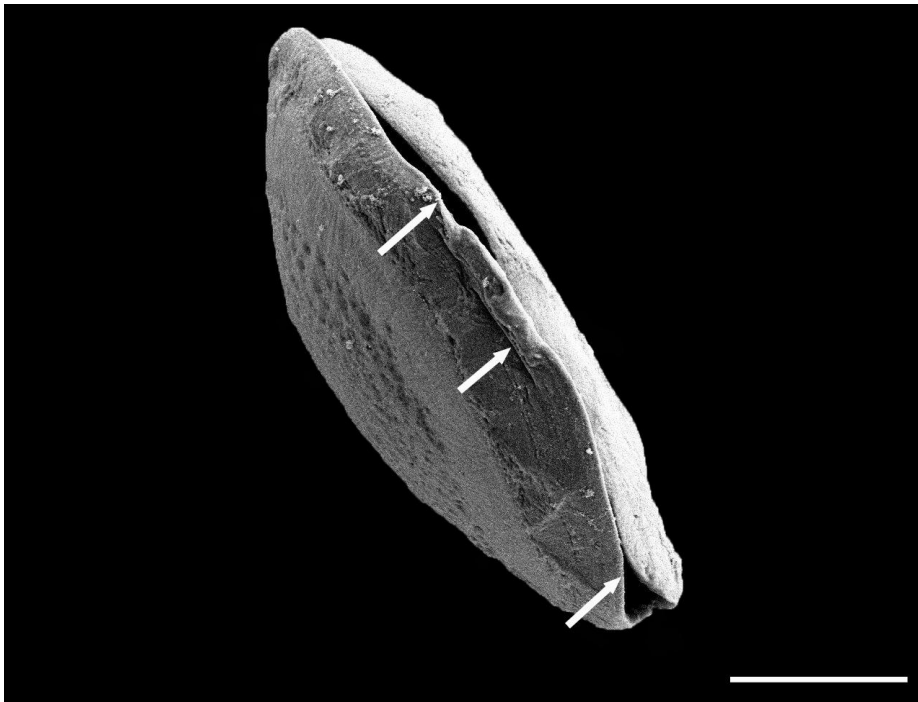


Figure 3.6. Larva (5 days post-fertilisation) cryopreserved at trochophore stage. White unlabelled arrows = abnormalities to shell. Scale bar = 20 μ m.

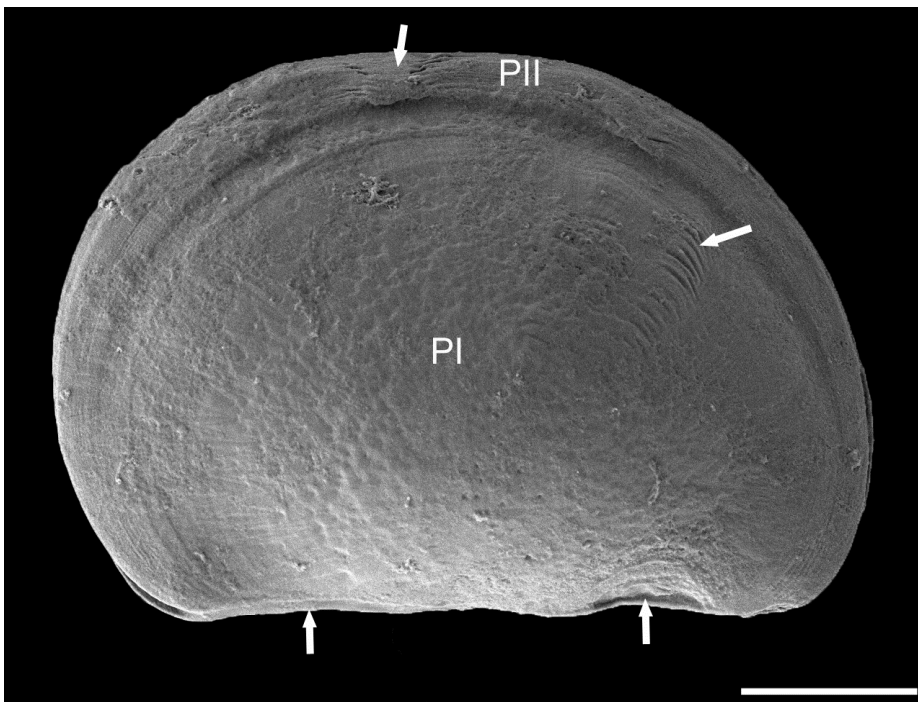


Figure 3.7. Larva (7 days post-fertilisation) cryopreserved at trochophore stage. Abbreviations: PI, prodissoconch I; PII, prodissoconch II. White unlabelled arrows = abnormalities in the hinge. Scale bar = 20 μ m.

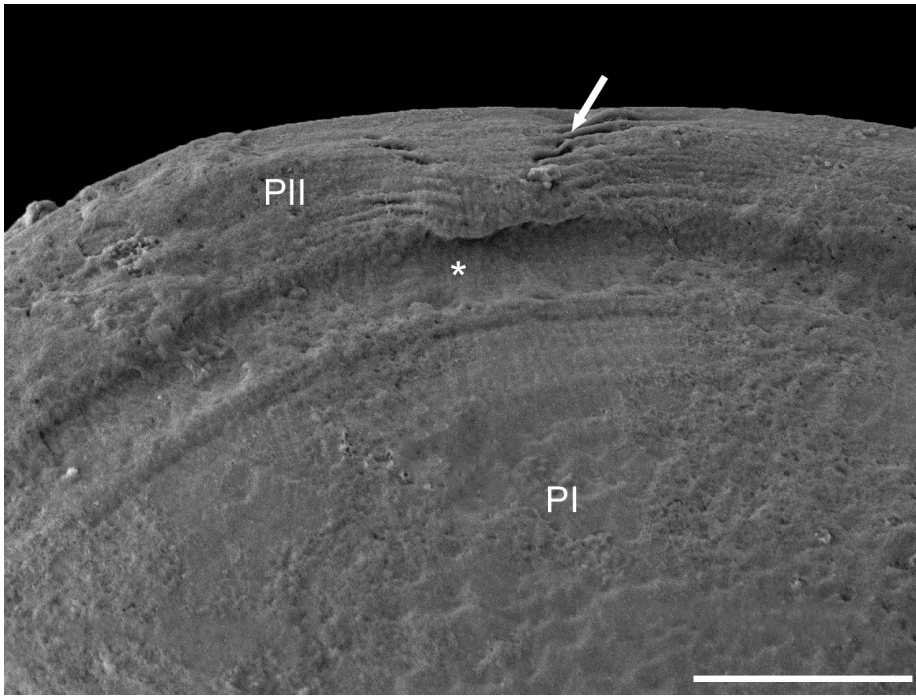


Figure 3.8. Larva (7 days post-fertilisation) cryopreserved at trochophore stage. Abbreviations: PI, prodorsoconch I; PII, prodorsoconch II; * = transition zone. White unlabelled arrows = abnormalities. Scale bar = 10 μ m.

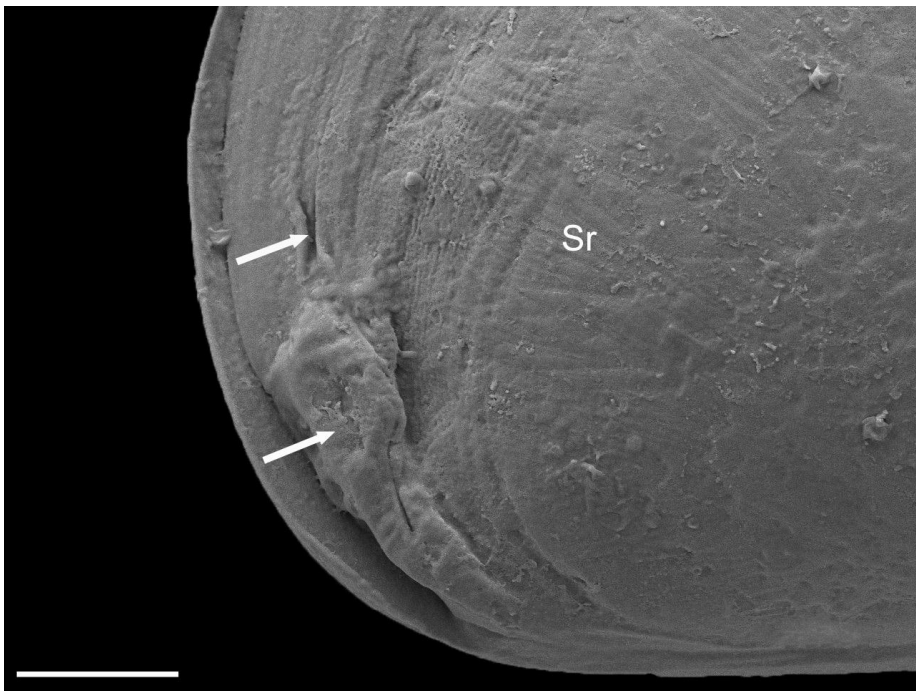


Figure 3.9. Larva (11 days post-fertilisation) cryopreserved at trochophore stage. Abbreviations: Sr, stellate-radial region. White unlabelled arrows = abnormalities. Scale bar = 10 μ m.

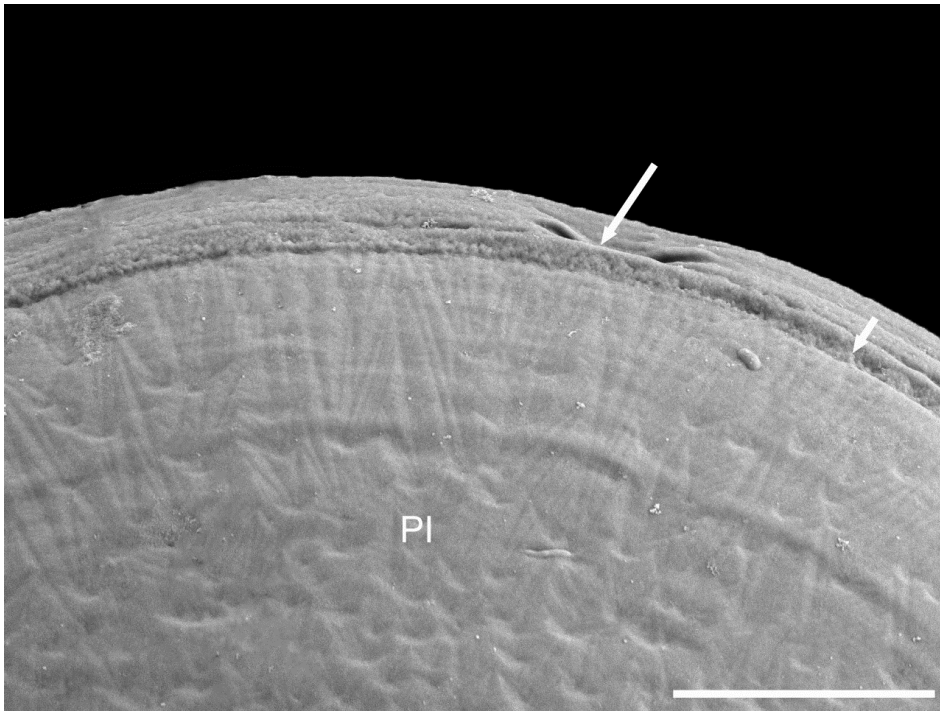


Figure 3.10. Larva (8 days post-fertilisation) cryopreserved at D-stage. Abbreviations: PI, prodissoconch I. White unlabelled arrows = abnormalities. Scale bar = 10 μ m.

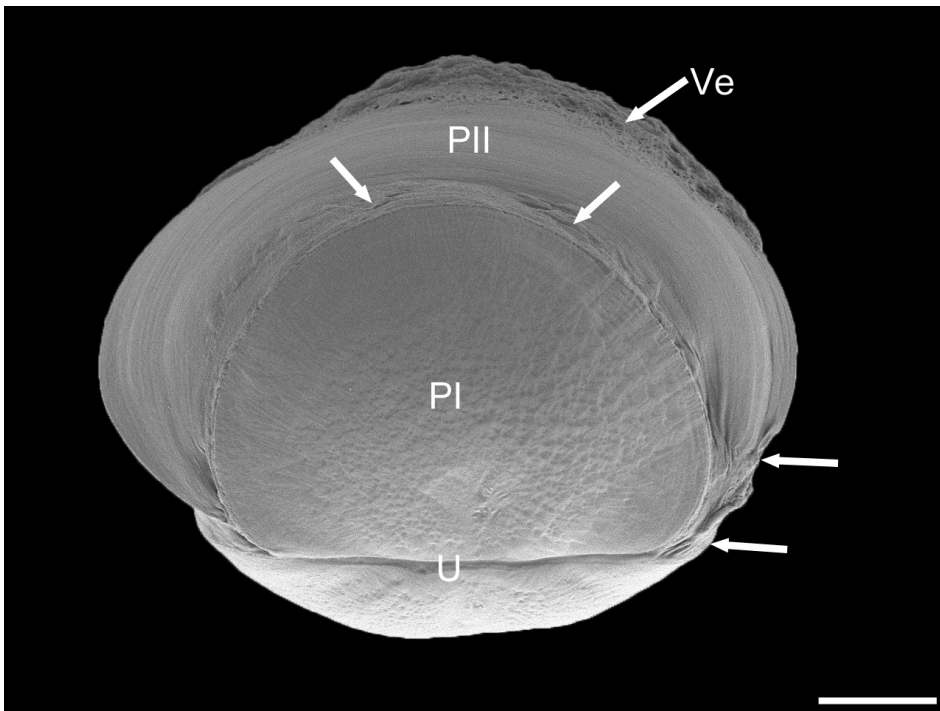


Figure 3.11. Larva (15 days post-fertilisation) cryopreserved at D-stage. Abbreviations: PI, prodissoconch I; PII, prodissoconch II, U, umbo; Ve, velum. White unlabelled arrows = abnormalities. Scale bar = 20 μ m.

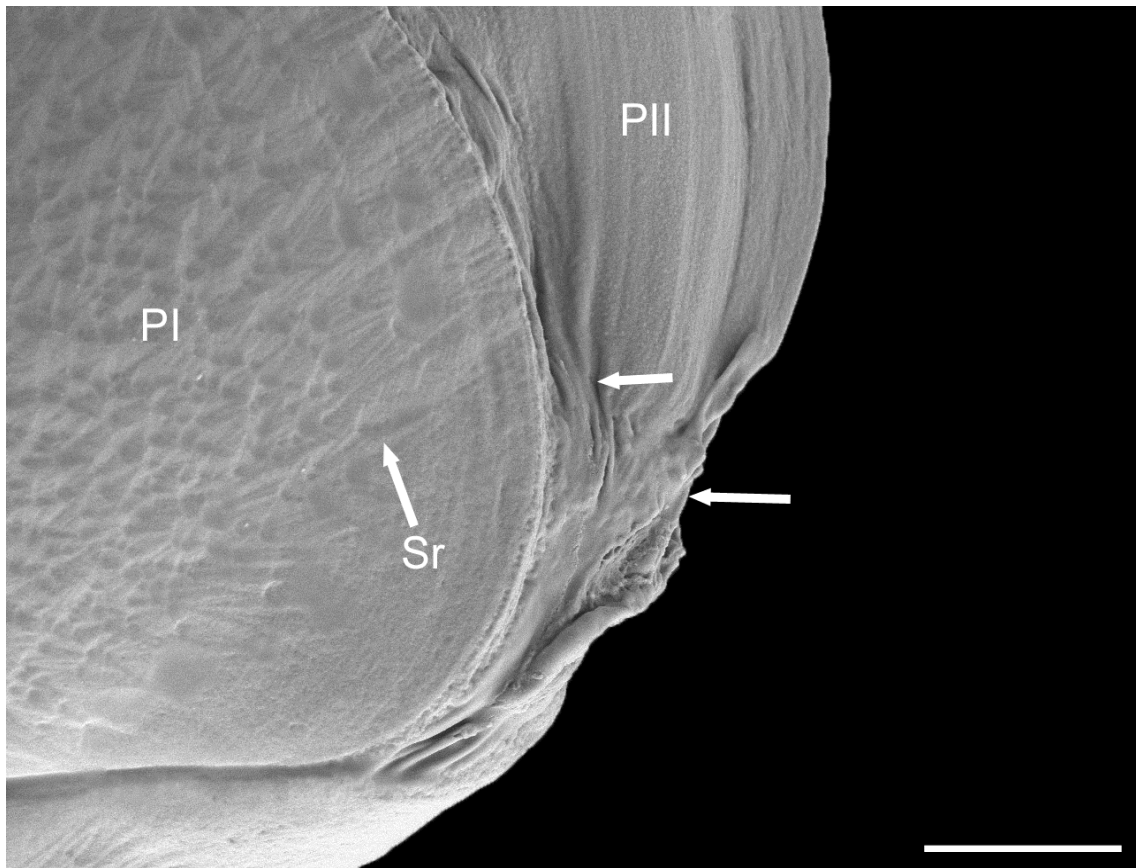


Figure 3.12. Larva (15 days post-fertilisation) cryopreserved at D-stage. Abbreviations: PI, prodossoconch I; PII, prodossoconch II, Sr, stellate-radial region. White unlabelled arrows = abnormalities. Scale bar = 10 μ m.

Table 2. Different larval stages of cryopreserved and controls of *Perna canaliculus* in days (d).

Time post-fertilisation	Control	Cryo D-stage	Cryo Trochophore
2 d	D-shaped	D-shaped	D-shaped
7 d	Early umbo	D-shaped	D-shaped
11 d	Late umbo	Early umbo	D-shaped
16 d	Umbonate	Late umbo	Early umbo
18 d	Pediveliger		
21 d	Post-larva		

3.5.5 Organogenesis

Control larvae

Histological sections and light microscopy showed larvae at the D-stage had gone through limited organogenesis. At 2 days old, the D-stage larvae had undistinguishable features apart from the cilia, and microalgal material was apparent in the digestive diverticulum or stomach (Fig. 3.13-1A; Table 2). A frontal section of a larva from a histological section revealed an apical ganglion lying dorsal of the velum and a stomach present at 3 days old (Fig. 3.14). A sagittal section showed larvae had developed an anterior adductor muscle, and a well-developed alimentary system composing of a large stomach, with an intestine lying dorsal of the stomach (Fig. 3.15). At 4 days old, the larvae had a small accumulation of algae in the stomach indicated by the presence of a brown pigmentation (3.13-1B). There was evidence of further accumulation of algae and an extended velum at 5 days old (3.13-1C). Larvae then progressed in organogenesis with the appearance of an esophagus and velum retractor muscles connected to the velum and extending dorsally towards the stomach. These were characteristics of an early umbo larva at 7 days old (Fig. 3.16; Table 2). At 11 days (late umbo stage) larvae had a well-developed digestive diverticulum and style sac surrounding the inner lining of the stomach (Fig. 3.17; Table 2). Further organogenesis (day 12) in the late umbo stage had developed a pronounced umbo with a large digestive diverticulum and stomach containing large quantities of consumed algae (Fig. 3.13-1D; Table 2). Finally at day 15, the larva were deemed to be in the late umbo to umbonate stage with

the presence of a foot, pedal ganglion which lies dorsal of the foot, and a visceral ganglion lying dorsal of the anterior adductor muscle (Fig. 3.18; & Table 2). Large quantities of algae were still present in the digestive diverticulum and stomach (Fig. 3.13-1E). At 20 days, larva had successfully metamorphosed and developed well-defined structures associated with the pediveliger stage, such as the anterior and posterior adductor muscles, the visceral ganglia, an enlarged digestive diverticulum, and a gill rudiment (Fig. 3.19, 3.20; & Table 2). Visual observations showed eye spots in most individual larvae.

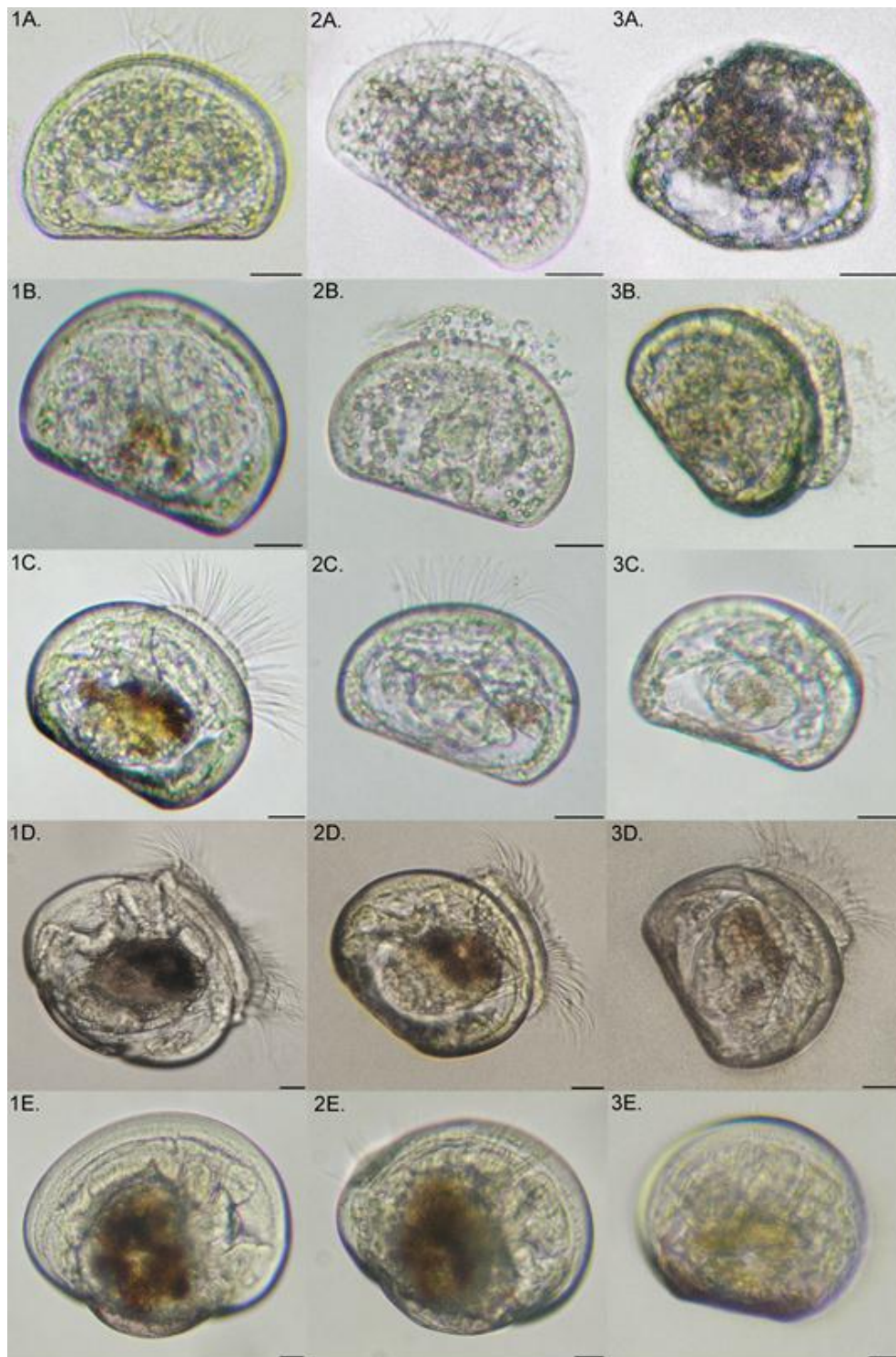


Figure 3.13. 1A-3E. *Perna canaliculus*. Light images of D-stage to late umbo-stage larvae showing overall organogenesis and microalgae (brown pigmentation) content in stomach. Control = 1A-1E, cryopreserved at D-stage larvae = 2A-2E, & cryopreserved at trochophore larvae = 3A-3E. A = 2 days old, B = 4 days old, C = 5 days old, D = 12 days old, E = 15 days old. Scale bars = 20 μ m.

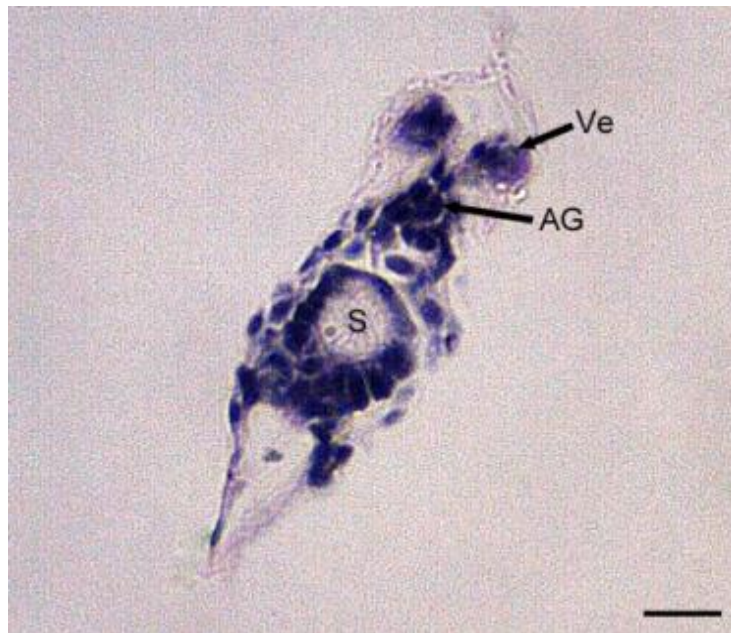


Figure 3.14. Frontal section of unfrozen D-stage larva (3 days post-fertilisation). Abbreviations: AG, apical ganglion; S, stomach; Ve, velum. Scale bar = 20 μ m.

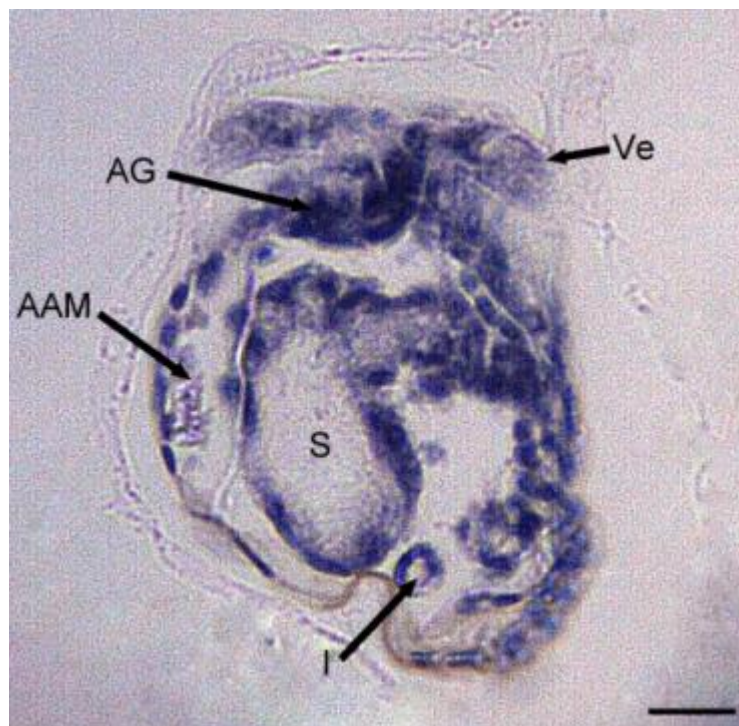


Figure 3.15. Sagittal section of unfrozen D-stage larva (3 days post-fertilisation). Abbreviations: AAM, anterior-adductor muscle; AG, apical ganglion; I, intestine; S, stomach; Ve, velum. Scale bar = 20 μ m.

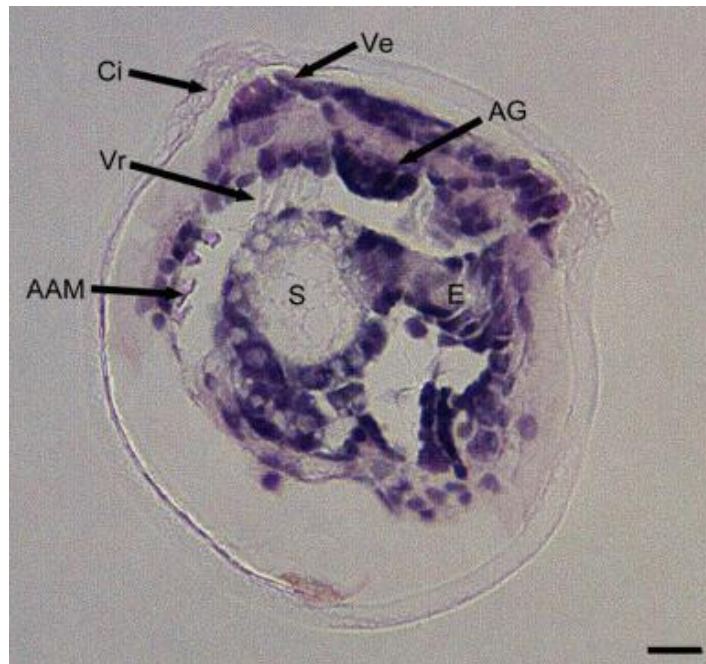


Figure 3.16. Sagittal section of unfrozen early-umbo larva (7 days post-fertilisation).
 Abbreviations: AAM, anterior-adductor muscle; AG, apical ganglion; Ci, cilia; E, esophagus; S, stomach; Ve, velum, Vr, velum retractor muscle. Scale bar = 20 μ m.

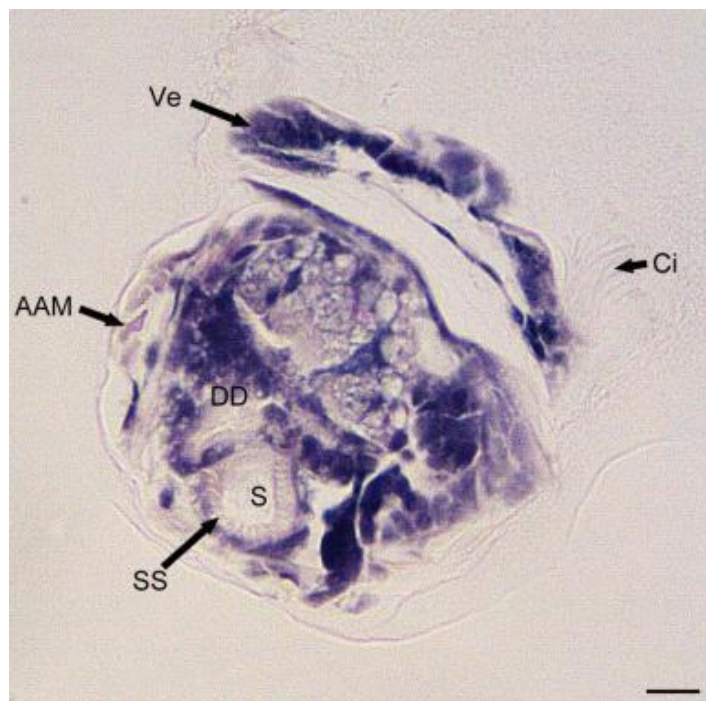


Figure 3.17. Sagittal section of unfrozen late-umbo larva (11 days post-fertilisation).
 Abbreviations: AAM, anterior-adductor muscle; Ci, cilia; DD, digestive diverticulum; S, stomach; SS, style sac, Ve, velum. Scale bar = 20 μ m.

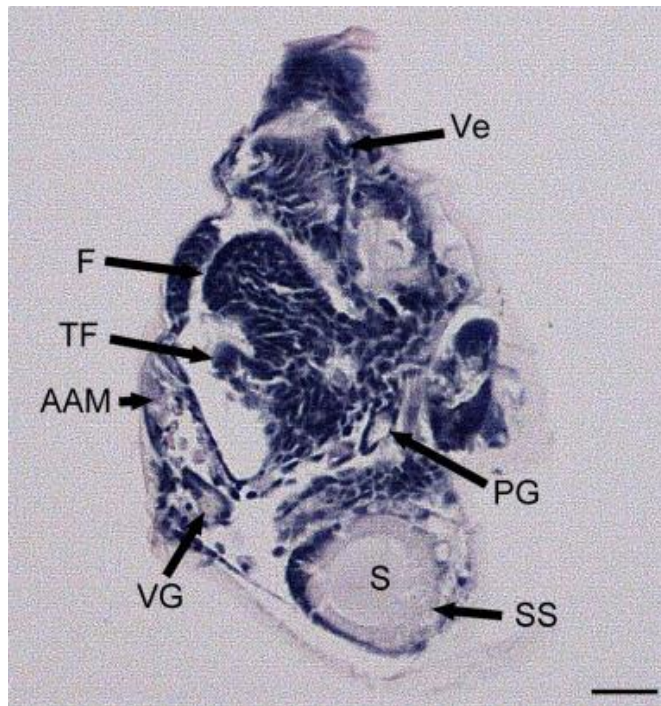


Figure 3.18. Frontal section of unfrozen late-umbo larva (15 days post-fertilisation). Abbreviations: AAM, anterior adductor muscle; F, foot; PG, pedal ganglion; S, stomach; SS, style sac; TF, toe of foot; Ve, velum, VG, visceral ganglion. Scale bar = 20 μ m.

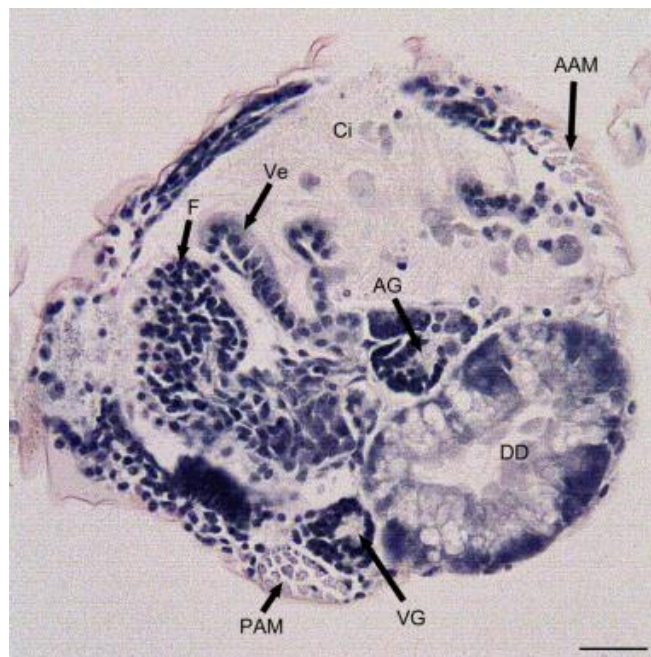


Figure 3.19. Sagittal section of unfrozen pediveliger (20 days post-fertilisation). Abbreviations: AAM, anterior adductor muscle; AG, apical ganglion; Ci, cilia; DD, digestive diverticulum; F, foot; PAM, posterior adductor muscle; Ve, velum, VG, visceral ganglion. Scale bar = 20 μ m.

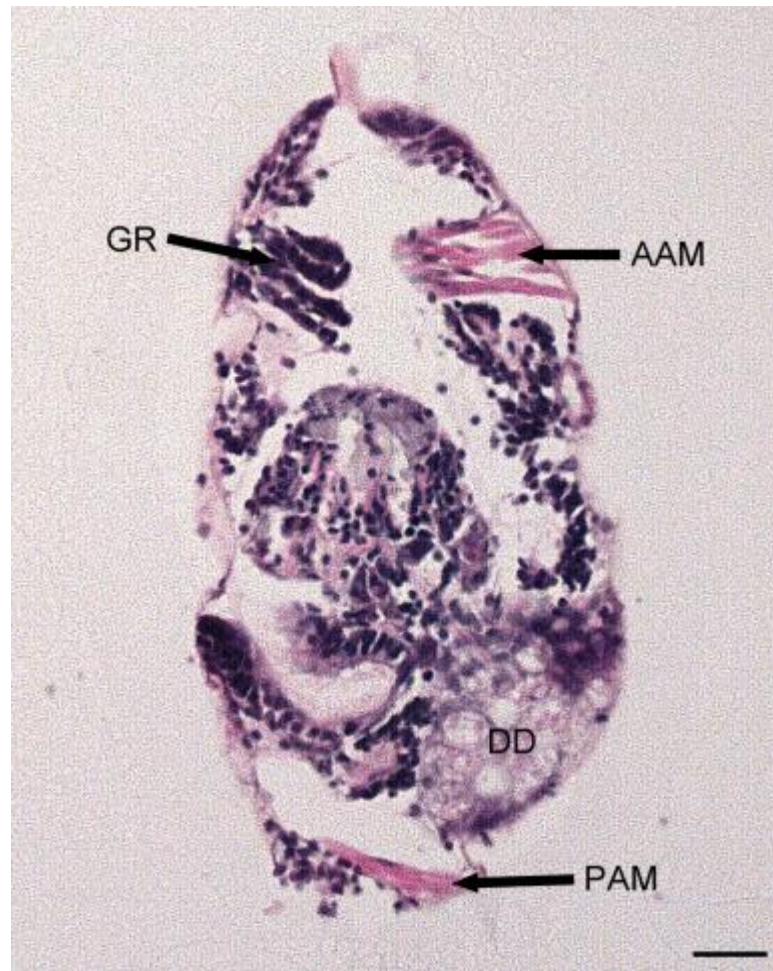


Figure 3.20. Frontal section of unfrozen pediveliger (20 days post-fertilisation). Abbreviations: AAM, anterior adductor muscle; DD, digestive diverticulum; GR, gill rudiment; PAM, posterior adductor muscle. Scale bar = 20 μ m.

Cryopreserved at trochophore

Microscopic observations of cryopreserved trochophore larvae revealed limited organogenesis with some abnormalities to shell morphology and internal organs at 2 days old (Fig. 3.13-3A). At day 3, velum retractor muscles were observed extending towards the projected velum, along with an esophagus, and digestive diverticulum through histological sections (Fig. 3.21 & 3.22). By day 4, organs were still unrecognisable through light microscopy with only an extended velum

being observed, and little algae within the larvae (3.13-1B). Larvae at 5 days old revealed a circular stomach containing little algae (3.13-1C). However, by day 12, a small accumulation of algae in the stomach was clearly visible with a velum and beating cilia (3.13-1D). At day 13, the larvae had not progressed and were still at D-stage with only some enlargement to overall organs and the appearance of a style sac lining the stomach interior (Fig. 3.23). Larvae from this period onwards experienced low survivability and histological sectioning was not viable given the low numbers. At around day 15 and 16, light microscopy showed the larvae had developed to the early umbo stage with little algae accumulation in the stomach (Fig. 3.13-3E).

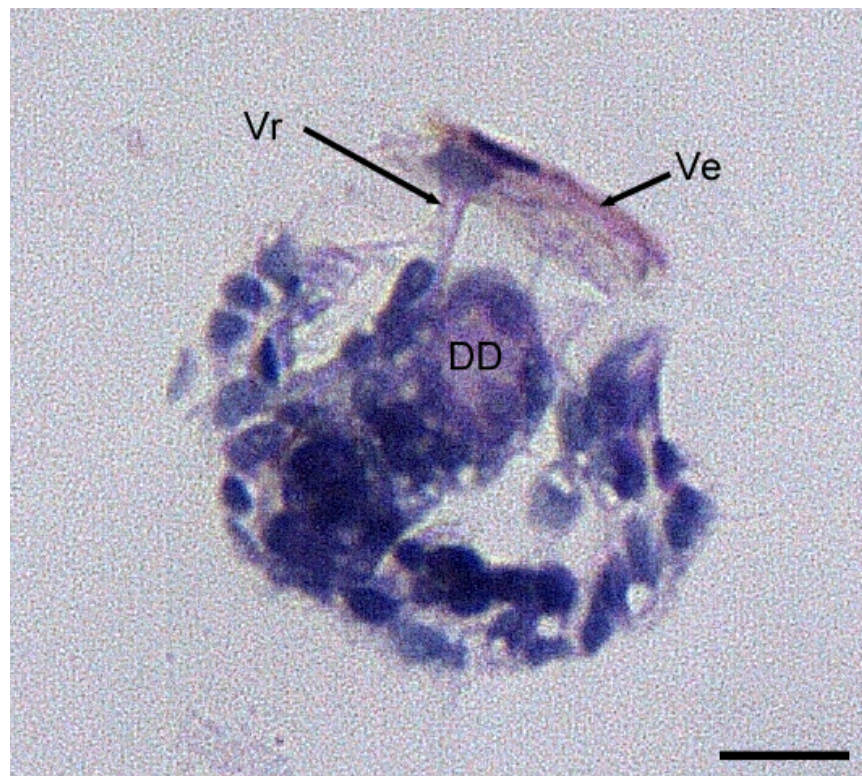


Figure 3.21. Sagittal section of D-stage larva (3 days post-fertilisation) cryopreserved at trochophore. Abbreviations: DD, digestive diverticulum; Ve, velum; Vr, velum retractor muscle. Scale bar = 20 μ m.

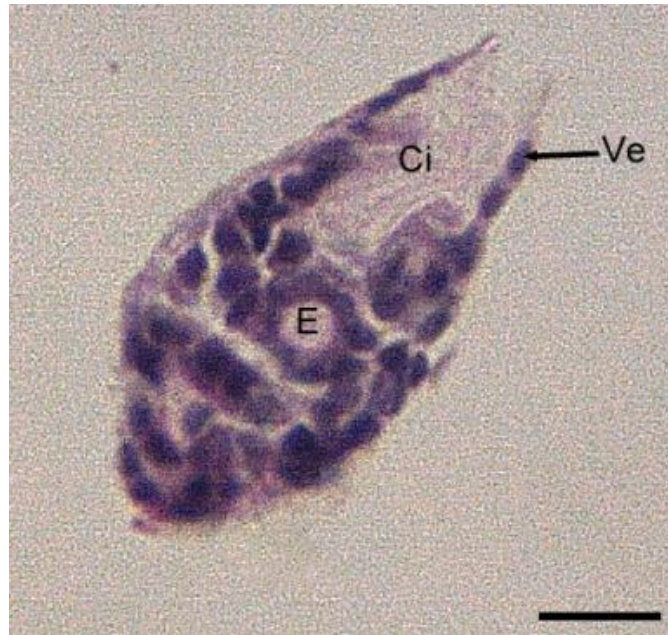


Figure 3.22. Frontal section of D-stage larva (3 days post-fertilisation) cryopreserved at trochophore. Abbreviations: E, esophagus; Ci, cilia; Ve, velum. Scale bar = 20 μ m.



Figure 3.23. Frontal section of late-umbo larva (13 days post-fertilisation) cryopreserved at trochophore. Abbreviations: S, stomach; SS, style sac; Ve, velum. Scale bar = 20 μ m.

Cryopreserved at D-stage

At day 2, cryopreserved D-stage larvae had a stomach and esophagus travelling dorsally from the ventral valves (Fig. 3.24), and showed limited organogenesis. The stomach of the larvae at day 4 appeared empty with no algae (Fig. 3.13-2B). However, at day 5 larvae showed the first accumulation of algae in the stomach (Fig. 3.13-2C). Larvae that progressed onwards had a well-developed velum, an enlarged stomach, and also the appearance of an anterior adductor muscle at 11 days old (Fig. 3.25). At day 12, larvae were classed as early umbo stage and by this time an umbo had developed, and a good accumulation of algae in the stomach and an extended velum were observed (Fig. 3.13-2D). Progressing further in the late umbo stage (15 days), a progression in organogenesis had occurred with the presence of a developing foot, and enlarged stomach with a style sac lining the interior circumference. An apical ganglion was observed lying dorsal of the velum and a pedal ganglion dorsal of the foot. Dorsal from the pedal ganglion is the intestine depicted by the circular impressions which are thought to be the overlapping portions of the intestinal tract (Fig. 3.26). A large quantity of algae was visible in the stomach (Fig. 3.13-2E). Histological sectioning from this time period onwards was not achievable due to low survivorship.

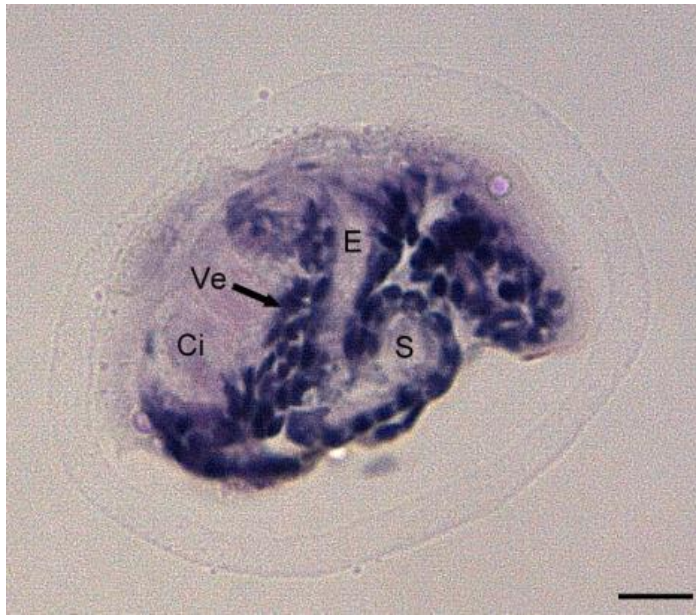


Figure 3.24. Sagittal section of D-stage larva (3 days post-fertilisation) cryopreserved at D-stage. Abbreviations: E, esophagus; Ci, cilia; S, stomach; Ve, velum. Scale bar = 20 μ m.

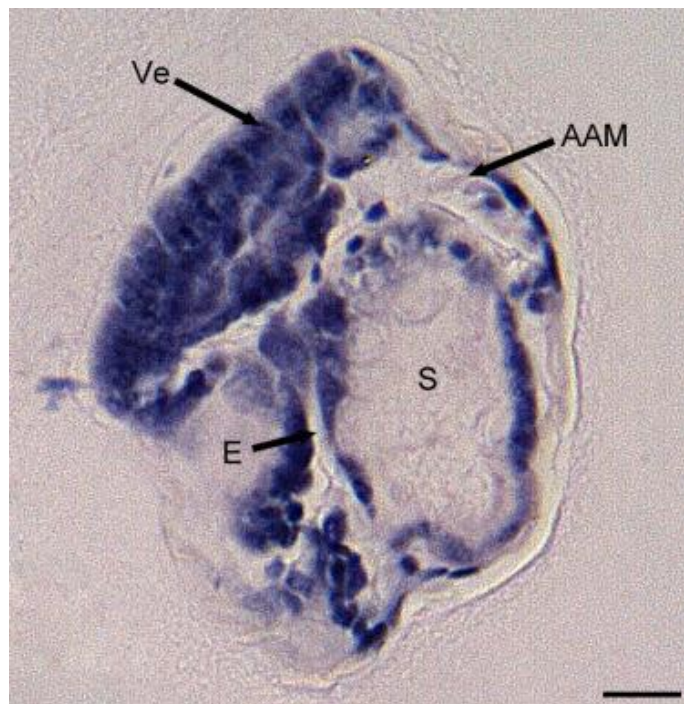


Figure 3.25. Sagittal section of late-umbo larva (11 days post-fertilisation) cryopreserved at D-stage. Abbreviations: AAM, anterior adductor muscle; E, esophagus; S, stomach; Ve, velum. Scale bar = 20 μ m.

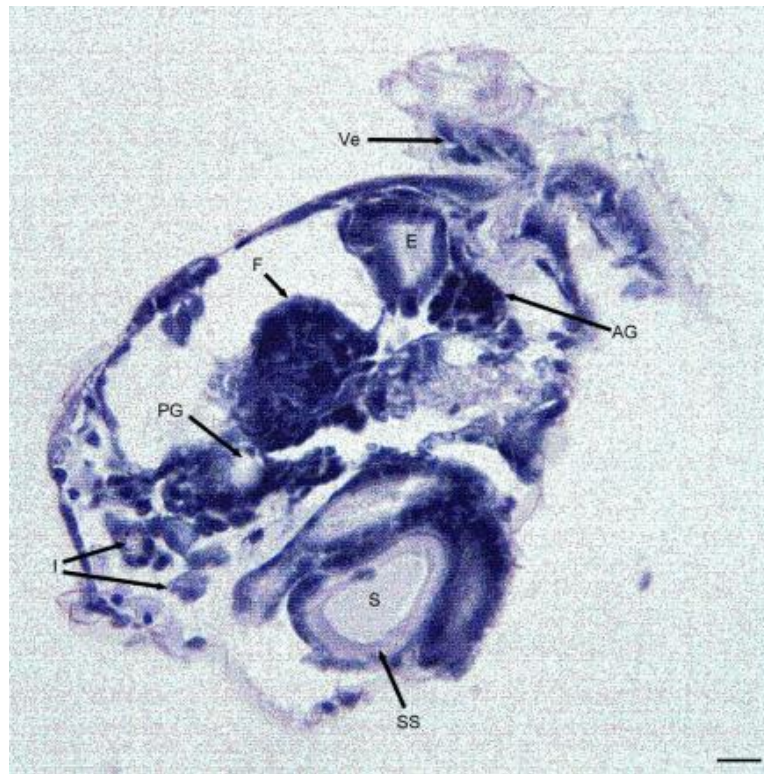


Figure 3.26. Transverse section of late-umbo larva (15 days post-fertilisation) cryopreserved at D-stage. Abbreviations: AG, apical ganglion; E, esophagus; F, foot; I, intestine; PG, pedal ganglion; S, stomach; SS, style sac; Ve, velum. Scale bar = 20 μ m.

3.5.6 Neurogenesis

Control larvae

Results from FMRamide-like (Phe-Met-Arg-Phe) immunoreactive staining for neuropeptides were used to observe neurogenesis on larvae from controls. These results were used to describe 'normal' development of mussel larvae (Chapter 2) and to compare with frozen larvae. Histological sections highlighting ganglia were used from controls within this chapter. The following

summary with illustrated images was used as a reference to compare neurogenic development between trochophore and D-stage frozen treatments.

An early D-stage (2 dpf) larva had few FMRFamide-like immunoreactive cells present, and location of these sites suggested it to be the apical or cerebral ganglion (Fig. 3.27). Histological sections at days 3 and 7 show the presence of an apical ganglion. Larvae at the D-stage (5 dpf) showed the beginning of a peripheral system with thin fibres running from the anterior-adductor muscle through to the cerebral ganglion. However, the mantle nerve was brightly stained and the stomach consisted of two unknown immunoreactive sites (Fig. 3.28). Early umbo larvae (10 dpf) had developed a complete nervous system with weak peripheral innervations running throughout the larvae (Fig. 3.29). A mantle nerve completely encompassing the mantle region was observed. Dorsal to the velum, the ventral osphradial nerve runs dorsally from the cerebral ganglion and connects to the fibre that runs from the anterior adductor muscle to the pedal ganglion. The plero-visceral connective projects onto the pedal ganglion and travelling posteriorly separates into two connective fibres that connect to the visceral ganglion. There appeared to be two weakly stained connectives running from the pedal ganglion to the visceral ganglion. Larvae at the late umbo stage (14 dpf) show innervations running throughout the anterior adductor muscle, which join to a single fibre which runs posterior to the pedal ganglion (Fig. 3.30). No fibres within the anterior adductor muscle were observed extending to the ventral osphradial nerve. The ventral osphradial nerve progressed anterior of the anterior adductor muscle and travelled dorsally

terminating before the umbo. The pedal ganglion itself composes of two heavily immunoreactive sites, and this suggests the pedal ganglion is composed of two neuronal sites with interconnecting fibres (Fig. 3.30). The intestine had some weak innervations running along the intestinal tract. Larvae at 15 dpf had a visceral and pedal ganglion (Fig. 2.26). By 18 dpf, larvae had progressed to the pediveliger stage and had developed a functional foot with cerebral ganglion appearing more intensely stained, indicating further neurogenic development (Fig. 3.31). The anterior adductor muscle is highly innervated with a series of network fibres extending throughout the muscle and interconnecting with several neuronal sites. At this stage, the ventral osphradial nerve connects to the mantle nerve anterior to the anterior adductor muscle. The posterior adductor muscle also is innervated with fibres that extend posteriorly to two unknown neurons that are connected to the mantle nerve that encompasses the entire mantle region. At 20 dpf, larvae at the settlement stage had a large visceral ganglion lying ventral and adjacent to the posterior-adductor muscle as seen in a sagittal section (Fig. 3.19).

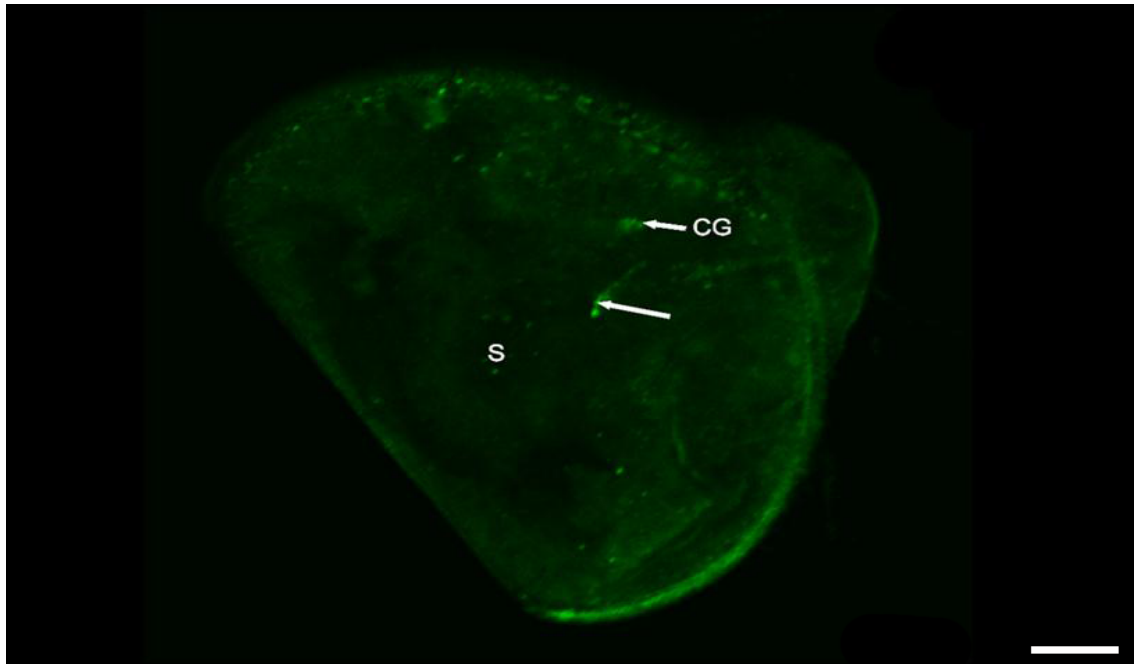


Figure 3.27. FMRFamide-like green immunoreactivity in day 2 control larva ($29 \times 0.97\mu\text{m}$). Abbreviations: CG, cerebral ganglion; S, stomach. White arrow = unknown immunoreactive site. Scale bar = $20\mu\text{m}$.

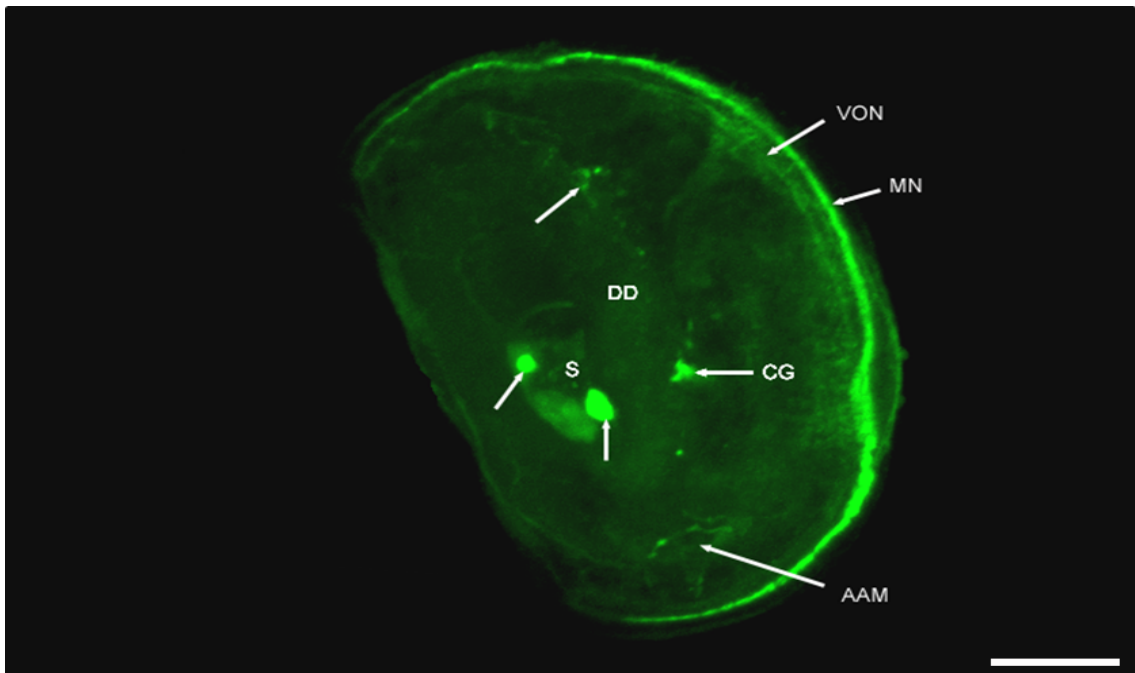


Figure 3.28. FMRFamide-like green immunoreactivity in day 5 control larva ($12 \times 0.97\mu\text{m}$). Abbreviations: AAM, anterior adductor muscle; CG, cerebral ganglion; DD, digestive diverticulum; MN, mantle nerve; S, stomach; VON, ventral osphradial nerve. White unlabelled arrow = unknown immunoreactive site. Scale bar = $20\mu\text{m}$.

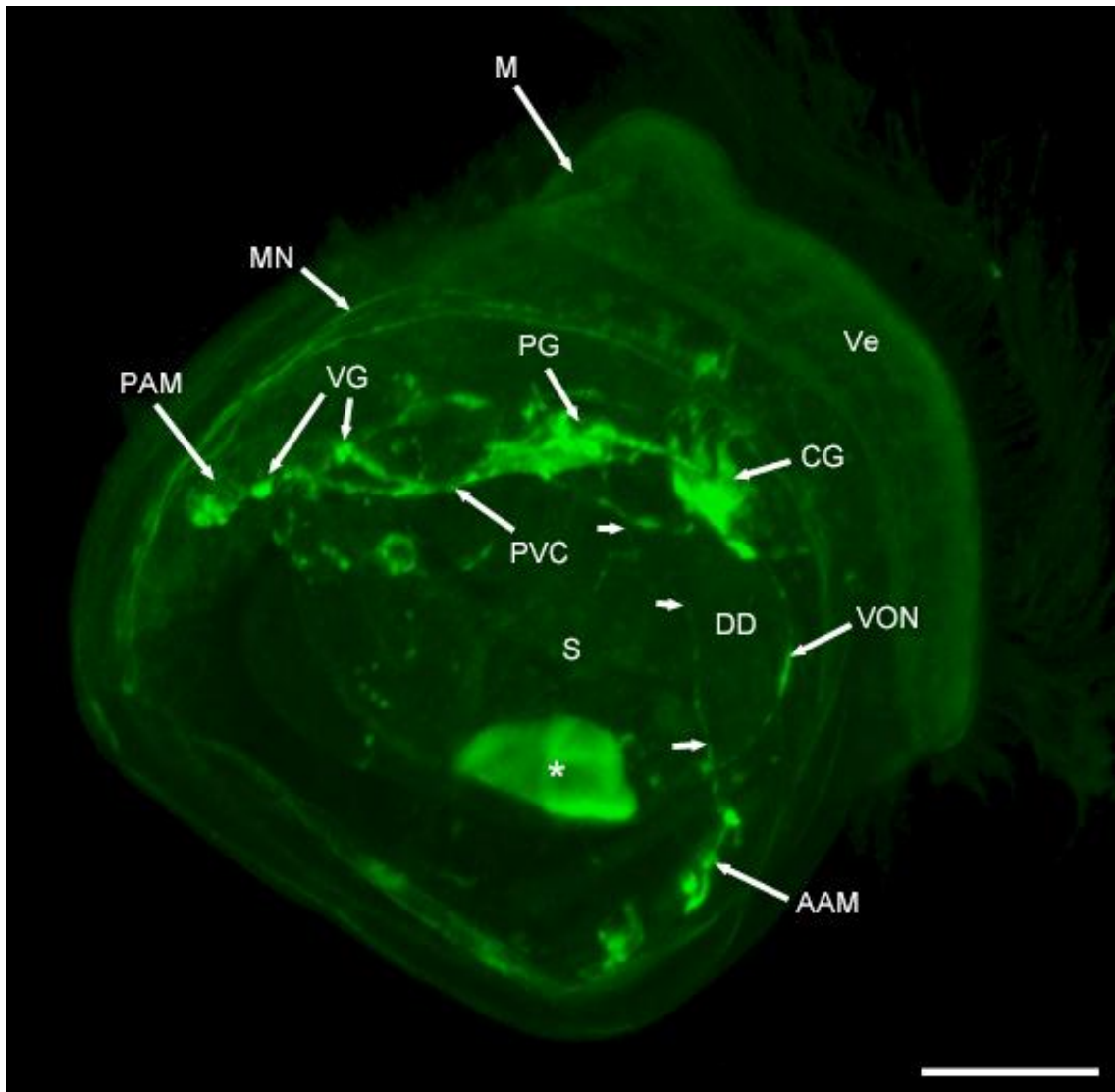


Figure 3.29. FMRFamide-like green immunoreactivity in day 10 control larva ($30 \times 1.07\mu\text{m}$). Abbreviations: AAM, anterior adductor muscle; CG, cerebral ganglion; DD, digestive diverticulum; MN, mantle nerve; PAM, posterior adductor muscle; PG, pedal ganglion; PVC, pleuro-visceral connective; S, stomach; VG, visceral ganglion; VON, ventral osphradial nerve. White unlabelled arrows; innervation from AAM to PG. * = autofluorescence. Scale bar = $20\mu\text{m}$.

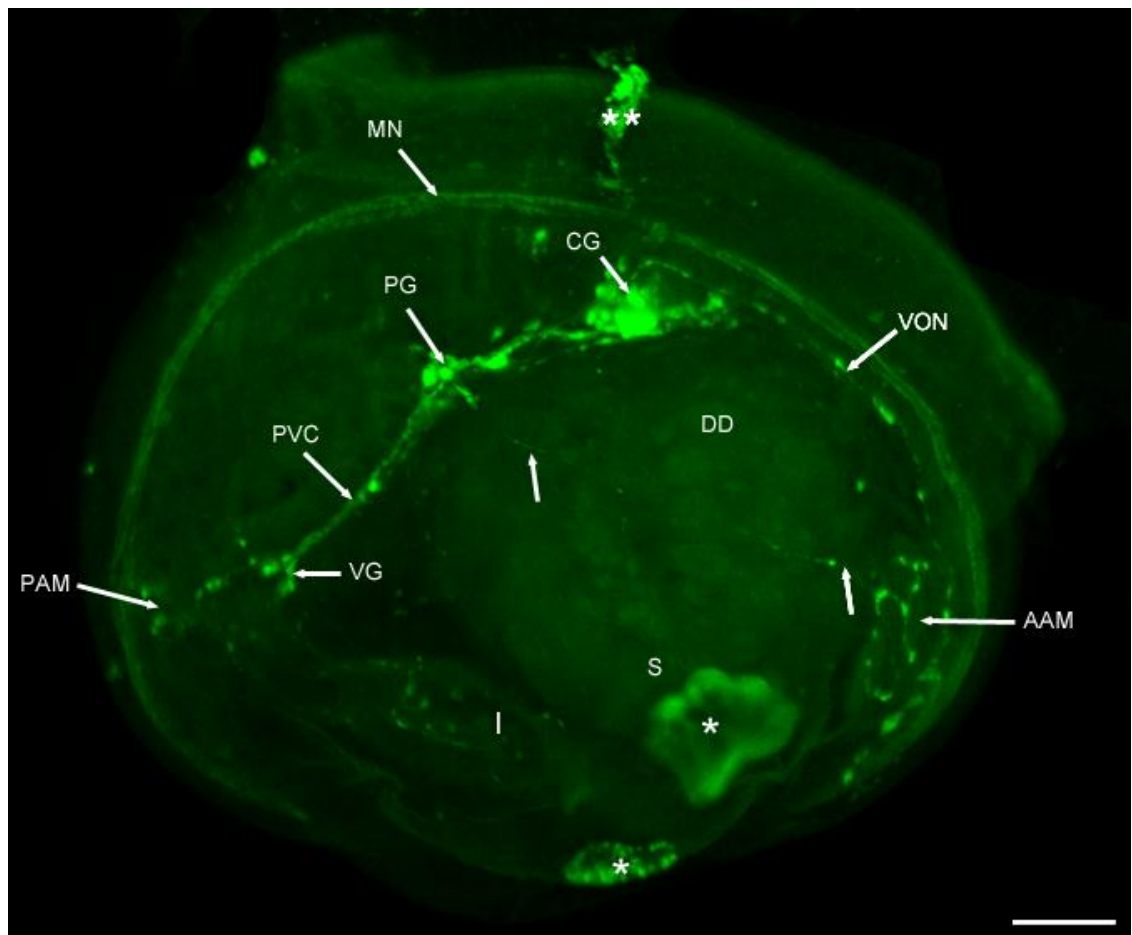


Figure 3.30. FMRFamide-like green immunoreactivity in day 14 control larva (52×0.97). Abbreviations: AAM, anterior adductor muscle; CG, cerebral ganglion; DD, digestive diverticulum; MN, mantle nerve; PAM, posterior adductor muscle; PG, pedal ganglion; PVC, pleuro-visceral connective; S, stomach; VG, visceral ganglion; VON, ventral osphradial nerve. White unlabelled arrows; innervation from AAM to PG. * = autofluorescence, ** = artefacts. Scale bar = $20\mu\text{m}$.

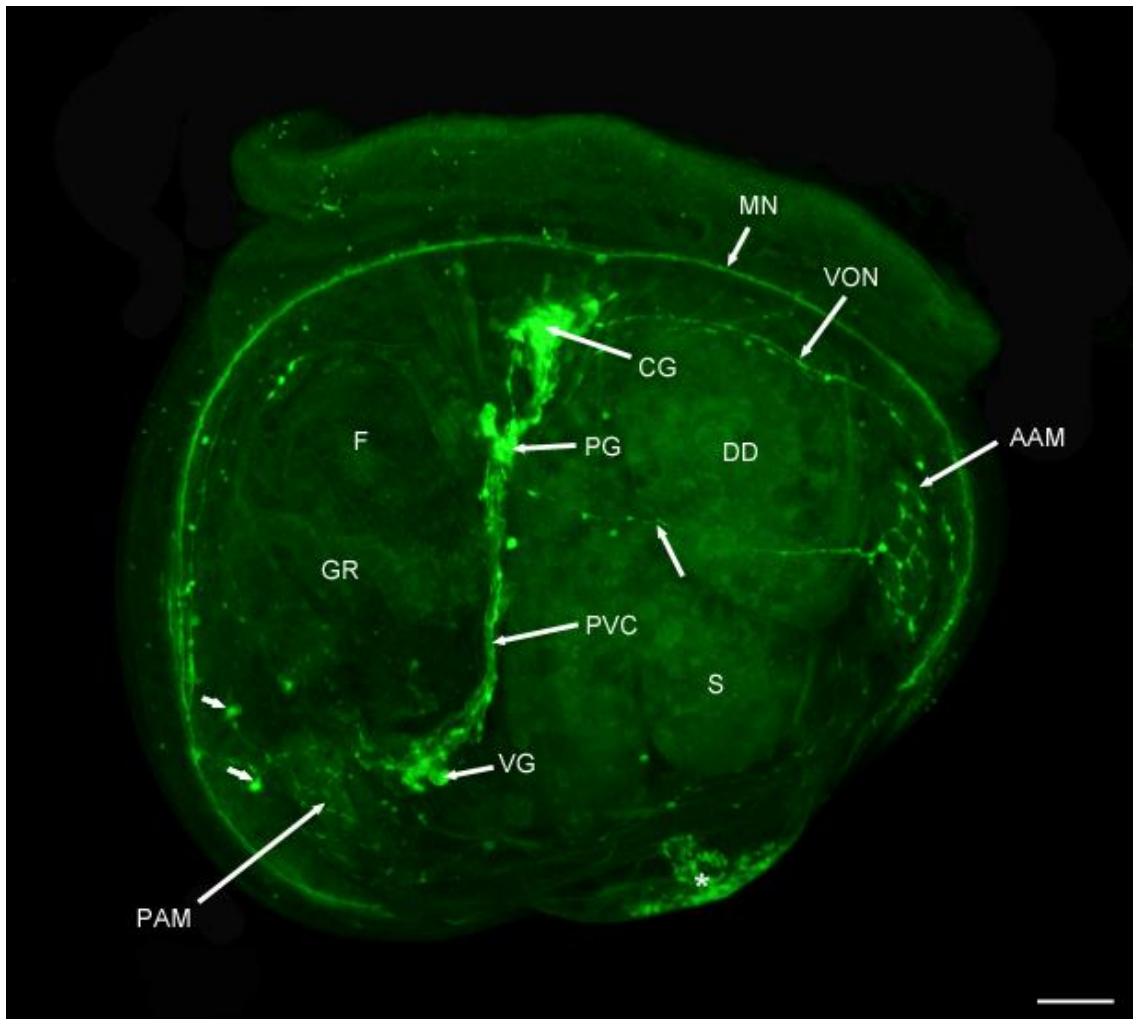


Figure 3.31. FMRFamide-like green immunoreactivity in day 18 control larva ($54 \times 1.07 \mu\text{m}$). Abbreviations: AAM, anterior adductor muscle; CG, cerebral ganglion; DD, digestive diverticulum; E, esophagus; F, foot; G, gill rudiment; MN, mantle nerve; PAM, posterior adductor muscle; PG, pedal ganglion; PVC, pleuro-visceral connective; S, stomach; VG, visceral ganglion; VON, ventral osphradial nerve. White short arrows; unknown neurons. White long unlabelled arrow; innervation from AAM to PG. * = autofluorescence, Scale bar = $20\mu\text{m}$.

Cryopreserved at D-stage

Solitary FMRFamidergic cells were present in various portions of the D-stage larva (2 dpf), but no connective or commissures were observed between these immunoreactive sites, which suggest that neurogenesis was still in its simplest form (Fig 3.32). In the mid D-stage (5 dpf), cells within the cerebral ganglia and

pedal ganglia were observed with a connective between these two ganglia (Fig. 3.33). At late D-stage (10 dpf), a pluro-visceral connective extends posteriorly to the visceral ganglia. A thin fibre extends from the pluro-visceral ganglia and extends towards the stomach and terminates before reaching the upmost anterior region (Fig. 3.34). The early umbo stage (14 dpf) shows further neurogenic development, with paired cerebral ganglia lying ventral of the mantles edge within the velum (Fig. 3.35). Connectives to each of the visceral ganglia travel dorsally connecting to one short single fibre before dividing connectives diverge to a pair of pedal ganglia. A pluro-visceral connective extends dorsally from the pedal ganglia to the paired visceral ganglia. A single thin fibre projects from the pedal ganglia and travels towards the anterior-adductor muscle, but terminates before reaching the muscle. The anterior-adductor itself composes of two ring like fibres with bulbous like cells extending around the muscle. The ventral osphradial nerve appears to connect or terminate near the connective fibres which extend between the visceral ganglia and pedal ganglia. However, no confirmation through rotatable 3D imagery could confirm this. Two clear mantle nerves were observed lying on the mantles edge of the right and left valve extending towards the hinge of the larvae.

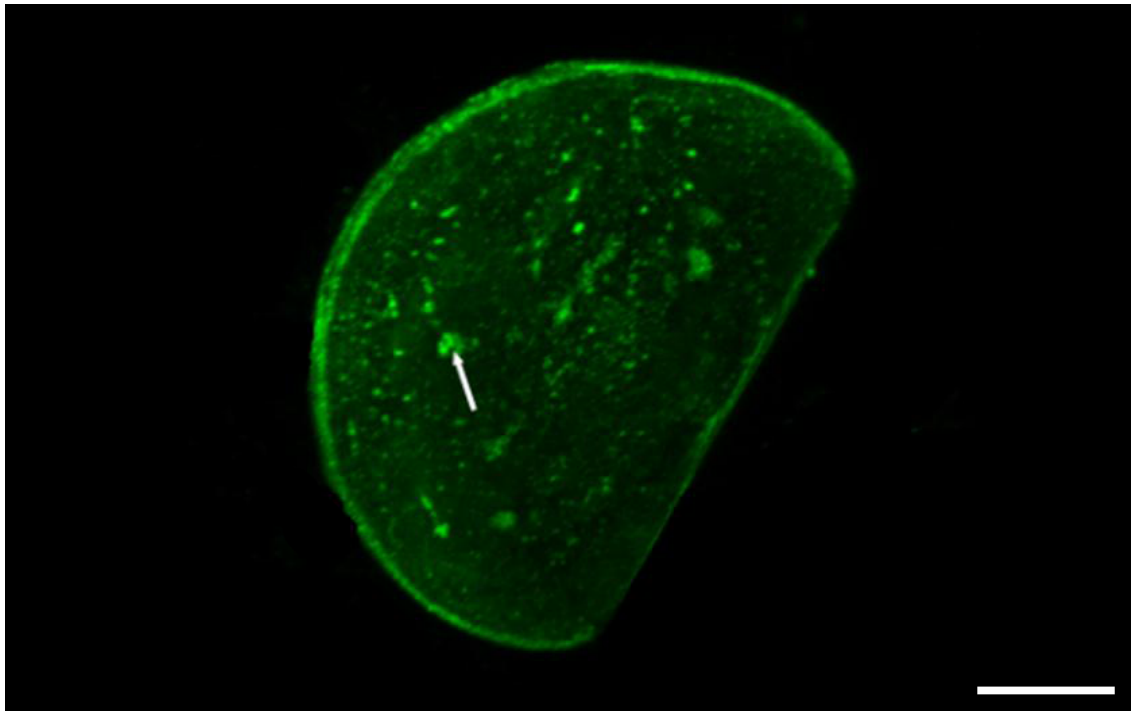


Figure 3.32. FMRFamide-like green immunoreactivity in day 2 larva cryopreserved at D-stage ($20 \times 1.07 \mu\text{m}$). White unlabelled arrow = unidentifiable immunoreactive site. Scale bar = $20\mu\text{m}$.

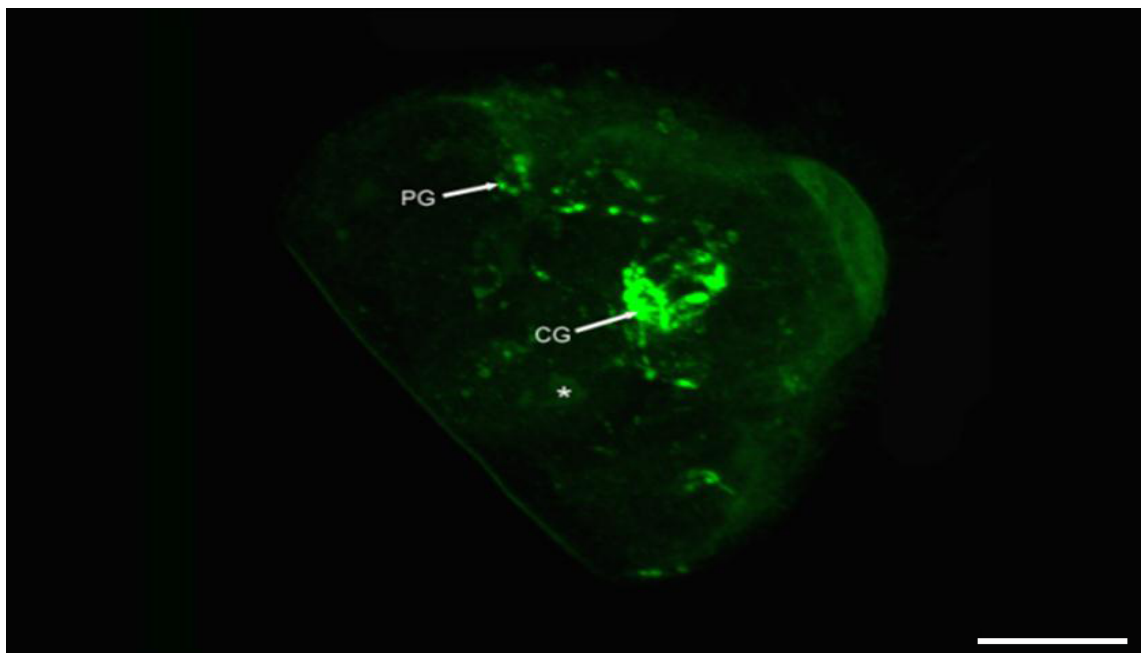


Figure 3.33. FMRFamide-like green immunoreactivity in day 5 larva cryopreserved at D-stage ($18 \times 0.97 \mu\text{m}$). Abbreviations: CG, cerebro-pleural ganglion; PG, pedal ganglion. * = autofluorescence. Scale bar = $20\mu\text{m}$.

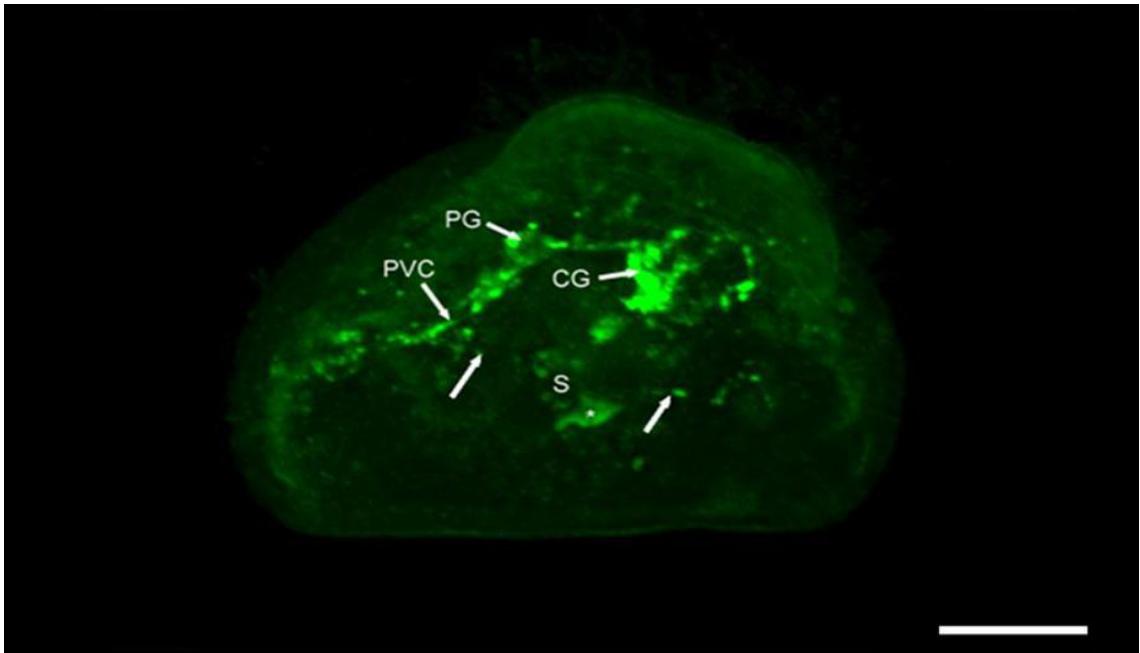


Figure 3.34. FMRFamide-like green immunoreactivity in day 10 larva cryopreserved at D-stage ($60 \times 0.34 \mu\text{m}$). Abbreviations: CG, cerebro-pleural ganglion; PG, pedal ganglion; PVC, pleuro-visceral connective; S, stomach. White unlabelled arrows = thin fibre. * = autofluorescence. Scale bar = $20\mu\text{m}$.

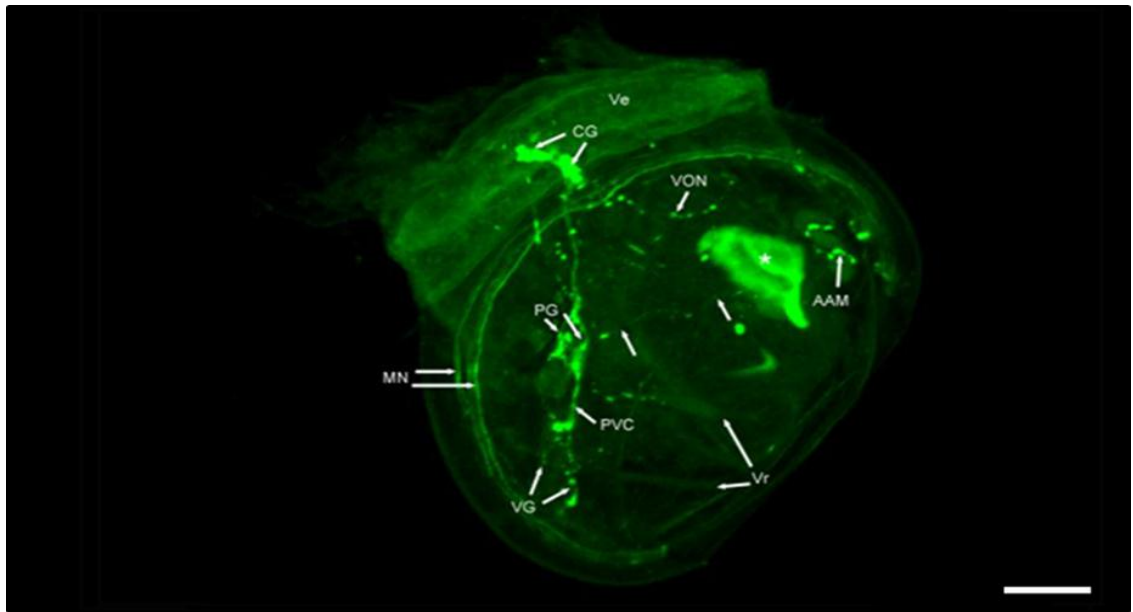


Figure 3.35. FMRFamide-like green immunoreactivity in day 14 larva cryopreserved at D-stage ($33 \times 0.97 \mu\text{m}$). Abbreviations: AAM, anterior adductor muscle; CG, cerebro-pleural ganglion; MN, mantle nerve; PG, pedal ganglion; PVC, pleuro-visceral connective; Ve, velum; VG, visceral ganglion; VON, ventral osphradial nerve; Vr, velum retractor muscle. White unlabelled arrows; innervation from AAM to PG. * = autofluorescence. Scale bar = $20\mu\text{m}$.

Cryopreserved at trochophore

FMRMamidergic cells in the cryopreserved trochophore larva that have progressed to D-stage larvae showed little immunopositive cells at 2 days old. Only two immunoreactive cells were apparent with one cell in the posterior region and another in the anterior region (Fig. 3.36). In the D-stage (5 dpf), larvae showed the first appearance of a cerebral ganglia with a faint cell in the region where the pedal ganglia will later develop (Fig. 3.37). Older D-stage larvae (10 dpf) showed further neurogenic development with paired cerebral ganglia with a connective fibre extending to the pedal ganglia. The posterior adductor muscle has a singular fibre with bulbous like cells extending along the length of the muscle which terminates at both ventral and posterior ends. The mantle nerve showed intense staining which travels adjacent to the mantle edge (Fig. 3.38). Larvae at day 14 showed an unexpected reduction in neurogenesis due mostly to variability with few larvae remaining. The cerebral ganglia and pedal ganglia were present with a pleuro-visceral connective between the two ganglia. However, the mantle nerve seems to be under developed (Fig. 3.39).

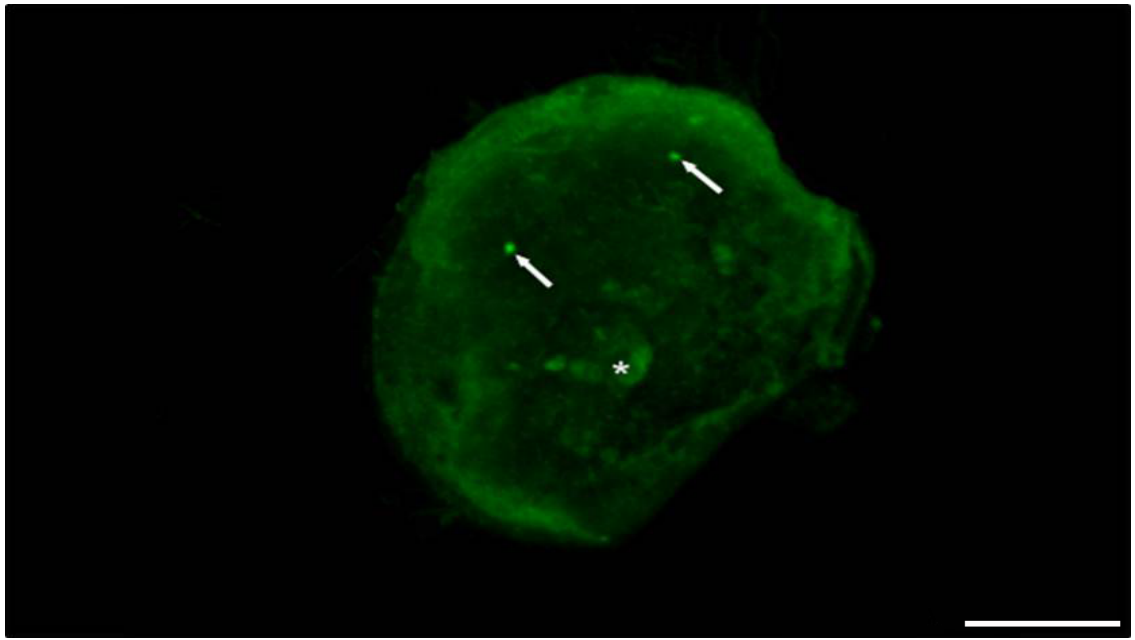


Figure 3.36. FMRFamide-like green immunoreactivity in day 2 larva cryopreserved at trochophore ($27 \times 1.07 \mu\text{m}$). Abbreviations: White unlabelled arrows; immunoreactive sites. * = autofluorescence. Scale bar = $20\mu\text{m}$.

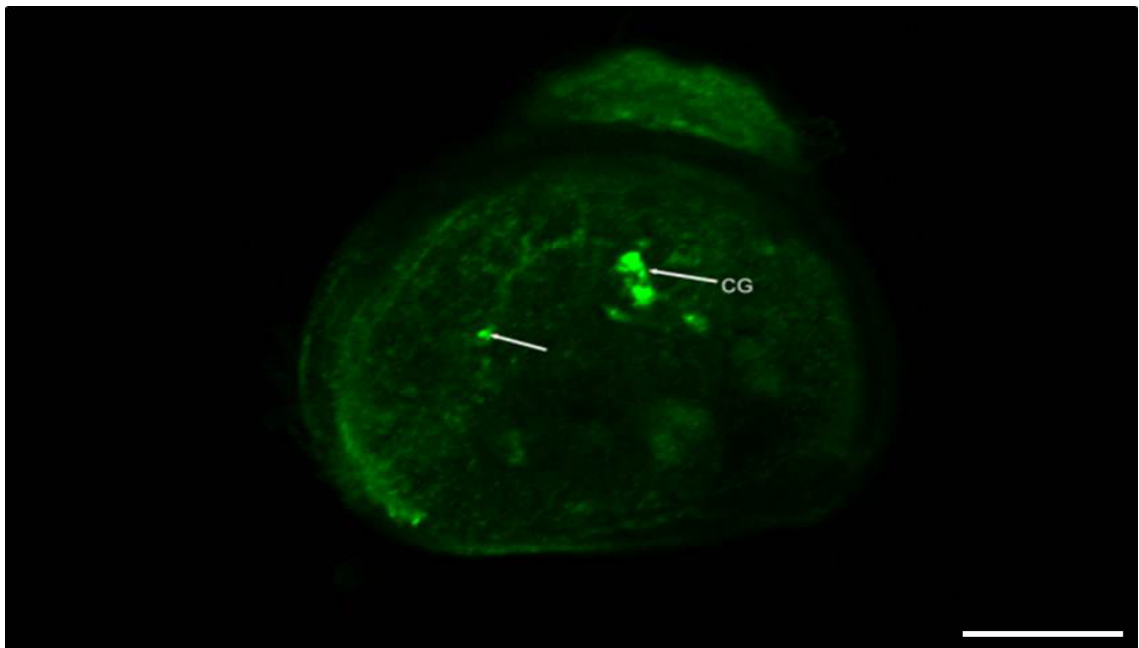


Figure 3.37. FMRFamide-like green immunoreactivity in day 5 larva cryopreserved at trochophore ($19 \times 0.97 \mu\text{m}$). Abbreviations: CG, cerebro-pleural ganglion; White unlabelled arrow; possible immunoreactive site within pedal ganglion region. Scale bar = $20\mu\text{m}$.

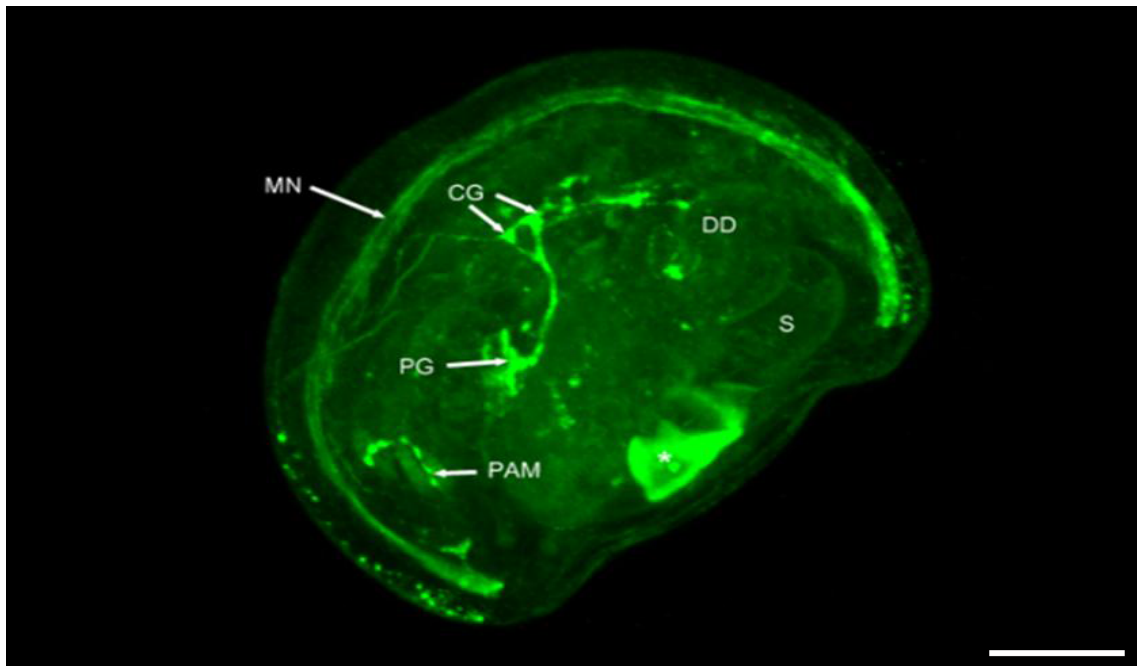


Figure 3.38. FMRFamide-like green immunoreactivity in day 10 larva cryopreserved at trochophore ($33 \times 0.97 \mu\text{m}$). Abbreviations: CG, cerebral ganglion; DD, digestive diverticulum; MN, mantle nerve; PAM, posterior adductor muscle; PG, pedal ganglion; S, stomach. * = autofluorescence. Scale bar = $20\mu\text{m}$.

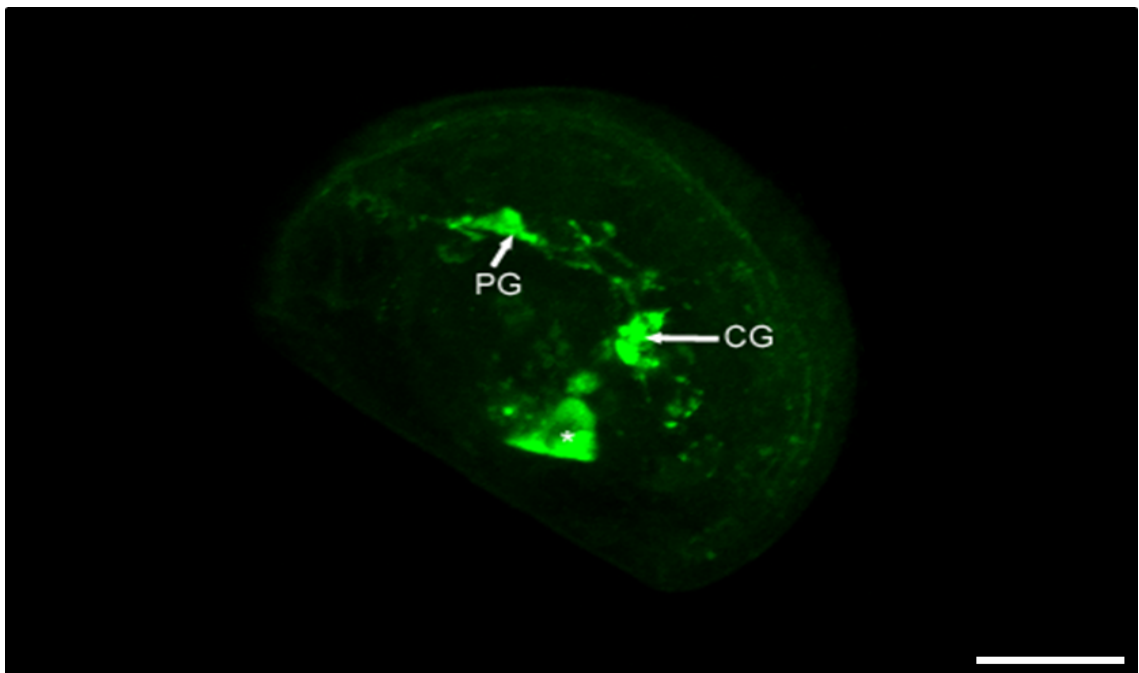


Figure 3.39. FMRFamide-like green immunoreactivity in day 14 larva cryopreserved at trochophore (day 14) ($33 \times 0.97 \mu\text{m}$). Abbreviations: CG, cerebral ganglion; PG, pedal ganglion. * = autofluorescence. Scale bar = $20\mu\text{m}$.

3.6 DISCUSSION

A few studies have focussed on the success of cryopreserving mussel oocytes, sperm, embryos, and larvae, which generally is assessed through survivability, shell growth, and successful transition to settlement (Adams et al., 2009; Di Matteo, Langellotti, Masullo, & Sansone, 2009; Wang et al., 2011; Paredes et al., 2012; Smith et al., 2012a,b). A good understanding of the processes involved in successful cryopreservation of mussel larvae is species-specific and dependent on the cryopreservation method used. Cryopreservation on *Perna canaliculus* has been investigated previously, including post-thaw oocyte viability (Adams et al., 2009), sperm function and post-thaw fertility (Smith et al., 2012a,b), and trochophore larvae (Paredes et al., 2012). These studies have primarily focussed on overall survivability, and shell length. However, studies on cryopreserving D-stage larvae are still lacking for this species. Paredes et al. (2012) concluded that further studies on *Perna canaliculus* development from D-larvae to settlement in the larval rearing process were required in order to increase survival. For example, the effect of cryopreservation on shell formation, organogenesis, and feeding during larval rearing had not been investigated prior to this study. Previous studies on both *Perna canaliculus* (Paredes et al., 2012) and *Mytilus galloprovincialis* (Wang et al., 2011) have suggested that looking at longer time frames of days as opposed to immediately after post-thawing would be an effective way of evaluating sub lethal cryo-injuries that may not manifest until during larval development.

In the present study we have investigated the effects of cryopreservation on subsequent larval development to post-settlement. Overall, results indicated some differences observed in cryopreserved treatments when compared to controls. Larvae frozen at D-stage slightly outperformed frozen trochophore larvae on average. However, controls still developed substantially better than frozen treatments in all parametric tests. Cryopreservation is a useful tool in selective breeding and hatchery production with a growing interest in using hatchery reared larvae as opposed to wild spat collection. Another implication of cryopreservation on *Perna canaliculus* larvae is to reduce the uncertainty of any risk associated with biological or commercial factors such as disease or economic changes. With this in mind, hatchery's adopting a successful cryopreservation method will ultimately allow a year round supply of spat and improve mussel hatchery production.

3.6.1 Survivability

The survivability of cryopreserved larvae over the 21-day rearing period followed a general declining linear trend with significant differences between controls and cryopreserved trochophore and D-stage larvae. However, there were no significant differences observed in percent survivability between cryopreserved trochophore and D-stage larvae. Survivability across cryopreserved treatments and controls were similar up to 4 dpf. However, between days 4 and 7, cryopreserved larvae differentiated with a considerable

decline in survivability and a continued decline in percent survival for the remainder of the 21 day rearing period. This trend was similar to Wang et al. (2011) who described a significant decline in survival for the cryopreserved blue mussel *Mytilus galloprovincialis* D-larvae for days 3 to 6 post-fertilisation. Within this study, only 0.03% of trochophore and 0.5% of D-stage larvae survived to day 18, but they were not competent pediveligers as observed in controls. This result differed to a study by Paredes et al. (2012) where 2.8% of cryopreserved *Perna canaliculus* trochophore successfully developed into competent pediveligers. Possible reasons for these survival differences could be seasonal batch variation or subsequent differences in genetic lines from selected broodstock. Alternatively, Paredes et al. (2012) did not sample as intensively as in our study, and low larval density could have affected overall survivability in this study.

These low survivability rates from cryopreserved *Perna canaliculus* larvae when compared to controls were similar to findings by Suquet et al. (2012) on the Pacific oyster (*Crassostrea gigas*) where cryopreserved D-stage survivability was different to normally reared larvae after 2 and 7 dpf. The CPA used by Suquet et al. (2012) (10% EG with 1% Polyvinyl pyrrolidone and 200mM trehalose in Milli-Q water, dilution rate: 1:1) was similar to our CPA (10% EG and 0.4 M trehalose (final concentrations), Milli-Q water, dilution rate: 1:1) used on both cryopreserved *Perna canaliculus* D-stage and trochophore larvae. For *Perna canaliculus*, the effectiveness of cell uptake when exposed to this CPA was investigated later on D-stage larvae using the same CPA to see if the

larvae would reject the applied CPA by discontinued swimming and shell closure (Serean Adams, personal communication). Initial CPA dilution with the D-stage larvae showed a 50% swimming response, and after 15 and 30 mins a 100% swimming response. This swimming behaviour suggests that in our study, successful exposure time (~20mins) to the CPA for both trochophore and D-stage larvae was given to help prevent cryo-injury. This also suggests the CPA is able to be taken up by the larvae as they are not rejecting the addition of CPA by closing their shells. A study by Paredes et al. (2012) investigated the chilling effect for *Perna canaliculus* trochophore using a similar CPA and same cooling rate ($0.5^{\circ}\text{Cmin}^{-1}$) and found that there was no effect of cooling rates between $0.5^{\circ}\text{Cmin}^{-1}$ and $1.0^{\circ}\text{Cmin}^{-1}$ down to -35°C on larvae developing to normal D-stage. This evidence reinforces the idea that our study used an optimised cooling rate and CPA for trochophore larvae to help reduce any cryo-injury. However, optimising a cool rate and CPA for D-stage larvae is yet to be determined through future experiments. Tolerances to chilling for various mussels is species-specific as demonstrated for the mussel *Mytilus galloprovincialis* (Statuito, Bao, Yang, & Kitamura, 2005) where straight-hinged larvae grew to umbo-veliger larvae in a $4\text{--}5^{\circ}\text{C}$ refrigerator after 2 months. There was a 79% survival rate after 1 month, but did not reach the pediveliger after 3 months with only 22% survival. This survival rate is overall considerably better than *Perna canaliculus* with or without cryopreservation and reinforces the idea that each species has its own tolerance to chilling prior to cryopreservation.

From visual observations, cryopreserved D-stage and trochophore larvae of *Perna canaliculus* showed normal swimming behaviour when compared with controls. However, no swimming behavioural tests were performed. This swimming behaviour after cryopreservation also was reported by Suquet et al. (2012) when they determined that D-stage *Crassostrea gigas* larvae had a reduced Average Path Velocity (AVP) after thawing. This suggested the ability of larval movement velocity as a measure of assessing the decrease in quality of thawed oyster larvae. This measurement of swimming behaviour assessment could be utilised in future cryopreservation studies on *Perna canaliculus* to help estimate the quality of thawed larvae at an early stage of development.

3.6.2 Shell length

Shell length between the control and frozen treatments over the 21-day rearing period showed a general incline in shell length with some differences. The control larvae showed differences in shell length compared to frozen trochophore and D-stage larvae. Frozen trochophore larvae had the greatest differences when compared to controls. However, the differences between shell length of cryopreserved trochophore and D-stage larvae were not significantly different. Low yields of cryopreserved D-stage larvae that made it to 18 days post-fertilisation and trochophore to 13 days post-fertilisation accounted for the high variation in shell length. These shell length differences

in cryopreserved larvae have been observed in other bivalve species, including mussels (Wang et al., 2011; Paredes et al., 2012), and oysters (Yankson & Moyse., 1991; McFadzen, 1992; Suquet et al., 2012). A similar trend was observed by Paredes et al. (2012) on cryopreserved *Perna canaliculus* trochophore larvae from the moment they became D-stage larvae. Over 18 days, Paredes et al. (2012) had significant differences in shell length between cryopreserved trochophore larvae and controls with frozen trochophores being ~20% smaller than unfrozen control larvae. Over this rearing period, cryopreserved larvae remained smaller than those in controls. No differences were observed at 18 days due to increase in high variability among frozen larvae. This variability was observed in our study between trochophore and D-stage larvae around the time when there was low survivability. Also the trend of cryopreserved larvae being generally smaller than controls was similar to Paredes et al. (2012) findings. However, another study by Wang et al. (2011) showed no shell length differences in frozen D-stage or unfrozen larvae of the blue mussel *Mytilus galloprovincialis* with differences only observed at 6 dpf. This differed to this study on *Perna canaliculus* frozen D-stage with significant differences across all days, except for 15 and 19 dpf due to high variability in cryopreserved and control larvae. We therefore suggest that shell length differences are a likely cause of cryo-injury to organs, such as the shell gland and mantle which are responsible for PI and PII shell secretion, respectively. More research is needed to assess the effects of cryo-injuries on shell length of *Perna canaliculus* which could be affiliated with a delay in successful development.

3.6.3 Feeding consumption

Feeding consumption was overall different over the 21-day rearing period with differences in feeding consumption for cryopreserved and control larvae. However, there were no differences in the interaction between larval age and treatments. Generally, the feeding consumption of the controls was significantly higher than those of the cryopreserved trochophore and D-stage larvae which had low feeding consumption throughout the 21-day rearing period. This difference in feeding consumption for cryopreserved larvae was seen by Wang et al. (2011) on the mussel *Mytilus galloprovincialis* cryopreserved at the D-stage. On day 3 post-fertilisation, only half of the swimming D-larvae after post-thaw, had microalgae in their stomachs in comparison with about 80% in the control group. A similar feeding response to cryopreservation also was seen in a study by Suquet et al. (2012) on Pacific oyster larvae frozen at D-stage. Results in that study showed 85% of Pacific oyster larvae were actively swimming 3 h after thawing, while only half of these larvae showed microalgae in their stomach, compared to 80% for the control group. This result was similar to our findings where low microalgae was observed in the stomachs of both cryopreserved trochophore and D-stage larvae between 2 and 5 dpf, but a large amount was observed in control larvae. There was no increase in feeding consumption for larvae cryopreserved at trochophore or D-stage over subsequent days, but some surviving individual larvae cryopreserved at D-stage had large amounts of microalgae in the stomach that appeared equivalent to control larvae. This suggests that D-stage larvae had avoided cryo-injury and were capable of ingesting microalgae as well as controls. This reduced feeding

consumption in *Perna canaliculus* could be affiliated with cryo-injury to important feeding organs, such as the velum, digestive diverticulum, or stomach during the cryopreservation process. However, this study could not identify any of these injuries to such organs and could be more obtrusive at a cellular level.

A study by Aoki et al. (2007) using cryopreserved sperm of the Japanese pearl oyster *Pinctada fucata martensii* for oocyte fertilisation showed that there was no difference in feeding consumption of the larvae over a 22-day rearing period. While the conditions of that study were not similar to those in our study, it is possible that the cryopreservation of larval stages for *Perna canaliculus* has an effect on feeding behaviour, organs, or neuronal system through either chilling or IIF damage. Further research to identify the causes of this reduced feeding consumption would be of significant interest to successful cryopreservation of *Perna canaliculus* larvae and various other species. Consequently, low microalgae in the stomachs of larvae could be used as an early assessment tool to determine the quality of larvae after cryopreservation.

3.6.4 Shell morphology

The shell morphology of cryopreserved larvae was different to observed controls without cryopreservation. The cryopreserved trochophore larvae that went on to develop a D-shell showed the greatest abnormalities at the very first stages of an early D-stage (2 days old) through to 14-day old larvae. Common abnormalities observed with frozen trochophore larvae were wrinkle type

appearances on the outer shell surface situated from the punctuate region of the PI layer extending ventrally through the PII layer towards the mantle edge. Unsymmetrical left and right valves also were observed in the early D-stage form. Frozen D-stage larvae showed fewer shell abnormalities than frozen trochophore larvae. The frozen D-stage larvae had abnormalities to the shell immediately after cryopreservation and when the D-stage larvae were progressing on with PII shell secretion throughout development. These abnormalities to both frozen stages suggests some form of cryo-injury occurred on the shell gland in the frozen trochophore larvae which is responsible for shell secretion in the PI region, or to the mantle in the frozen D-stage which is responsible for shell secretion in the PII region (Gosling, 2003). A detailed study on abnormalities of bivalve larval shell morphology is lacking. However, a study by Nascimento et al. (2005) on the toxic effects of cryoprotectants on embryos and gametes of oyster (*Crassostrea rhizophorae*) identified similar shell abnormalities. These abnormalities were described as larvae having irregular or misshapen shells, completely or incompletely formed. Also any embryos that had not developed to a D-stage larva (24 hours post-fertilisation) were deemed abnormal due to unsuccessful development. Overall, 15% of the population had abnormal larvae within 24 hours post-fertilisation for oyster embryos and gametes. While our study did not quantify abnormal larvae of *Perna canaliculus* when exposed to CPA for frozen trochophore larvae, the majority of post-thaw larvae were observed to have these shell abnormalities during the early stages of development with few abnormal larvae making it to a later development stage. Shell abnormalities observed at the mantle edge in

frozen trochophore larvae that had developed a D-shell, could allow an increase in the likelihood of ciliates disrupting the larvae and causing low survivability. Ciliates are considered opportunistic at the expense of necrotic tissue or weakened larvae as seen in *Crassostrea virginica* larvae (Brown, 1973). A study on juvenile oyster *Crassostrea gigas* and *Crassostrea sikamea* has shown that ciliates are able to bypass the outer mantle lobe and gain entry to the extrapallial space *via* the mantle tissue separating the extrapallial space from the coelomic cavity (Elston, Cheney, Frelter, & Lynn, 1999). Once invaded, the juveniles became infected and appeared to be irreversible with cultures usually exceeding 50% mortality (Elston et al., 1999). These studies infer that damage to the shell margins in *Perna canaliculus* could provide favourable conditions for ciliate propagation. Our findings are therefore a representation of the effects cryopreservation has on shell morphology, and further research could endeavour to determine the exact cause of shell deformities. Overall, results indicate that frozen D-stage larvae with less shell abnormalities are more tolerant to cryo-injury than frozen trochophores that go on to develop abnormal shells.

3.6.5 Organogenesis

Cryopreservation delayed organogenesis of larvae when compared to control larvae, irrespective of the larval stage frozen. Within this study, delays in organogenesis were determined using a combination of histology, light

microscopy, and SEM observations. Larvae frozen at trochophore stage had a slower rate of organogenesis when compared to larvae frozen at D-stage which developed quicker. Control larvae were able to progress to the settlement stage where eye spots were evident with developed organs, such as the gill rudiment and a functioning foot where as cryopreserved larvae did not. Cryo-injuries were not evident through histological slides, but light microscopy showed some minor deformities to frozen trochophore and D-stage larvae. These cryo-injuries of certain organs or cell types have been shown to cause a delay in development and recovery of cryopreserved Sydney rock oyster (*Saccostrea glomerata*) D-larvae and subsequent injuries to other organs may also result in death (Liu & Li, 2008). Our study supports this notion since cryopreserved trochophore larvae had progressed only to the early umbo larvae stage by around 15–16 dpf whereas control larvae at that time had developed progressively more to the umbonate larvae with a functional foot, visceral and pedal ganglia. Few cryopreserved D- larvae and no trochophore larvae were observed to develop to competent pediveligers with a functional foot, and no cryopreserved larvae developed to post-larva with an eye spot. Wang et al. (2011) observed a similar delay in development for cryopreserved *Mytilus galloprovincialis* D-stage larvae, where less than 10% of frozen larvae developed an eye spot at 16 days post-fertilisation. This was suggested to be due to possible cryo-injuries or temporary interruption to biological processes in development. However, at 21 days post-fertilisation, the cryopreserved larvae had a higher rate (78%) of larvae developing eye spots which reinforces the idea of a delay in organogenesis.

Overall, intracellular ice formation damage to cryopreserved larva cells was not distinguished through histological sections or light microscopy. The addition of CPA (10% EG + 0.4 M trehalose) seems efficient at preventing the majority of cooling and post thaw damage from cryopreservation, but further research is needed to investigate any cryo-injuries at a cellular level.

3.6.6 Neurogenesis

Cryopreservation of trochophore and D-stage larvae that progressed on with larval development showed neurogenic differences between the two cryopreserved stages. At 14 dpf, the frozen D-stage larvae had a complete nervous system with paired cerebral, pedal, and visceral ganglia, along with an innervation extending from the pedal ganglia towards the anterior adductor muscle. At the same time, frozen trochophore larvae showed differences with only a cerebral and pedal ganglia present with an interconnecting plero-visceral connective, but no visceral ganglia were visible. Central neurons of the visceral ganglia are suggested to influence the rate of beating of the lateral cilia via the release of biogenic amines in the gill of adult *Mytilus edulis* (Audesirk, McCaman, & Willows, 1979). The fact that the visceral ganglion were absent or yet to develop in frozen *Perna canaliculus* trochophore, leaves possible cilia functional issues. The visceral ganglia are suggested to influence the rate of beating movement in cilia, and also connect to the branchia gill. This leaves doubt as to whether the larvae were having cilia functional problems. This may

well explain the lack of microalgae seen in the stomach of cryopreserved larvae as most bivalve larvae are known to use selective particle manipulation during feeding as seen in *Mercenaria mercenaria* larvae (Gallager, 1988). Also, no innervations extending from the pedal ganglia towards the anterior adductor muscle, and ventral osphradial nerve were observed in frozen trochophore larvae. The function of this fibre is still unexplained.

These observable changes suggest some delay in neurogenesis after cryopreservation, which is most likely affiliated with the delay in organogenesis. At present, no studies have investigated the effects of cryopreservation on neuronal processes through larval development of any bivalve. Therefore this is one of the first known studies to effectively observe any changes in the nervous system of cryopreserved mussel larvae. Detailed studies on the larval nervous system of mussel, *Mytilus trossulus* (Voronezhskaya et al., 2008) and oysters *Ostrea edulis* (Erdmann, 1935) and *Crassostrea virginica* (Ellis, 2010) have been carried out which showed very similar neural processes to controls of *Perna canaliculus*. However, studies assessing the role of how these neuronal processes develop after exposure to chemical or thermal responses are still lacking. These neural processes of *Mytilus trossulus* involved innervated anterior-adductor muscles, a fibre extending from the pedal ganglia to the anterior-adductor muscle, and paired cerebral, pedal, and visceral ganglia which were very similar to those of *Perna canaliculus* larval development over a 21-day rearing larval development. Within this study, it is possible that intracellular damage inhibited or disrupted biological processes in

neuromodulation (epinephrine, norepinephrine, serotonin, and dopamine) that are responsible for behavioural, settlement and overall neuronal development in molluscs (Kreiling, Jessen- Eller, Miller, Seegal, & Reinisch, 2001). A detailed study on the effects of cryopreservation on neurogenesis and how these changes inhibit or release certain neural processes that are fundamental to overall larval development would be of considerable value to neurobiologists and cryobiologists.

In summary there were significant differences observed between cryopreserved treatments and controls due most likely to cryo-injuries sustained in the chilling or thawing process. A great deal of cryopreservation work has been focussed on the survival success of freezing earlier stages of *Perna canaliculus* development involving oocytes, sperm, and trochophore larvae. Good success has been achieved immediately after post-thaw, but on-going larval development proves to be problematic with low survival. Within this study, survivability, shell length, and feeding consumption of both frozen trochophore and D-stage were shown to be significantly different to those of control larvae. However, in all analyses mentioned, there were no significant differences among frozen treatments. Shell morphology between both frozen treatments revealed abnormalities to regions of the shell incorporating the prodissoconch I & II layer suggesting the mantle and shell gland were damaged in the cryo process. Shell abnormalities in frozen trochophore were slightly more pronounced in the mantle region with fewer abnormalities observed in frozen D-stage larvae. This could account for more ciliates. Organogenesis between the

frozen treatments showed a delay in development with frozen D-stage larvae progressing further to the late umbo stage, than trochophore larvae that reached only the early umbo stage. Neurogenesis between the frozen treatments was different among frozen D-stage larvae and trochophore larvae, but differentiation between controls and D-stage larvae were similar. Trochophore larvae were largely different in neurogenesis with a delay in neural processes when compared to controls. Overall, this study highlights the importance of further on-going research on the effects cryopreservation has on subsequent larval development of *Perna canaliculus*.

CHAPTER FOUR: General Discussion

4.1 DISCUSSION

Research on the green-lipped mussel *Perna canaliculus* has investigated extensively the dynamic aspects of biology and ecology of the larval, juvenile, and adult stages. This endemic New Zealand species is of great cultural and economic significance, since it represents an iconic symbol for New Zealand in the international seafood market. Earlier studies for this species have primarily focussed on population dynamics (Paine, 1971; Hickman, 1991; Lachowicz, 2005; Alfaro et al., 2008) shell morphology (Redfearn, 1986; Buchanan, 1999; Ericson, 2010), settlement (Alfaro, 2005; Young, 2009; Young et al., 2010; Young et al., 2011), and reproduction (Flaws, 1975; Hickman & Illingworth, 1980; Jenkins, 1985; Alfaro et al., 2001; Alfaro et al., 2003). More recent research directions have been on larval behaviour, settlement cues, and nutrition across different larval stages within hatchery or laboratory settings (Young, 2009; Ganesan et al., 2010; Ragg et al., 2010; Young et al., 2011). The findings of this thesis address for the first time, the detailed larval development and the effects of cryopreservation on post-thawed larvae in hatchery-reared *Perna canaliculus*. This research contributes greatly to our knowledge on invertebrate larval biology and cryobiology for this mussel species, and it is relevant for other marine invertebrate species.

This study has identified specific characteristics of larvae during their development that have not been documented before. Supplementing this research was a study on the effects of cryopreservation on subsequent developmental processes. Of particular interest is the nervous system

(FMRFamide-like immunoreactivity) which was found to develop completely at the pediveliger stage. This is the first study to document such developmental characteristics for *Perna canaliculus*, and these findings open new directions for further work on larval neurological functioning and chemoreception. These advanced methods allow for a more in-depth characterisation of neuronal development, which was not available previously. Recently, techniques in the field of immunocytochemistry, histochemistry, and immunocytochemistry have been used to identify cells affiliated with physiological processes in mussel larval development (Croll et al., 1997; Flyachinskaya, 2000; Voronezhskaya et al., 2008; Dyachuk et al., 2012). These new techniques have been used in the identification of FMRFamide, serotonin, and catecholamine-containing cells which are formed through neurodevelopment (Croll et al., 1997; Voronezhskaya et al., 2008; Dyachuk et al., 2012). Neurogenesis through FMRF-amide, such as immunocytochemistry, has only recently been used to elucidate the complete nervous systems at the pediveliger stage for *Mytilus edulis* and *Crassostrea gigas* (Voronezhskaya et al., 2008; Dyachuk et al., 2012). However, other neurological development, such as catecholamine sites could provide insightful knowledge into mechanisms involved in larval behaviour and chemoreception for *Perna canaliculus*. Further studies in neurodevelopment of *Perna canaliculus* may help improve our knowledge on behavioural, settlement, and development aspects that constantly hinder successful larval rearing. Past studies on shell morphology and shell length for *Perna canaliculus* have provided basic and general knowledge, but more in-depth investigations are needed in order to fully understand shell secretion processes (Redfearn et al.,

1986; Petrone et al., 2009; Ericson, 2010). Thus, the present study identified important shell morphology characteristics from early D-stage to post-settlement which can be used to characterize the developmental stage of wild larvae and those cultivated in hatcheries. These findings also identified in detail the large variation in shell abnormalities and shell lengths resulting from cryopreservation. Scanning electron microscopy was used to assist in a higher detailed study on shell secretion, which improves on the depth of field limitations of normal light microscopy (Bozzola et al., 1999; Silberfeld et al., 2006). These findings draw attention to problematic areas in larval rearing techniques, such as grading practices through larval development, which often damage the larvae. A histological approach was used in this study to add to our knowledge of immunochemistry of the mussel nervous system, and at the same time to demonstrate ontogenesis processes that are involved in larval development. The integration of these techniques, such as histology (Hickman et al., 1971; Elston, 1999; Ellis, 2010), and immunochemistry (Voronezhskaya et al., 2008; Dyachuk et al., 2012) allows for a direct approach to understand the form and function of developing organs and neurons affiliated with the FMRFamide system. For example, the anterior adductor muscle of the pediveliger stage in *Perna canaliculus* is highly innervated with FMRFamide fibres. Recent findings by Dyachuk et al. (2012) found that anterior and posterior adductor muscles in the pediveliger *Crassostrea gigas* and *Mytilus trossulus* were innervated with FMRFamide fibres, which were similar to our findings. It was suggested that the role of FMRFamide can be released by neuronal excitation which acts on muscle fibres. However, no detailed

morphological or physiological study has defined mussel development and its correlation with the nervous system. Therefore, a detailed study involving the nervous system of bivalve pediveliger or post-larva would be of considerable value to neurobiologists.

As a first step to address the lack of integrated knowledge of larval development, an integrated multi-technique approach was used to investigate *Perna canaliculus* larval development. In addition to providing a catalogue of normal developmental stages in organogenesis, neurogenesis, shell morphology, shell length, survivability and feeding consumption, this study also provides a comparison of developmental processes between normal and cryopreserved larvae. The findings of this research and the approach used within may be used for a multitude of related studies with this species and other marine invertebrates. Furthermore, the catalogue of developmental stages for this mussel species can be used to identify on-going larval health problems, such as parasitism or diseases that affect on-going larval development. Additionally, this catalogue can be used as a template to identify healthy larval batches and distinguish larvae that are likely to not survive. This tool has the potential to significantly reduce larval rearing costs and time spent in unsuccessful larvae rearing.

Successfully cryopreserving viable mussel *Perna canaliculus* larvae from seasoned and conditioned broodstock on demand would be of considerable value to the aquaculture industry. At present, spat collected commercially from the wild make up a large contribution to the mussel industry (Alfaro et al., 2011).

This reliance on a source of spat washing up has its potential risks, and even spat collected on ropes are subject to losses in spat detachment, predation, and mortality cascades due to environmental conditions (Hay et al., 2004; Young, 2009; Alfaro et al., 2011). The demand to use hatchery-reared larvae within a growing mussel industry is a worthy area for research and development. The bottleneck of hatchery rearing is the lack of reliable larval supplies, which are highly susceptible to seasonal variations in gametogenesis and environmental conditions. Cryopreservation can be utilised as an alternative source of viable larvae from seasonally conditioned broodstock. A combination of both selective breeding and successful cryopreservation would be of benefit to any large scale hatchery production of *Perna canaliculus* or alternative species. The abnormalities described here are ultimately a guide to the cryo-injury effects obtained using this method. The fact that no cryopreserved larvae in this study went on to develop into competent pediveliger larvae was most likely due to a delay in organogenesis, which may have contributed to the low survivability, however cryo-injuries cannot be ruled out. Wang et al. (2011) had slightly better results to our findings with <10 % of cryopreserved *Mytilus edulis* larvae developing an eye spot compared to controls with 80% developing an eye spot at 16 days post-fertilisation. This was thought to be the result of temporary interruption in biological processes during cryopreservation due to a significant increase (78%) of older (21 days post-fertilisation) cryopreserved larvae developing eye spots. Understanding these biological processes, which take place immediately post-thawing, may help overcome some of these cryopreservation hurdles. This would be of considerable importance to

developing future cryopreservation methods for *Perna canaliculus* and ascertaining whether this is an effective method for the industry to invest in. These cryobiology assessment tools also can be applied to other species which have not been cultivated with the success of this mussel species.

A study involving lipid extractions from the tissues of this mussel species and the addition of antioxidants incorporated into a cryoprotectant has been shown to improve mussel viability (Odintsova et al., 2012). The bovine serum albumin used in this study has similar antioxidant properties, and previous studies indicate an increase in viability. This integration of antioxidants and lipids could ultimately be investigated in the cooling and thawing cycle of *Perna canaliculus* within cryopreserved trochophore and D-stage larva to see if this increases larval viability. Another avenue worth exploring and supplementing with cryo-experiments is to investigate the swimming behaviour of larvae. Measuring the average path velocity after thawing, as observed by Suquet et al. (2012) on D-stage *Crassostrea gigas*, suggests this to be a worthy method of measuring a decrease in larval quality. This could ultimately be used to indicate the quality of *Perna canaliculus* larvae as an early warning system before investing time and money into rearing unviable larvae.

In summary, this thesis has provided a significant foundation for further studies on larval development of *Perna canaliculus*, and the effects of cryopreservation on subsequent larval development. The future directions mentioned here would be of significant importance within hatchery rearing of *Perna canaliculus* and for general larval biology. In addition, this multi-technique research approach can

be applied to various other bivalve species. Integrating the findings from these different research areas will greatly enhance our understanding of larval developmental biology, effective cryopreservation of this endemic New Zealand species, and other marine invertebrate species throughout the world.

REFERENCES

- Adams, S.L., Smith, J.F., Roberts, R.D., Janke, A.R., Kasper, H.F., Tervit, H.R., Pugh, P.A., Webb, S.C., & King, N.G. (2004). Cryopreservation of sperm of the Pacific oyster (*Crassostrea gigas*): development of a practical method for commercial spat production. *Aquaculture*, 242, 271–282.
- Adams, S.L., Smith, J.F., Roberts, R.D., Janke, A.R., King, N.G., Tervit, H.R., & Webb, S.C. (2008). Application of sperm cryopreservation in selective breeding of the Pacific Oyster, *Crassostrea gigas* (Thunberg). *Aquaculture Research*, 39, 1434–1442.
- Adams, S.L., Tervit, H.R., McGowan, L.T., Smith, J.F., Roberts, R.D., Flores, L.S., Gale, S.L., Webb, S.C., Mullen, S.F., & Critser, J.K. (2009). Towards cryopreservation of Greenshell™ mussel (*Perna canaliculus*) oocytes. *Cryobiology*, 58, 69–74.
- Alfaro, A. C. (2005). Effect of water flow and oxygen concentration on early settlement of the New Zealand green-lipped mussel, *Perna canaliculus*. *Aquaculture*, 246, 285–294.
- Alfaro, A.C., Copp, B.R., Appleton, D.R., Kelly, S., & Jeffs, A.G. (2006). Chemical cues promote settlement in larvae of the green-lipped mussel *Perna canaliculus*. *Aquaculture International*, 14, 405–412.
- Alfaro, A. C., & Jeffs, A. G. (2002). Small-scale mussel settlement patterns within morphologically distinct substrata at Ninety Mile Beach, northern New Zealand. *Malacologia*, 44(1), 1–16.
- Alfaro, A.C., Jeffs, A.G., & Hooker, S.H. (2001). Reproductive behaviour of the green-lipped mussel, *Perna canaliculus*, in northern New Zealand. *Bulletin of Marine Science*, 69(3), 1095–1108.
- Alfaro, A.C., Jeffs, A.G., & Hooker, S.H. (2003). Spatial variability in reproductive behaviour of green-lipped mussel populations of northern New Zealand. *Molluscan Research*, 23, 223–238.
- Alfaro, A.C. (2006). Population dynamics of the green-lipped mussel, *Perna canaliculus*, at various spatial and temporal scales in northern New

Zealand. *Journal of Experimental Marine Biology and Ecology*, 334, 294–315.

Allen, J.A. (1961). The development of *Pandora inaequalis* (Linne). *Journal of Experimental Marine Biology and Ecology*, 9, 252–268.

Aoki, H., Hayashi, M., Isowa, K., Kawamoto, R., Ohta, H., Narita, T., & Komaru, A. (2007). Growth, mortality and feed intake of Japanese pearl oyster *Pinctada fucata martensii* larvae produced by cryopreserved sperm. *Bulletin of the Fisheries Research Division Mie Prefectural Science and Technology Promotion Centre*, (15), 1–6.

Arellano, S.M., & Young, C.M. (2009). Spawning, development, and the duration of larval life in a deep-sea cold-seep mussel. *Biol. Bull.*, 216, 149–162.

Audesirk, G., McCaman, R.E., & Willows, A.O.D. (1979). The role of serotonin in the control of pedal ciliary activity by identified neurons in *Tritonia diomedea*. *Comparative Biochemistry and Physiology*, 62(1), 87–91.

Bayne, B.L. (1964). Primary and secondary settlement in *Mytilus edulis* L. (Mollusca). *Journal of Animal Ecology*, 33, 513–523.

Bayne, B.L. (1971). *Some morphological changes that occur at the metamorphosis of the larvae of Mytilus edulis*. In: Crisp, D. J. (ed.) Fourth European Marine Biology Symposium, Bangor. London: Cambridge University Press.

Bayne, B.L., Gee, J.M., Daye, J.T., & Scullard, C. (1978). Physiological responses of *Mytilus edulis* L. to parasitic infestation by *Mytilicola intestinalis*. *J. Cons.perm. Int. Explor. Mer*, 38, 12–17.

Beaumont, A.R., & Budd, M.D. (1982). Delayed growth of mussel (*Mytilus edulis*) and scallop (*Pecten maximus*) veligers at low temperatures. *Marine Biology*, 71, 97–100.

Booth, J.D. (1977). Common bivalve larvae from New Zealand; Mytilacea. *Journal of marine and freshwater research*, 11(3), 407–440.

- Boss, K. J. (1982). Mollusca, in parkers. (ed.), *Synopsis and Classification of Living Organisms*. New York: McGraw-Hill.
- Bower, S. M., & Meyer, G.R. (1990). Atlas of anatomy and histology of larvae and early juvenile stages of the Japanese scallop (*Patinopecten yessoensis*). *Canadian Special Publication of Fisheries and Aquatic Sciences* 111. 51 p.
- Bozzola, J.J., & Russel, L.D. (1999). Specimen preparation for scanning electron microscopy. In: *Electron microscopy (Edn 2)* (J.J. Bozzola & L.D. Russell, eds). London: Jones and Bartlett Publishers.
- Brown, C. (1973). The Effects of Some Selected Bacteria on Embryos and Larvae of the American Oyster, *Crassostrea virginica*. *Journal of Invertebrate Pathology*, 21, 215–223.
- Brown, M.R. (1991). The amino-acid and sugar composition of 16 species of microalgae used in mariculture. *Journal of Experimental Marine Biology and Ecology*, 145, 79–99.
- Buchanan, S. (1997). Primary and secondary settlement by the Greenshell™ mussel *Perna canaliculus*. *Journal of Shellfish Research*, 16, 71–76.
- Buchanan, S. (1999). *Spat Production of the Greenshell mussel™ Perna canaliculus in New Zealand*. Thesis for Doctor of Philosophy in Zoology, University of Auckland, New Zealand.
- Buchanan, S. (2001). Measuring reproductive condition in the Greenshell™ mussel *Perna canaliculus*. *New Zealand Journal of Marine and Freshwater Research*, 35, 859–870.
- Buchanan, S., & Babcock, R. C. (1997). Primary and secondary settlement by the Greenshell™ mussel *Perna canaliculus*. *Journal of Shellfish Research*, 16(1), 71–76.
- Carriker, M.R., and Palmer, R.E. (1979). Ultrastructural morphogenesis of prodissoconch and early dissoconch valves of the oyster *Crassostrea*

virginica. *Proceedings of the national shellfisheries association*, 69, 103–128.

Casse, N., Devauchelle, N., & Le Penneec, M. (1998). Embryonic shell formation in the scallop *Pecten maximus* (Linnaeus). *Veliger*, 41, 133–141.

Chanley, P., and Andrews, J.D. (1971). Aids for identification of bivalve larvae of Virginia. *Malacologia*, 11, 45–119.

Chao, N.H., & Liao, I.C. (2001). Cryopreservation of finfish and shellfish gametes and embryos. *Aquaculture*, 197, 161–189.

Cheng, T.C., Peyre, J.F.L., Buchanan, J.T., Tiersch, T.R., & Cooper, R.K. (2001). Cryopreservation of heart cells from the eastern oyster. *In Vitro Cellular & Development Biology - Animal*, 37, 237–244.

Choi, Y.H., Chang, Y.J. (2003). The influence of cooling rate, development stage, and the addition of sugar on the cryopreservation of larvae of the pearl oyster *Pinctada fucata martensii*. *Cryobiology*, 46, 190–193.

Costa, F.D., Darriba, S., & Matinez-Patino. (2008). Embryonic and larval development of *Ensis arcutus* (Jeffreys, 1865) (Bivalvia: Pharidae). *Journal of Molluscan Studies*, 74, 103–109.

Cragg, S.M. (1985). The adductor and retractor muscles of the veliger *Pecten maximus* (L.) (Bivalvia). *Journal of Molluscan Studies*, 51, 276–283.

Croll, R.P. (2001). Catecholamine-Containing Cells in the Central Nervous System and Periphery of *Aplysia californica*. *The Journal of Comparative Neurology*, 441, 91–105.

Croll, R.P., & Dickinson, A.J.G. (2004). Form and function of the larval nervous system in molluscs. *Invertebrate Reproduction and Development*, 46, 173–187.

- Croll, R.P., Jackson, D.L., Voronezhskaya, E.E, (1997). Cetacholamine-containing cells in larval and postlarval bivalve molluscs. *Biological Bullentin*, 193, 116–124.
- Croll R.P., & Voronezhskaya, E.E (1995). Early FMRFamide-like immunoreactive cells in gastropod neurogenesis. *Acta Biologica Hungarica*, 46, 295–303.
- da Costa, F., Novoa, S., Ojea, J., & Martinez-Patino, D. (2012). Biochemical and fatty acid dynamics during larval development in the razor clam *Ensis arcuatus* (Bivalvia: Pharidae). *Aquaculture Research*, 1–14.
- Dickinson, A.J.G., Croll, R.P., & Voronezhskaya, E.E. (2000). Development of embryonic cells containing serotonin, catecholamines, and FMRFamide-related peptides in *Aplysia californica*. *Biology Bullentin*, 199, 305–315.
- Di Matteo, O., Langellotti, A.L., Masullo, P., & Sansone, G. (2009). Cryopreservation of the Mediterranean mussel (*Mytilus galloprovincialis*) spermatozoa. *Cryobiology*, 58(2), 145–150.
- Dong, Q., Huang, C., & Tiersch, T.R. (2007). Control of sperm concentration is necessary for standardization of sperm cryopreservation in aquatic species: Evidence from sperm agglutination in oysters. *Cryobiology*, 54, 87–98.
- Doroudi, M.S., & Southgate, P.C. (2003). Embryonic and larval development of *Pinctada margaritifera* (Linnaeus, 1758). *Molluscan Research*, 23, 101–107.
- Dyachuk, V., Wanninger, A., & Voronezhskaya, E.E. (2012). Innervation of bivalve larval catch muscles by serotonergic and FMRFamidergic neurons. *Acta Biologica Hungarica*, 63, 221–229
- Ellis, I.R. (2010). *Investigations of Neural Ontogeny in the Larval Oyster Crassostrea virginica and the nudibranch Berghia verrucicornis: A Histological an Immunohistochemical Approach*. Thesis for Master of Science, Auburn University, Alabama.

- Elston, R.A., Cheney, D., Frelierc, P., & Lynnd, D. (1999). Invasive orchitophryid ciliate infections in juvenile Pacific and Kumomotooysters, *Crassostrea gigas* and *Crassostrea sikamea*. *Aquaculture*, 174(1–2), 1–14.
- Elston, R.A. (1999). Health management, development and histology of seed oysters. World Aquaculture Society, Baton Rouge, LA.
- Erdmann, W. (1935). Untersuchungen über die Lebensgeschichte der Auster. Nr. 5 Über die Entwicklung und die Anatomie der “ansatzreifen” Larve von *Ostrea edulis* mit Bermerkungen über die Lebensgeschichte der Auster. Wissenschaftliche Meeresuntersuchungen herausgegeben von der Kommission zur wissenschaftlichen Untersuchung der deutschen Meere in Kiel und der Biologischen Anstalt auf Helgoland, Neue Folge, Band 19, Abteilung Helogland, Heft 3, Abhandlung Nr. 6, pp 1–25.
- Ericson, J. (2010). *Effects of ocean acidification on fertilisation and early development in polar and temperate marine invertebrates* (Unpublished master’s thesis). University of Otago, New Zealand.
- Espinoza, C., Valdivia, M., & Dupre, E. (2010). Morphological alterations in cryopreserved spermatozoa of scallop *Argopecten purpuratus*. *Latin American Journal of Aquatic Research*, 38(1), 121–128.
- Eyster, L.S. & Morse, M.P. (1984). Early shell formation during molluscan embryogenesis with new studies on the surf clam *Spisula solidissima*. *American Zoologist*, 24, 871–882.
- Faller, S., Staubach, S., & Kolb, A.K. (2008). Comparative immunohistochemistry of the cephalic sensory organs in Opisthobranchia (Mollusca, Gastropoda). *Zoomorphology*, 127, 227–239.
- Fallis, L.C., Stein, K.K., Lynn, J.W., & Misamore, M.J. (2010). Identification and role of carbohydrates on the surface of gametes in the Zebra Mussel, *Dreissena polymorpha*. *Biological Bullentin*, 218, 61–74.
- Flaws, D. E. (1975). *Aspects of the biology of mussels in the Cook Strait area* (Unpublished PhD Thesis). Victoria University, Wellington.

- Flyachinskaya, L.P. (2000). Localization of serotonin and FMRFamide in the bivalve mollusc *Mytilus edulis* at early stages of its development. *Journal of Evolutionary Biochemistry and Physiology*, 36(1), 66–70.
- Foighil, D.O. (1986). Prodissoconch morphology is environmentally modified in the brooding bivalve *Lasaea subviridis*. *Marine Biology*, 92, 517–524.
- Frontali, N., Williams, L., & Welsh, J.H. (1967). Heart excitatory and inhibitory substances in molluscan ganglia. *Comparative Biochemistry and Physiology*, 22, 833–841.
- Gallager, S.M., Mann, R., & Sasaki, G.C. (1986a). Lipid as an index of growth and viability in three species of bivalve larvae. *Aquaculture*, 56, 81–103.
- Gallager, S.M., & Mann, R. (1986b). Growth and survival of larvae of *Mercenaria mercenaria* (L.) and *Crassostrea virginica* (Gmelin) relative to broodstock conditioning and lipid content of eggs. *Aquaculture*, 56(2), 105–121.
- Ganesan, A. M., Alfaro, A. C., Brooks, J. D., & Higgins, C. M. (2010). The role of bacterial biofilms and exudates on the settlement of mussel (*Perna canaliculus*) larvae. *Aquaculture*, 306, 388–392.
- Gao, D. & Critser, J.K. (2000). Mechanisms of cryoinjury in living cells. *Journal of Experimental Biology*, 265, 187–196.
- Garcia-Lavandeira, M., Silva, A., Abad, M., Pazos, A.J., Sanchez, J.L., & Luz Perez-Paralle, M. (2005). Effects of GABA and epinephrine on the settlement and metamorphosis of the larvae of four species of bivalve molluscs. *Journal of Experimental Marine Biology and Ecology* 316, 149–156.
- Gaume, B., Fouchereaua-Peron, M., Badou, A., Helleouet, M-N., Huchete, S., & Auzoux-Bordenave. (2011). Biomineralization markers during early shell formation in the European abalone *Haliotis tuberculata*, Linnaeus. *Marine Biology*, 158, 341–353.
- Gerdes, D. (1983). The Pacific Oyster *Crassostrea gigas* Part I. Feeding behaviour of larvae and adults. *Aquaculture*, 31, 195–219.

- Goodsell, J.G., & Eversole, A.G. (1992). Prodissoconch I and II length in Mercenaria taxa. *Nautilus*, 106, 119–122.
- Gosling, E., (2003). *Reproduction, settlement & recruitment. Bivalve Molluscs, Biology, Ecology and Culture*. Oxford: Blackwell Publishing.
- Gros, O., Frenkiel, L., & Moueza, M. (1997). Embryonic, larval, and post-larval development in the symbiotic clam *Codakia orbicularis*. *Invertebrate Biology*, 116, 86–101.
- Gwo, J.-C. (1995). Cryopreservation of oyster *Crassostrea gigas* embryos. *Theriogenology*, 43(7), 1163–1174.
- Haag, W. R., & Warren, M.L. (1997). Host fishes and reproductive biology of 6 freshwater mussel species from the Mobile Basin, USA. *Journal of the North American Benthological Society*, 16, 576–585.
- Hay, B. & Grant, C. (2004). *An Introduction to Marine Resources in Taitokerau, with Examples from the Whangarei Region*. Research Programme on Sustainable Māori. The James Henare Māori Research Centre, University of Auckland.
- Hickman, R. W., & Gruffydd., L.D. (1971). *The histology of the larva of Ostrea edulis during metamorphosis*. In: Crisp, D. J. (ed.) Fourth European Marine Biology Symposium, Cambridge University Press: Cambridge.
- Hickman, R.W., Illingworth, J. (1980). Condition cycle of the Green-Lipped Mussel *Perna canaliculus* in New Zealand. *Marine Biology*, 60, 27–38.
- Hickman, R.W., Waite, R.P., Illingworth, J., Meredyth-Young, J.L., & Payne, G. (1991). The relationship between farmed mussels, *Perna canaliculus* and available food in Pelorus-Kenepuru Sound, New Zealand, 1983-1985. *Aquaculture*, 99, 49–68.
- Hodgson, C.A., & Burke, R.D. (1988). Developmental and larval morphology of Spiny Scallop, *Chlamys hastate*. *Biology Bullentin*, 174, 303–318.

- Holland, D.L., & B. E. Spencer, B.E. (1973). Biochemical changes in fed and starved oysters, *Ostrea edulis* L. during larval development, metamorphosis and early spat growth. *Journal of Experimental Marine Biology and Ecology*, 53, 287–298.
- Howard, D.W., & Smith, C.S. (1983). *Histological techniques for marine bivalve molluscs*. National Oceanic and Atmospheric Administration technical memorandum NMFS-F/NEC–25.
- Humphreys, W.J., (1969). Initiation of shell formation in the bivalve, *Mytilus edulis*. *Proceedings of electrochemical microscopy*, 272–273.
- Jaeckle, W.B. (1995). Variation in the size, energy content, and biochemical composition of invertebrate eggs: Correlates to the mode of larval development. In *Ecology of Marine Invertebrate Larvae* (ed, L. McEdward), pp. 49–78. CRC Press, Boca Raton, FL.
- Jardillier, E., Rousseau, M., Gendron-Badou, A., Fröhlich, A., Smith, D.C., Martin, M., Helléouet, M.N., Huchette, S., Doumenc, D., Auzoux-Bordenave, S. (2008). A morphological and structural study of the larval shell from the abalone *Haliotis tuberculata*. *Marine Biology*, 154, 735–744.
- Jefferies, A., R. Holland, S. Hooker and B. Hayden. (2000). Overview and bibliography of research on the greenshell mussel, *Perna canaliculus*, from New Zealand waters. *Journal of Shellfish Research*, 18, 1–14.
- Jenkins, R. J. (1985). *Mussel Cultivation in the Marlborough Sounds (New Zealand)* (2nd ed.). Wellington: New Zealand Fishing Industry Board.
- Kennedy, V.S. (1977). Reproduction in *Mytilus edulis aoteanus* and *Aulacomya maoriana* (Mollusca:Bivalvia) from Taylors Mistake, New Zealand. *New Zealand journal of marine and freshwater research*, 11, 255–267.
- Kniprath, E. (1980). Larval development of the shell and the shell gland in *Mytilus* (Bivalvia). *Wilhelm Roux's Archives of Developmental Biology*, 188, 201–204.

- Kreiling, J.A., Jessen- Eller, K., Miller, J., Seegal, R.F., & Reinisch, C.L. (2001). Early development of the serotonergic and dopaminergic nervous system in *Spisula solidissima* (surf clam) larvae. *Comparative Biochemistry and Physiology Part A*, 130, 341–351.
- Kristof, A., & Klusmann-Kolb, A. (2010). Neuromuscular development of *Aeolidiella stephanieae* Valdez, 2005 (Mollusca, Gastropoda, Nudibranchia). *Frontiers in Zoology*, 7(5).
- Lachowicz, L. S. (2005). *Population biology of mussels (Aulacomya maoriana, Mytilus galloprovincialis and Perna canaliculus) from rocky intertidal shores in Wellington Harbour, New Zealand.*
- Lin, T.T., Chao, N.H., & Tung, H.T. (1999). Factors affecting survival of cryopreserved Oyster (*Crassostrea gigas*) embryos. *Cryobiology*, 39, 192–196.
- Liu, B.Z., & Li, X. (2008) Preliminary studies on cryopreservation of Sydney Rock Oyster (*Saccostrea glomerata*) larvae. *Journal of Shellfish Research*, 27, 1125–1128.
- Lopez-Vera, E., Aguilar, M.B., & Heimer de la Cotera, E.P. (2008). FMRFamide and related peptides in the phylum mollusca. *Peptides*, 29, 310–317.
- MacDonald, I. H. (1963). *Studies in the biology of Mytilus edulis aoteanus Powell, 1958 and Perna canaliculus Gremlin, two intertidal molluscs of the rocky shore* (Unpublished MSc. Thesis). University of Canturbury, Christchurch.
- Mahmud, S., Mladenov, P.V., Sheard, P., & Chakraborty, S.C. (2008). Characterisation of neurons in the visceral ganglia of the Green-lipped mussel (*Perna canaliculus*) using antibodies raised against neuropeptides and neurotransmitters. *Bangladesh Journal of Animal Science*, 37 (1) 78–85.
- Marois, R., & Carew, T.J. (1997). Fine structure of the apical ganglion and its serotonergic cells in the larva of *Aplysia californica*. *Biology. Bullentin*, 192, 388–398.

- Martel, A., Hynes, T.M., & Nicks, J.B. (1995). Prodissoconch morphology, planktonic shell growth, and size at metamorphosis in *Dreissena polymorpha*. *Canadian Journal of Zoology*, 73, 1835–1844.
- McFadzen, I.R.B. (1992). Growth and survival of cryopreserved oyster and clam larvae along a pollution gradient in the German Bight. *Marine Ecology Progress Series*, 91, 215–220.
- Ministry of Fisheries (2010). Green-shell mussels. Retrieved 1 October, 2012, from <http://fs.fish.govt.nz/Page.aspx?pk=122>.
- Ministry of Fisheries (2011). Quaterly report. *Fisheries and aquaculture production and trade (Period ending December 2011)*. Retrieved 1 October, 2012, from <http://www.fish.govt.nz/NR/rdonlyres/B978D085-128A-4E63-83ADC3CA1BDC953D/0/QuarterlyreportDecember2011.pdf>.
- Ministry for Primary Industries (2012). Situation and Outlook for Primary Industries 2012. Wellington: Ministry for Primary Industries.
- Morton, J. E., & Miller, M. (1973). *The New Zealand Sea shore* (2nd ed.). London: Collins & Sons.
- Moueza, M., Gros, O., & Frenkiel, L. (2006). Embryonic development and shell differentiation in *Chione cancellata* (Bivalvia, Veneridae): an ultrastructural analysis. *Invertebrate biology*, 125(1), 21–33.
- Moueza, M., Gros, O., & Frenkiel, L. (1999). Embryonic, larval and postlarval development of the tropical clam, *Anomalocardia brasiliiana* (Bivalvia, Veneridae). *Journal of Molluscan Studies*, 65, 73–88.
- Nascimento, I.A., Leite, M. B., Sampaio de Araujo, M. M, Sansone, G., Pereira, S., Santo, M. (2005). Selection of cryoprotectants based on their toxic effects on oyster gametes and embryos. *Cryobiology*, 51, 113–117.

- New Zealand Government. (2007). *Our Blue Horizon; the Government's commitment to Aquaculture*. Ministry of Economic Development, New Zealand. 47pp.
- Nielsen, C. (2004). Trochophore Larvae: Cell-lineages, ciliary bands, and body regions. 1. Annelida and Mollusca. *Journal of Experimental Zoology (Mol. Dev. Evol.)* 302B, 35–68.
- Ockelmann, K.W. (1965). Developmental types in marine bivalves and their distribution along the Atlantic coast of Europe. In Proceedings of the First European Malacological Congress, London, 1962. Edited by L.R. Cox and J.F. Peake. Conchological Society of the Great Britain and Ireland and the Malacological Society of London, London. pp. 25–53.
- Odintsova, N.A., & Boroda, A.V. (2012). Cryopreservation of the Cells and Larvae of Marine Organisms. *Russian Journal of Marine Biology*, 38(2), 101–111.
- Paine, R. T. (1971). A short-term experimental investigation of resource partitioning in a New Zealand rocky intertidal habitat. *Ecology*, 52(6), 1096–1106.
- Paniagua-Chavez, C.G., Buchanan, J.T., Supan, J.E., & Tiersch, T.R. (2000). Cryopreservation of sperm and larvae of the Eastern oyster, in Cryopreservation in Aquatic species, Tiersch, T.R., & Mazik, P.M., Eds., The World Aquaculture Society, Baton Rouge, LA, pp. 230–239.
- Paniagua-Chavez, C.G., Tiersch, T.R. (2001). Laboratory Studies of Cryopreservation of Sperm and Trochophore Larvae of the Eastern Oyster. *Cryobiology*, 43, 211–223.
- Paredes, E., Adams, S.L., Tervit, H.R., Smith, J.F., McGowan, L.T., Gale, S.L., Morrish, J.R., & Watts, E. (2012). Cryopreservation of Greenshell™ mussel (*Perna canaliculus*) trochophore larvae. *Cryobiology*.
- Petrone, L., Ragg, N.L.C., Girvan, L., & McQuillan, A.J. (2009). Scanning Electron Microscopy and Energy Dispersive X-Ray Microanalysis of *Perna canaliculus* Mussel Larvae Adhesive Secretion. *The Journal of Adhesion*, 85, 78–96.

- Ponder, F. W., & Lindberg, D. R. (2008). *Phylogeny and Evolution of the Mollusca*. Berkeley: University of California Press.
- Powell, A. W. B. (1979). *New Zealand Mollusca: Marine land and freshwater shells*. Auckland: Collins.
- Price, D.A., & Greenberg, M.J. (1977). Structure of a molluscan cardioexcitatory neuropeptide. *Science*, 197, 670–671.
- Ragg N.L.C., King, N., Watts, E., & Morrish, J. (2010). Optimising the delivery of the key dietary diatom *Chaoceros calcitrans* to intensively cultured Greenshell™ mussel larvae, *Perna canaliculus*. *Aquaculture*, 306, 270–280.
- Raineri, M. (1995). Is a mollusc an evolved bent metatrochophore? A histochemical investigation of neurogenesis in *Mytilus* (Mollusca: Bivalvia). *Journal of the Marine Biological Association of the United Kingdom*, 75, 571–592.
- Redfearn, P., Chanley, P., & Chanley, M. (1986). Larval shell development of four species of New Zealand mussels: (Bivalvia, Mytilacea), *New Zealand Journal of Marine and Freshwater Research*, 20(2) 157–172.
- Renard, P. (1991). Cooling and freezing tolerances in embryos of the Pacific Oyster, *Crassostrea gigas*; methanol and sucrose effects. *Aquaculture*, 92, 43–57.
- Roche, M., Rondeau, P., Singh, N.J., Tarnus, E., & Bourdon, E. (2008). The antioxidant properties of serum albumin. *FEBS Letters*, 582, 1783–1787.
- Saier, B., (2002). Subtidal and intertidal mussel beds (*Mytilus edulis* L.) in the Wadden Sea: diversity differences of associated epifauna. *Helgoland Marine Research*, 56, 44–50.
- Sanchez-Lazo, C., & Martinez-Pita, Ines, (2012). Biochemical and energy dynamics during larval development of the mussel *Mytilus galloprovincialis* (Lamarck,1819). *Aquaculture*, 358–359, 71–78.

- Scheltema, R.S. (1967). The relationship of temperature to the larval development of *Nassarius obsoletus* (Gastropoda). *Biology Bullentin*, 132(2), 253–265.
- Siddall, S. E. (1980). A clarification of the genus *Perna* (Mytilidae). *Bulletin of marine science*, 30(4), 858–870.
- Silberfeld, T., & Gros, O. (2006). Embryonic development of the tropical clam *Tivela mactroides* (Born, 1778) (Veneridae: subfamily Meretricinae): a SEM study. *Cah Biology of Marine Journals*, 47, 243–251.
- Smith, J.F., Adams, S.L., Gale, S.L., McGowan, L.T., Tervit, H.R., & Roberts, R.D. (2012a). Cryopreservation of Greenshell™ mussel (*Perna canaliculus*) sperm. I. Establishment of freezing protocol. *Aquaculture*, 334–337, 199–204.
- Smith, J.F., Adams, S.L., McDonald, R.M., Gale, S.L., McGowan, L.T., & Tervit, H.R. (2012b). Cryopreservation of Greenshell™ mussel (*Perna canaliculus*) sperm. II. Effect of cryopreservation on fertility, motility, viability, and chromatin integrity. *Aquaculture*, 364–365, 322–328.
- Sprung, M., (1984). Physiological energetics of mussel larvae (*Mytilus edulis*). I. Shell growth and biomass. *Marine Ecology Progress Series*, 17, 283–293.
- Statuito, C.G., Bao, W., Yang, J., & Kitamura, H. (2005). Survival, growth, settlement and metamorphosis of refrigerated larvae of the mussel *Mytilus galloprovincialis* Lamarck and their use in settlement and antifouling bioassays. *Biofouling*, 21(3/4), 217–225.
- Stephenson, R.L., & Chanley, P.E. (1979). Larval development of the cockle *Chione stutchburyi* (Bivalvia: Veneridae) reared in the laboratory. *New Zealand Journal of Zoology*, 6, 553–560.
- Strathmann, R.R., Fenaux, L., Sewell, A.T., & Strathmann, M.F. (1993). Abundance of food affects relative size of larval and postlarval structures of a molluscan veliger. *Biology Bullentin*, 185, 232–239.

- Suquet, M., Mercier, A.L., Rimond, F., Mingant, C., Haffray, P., & Labbe, C. (2012). Setting tools for the early assessment of the quality of thawed Pacific oyster (*Crassostrea gigas*) D-larvae. *Theriogenology* 78, 462–467
- Tervit, H.R., Adams, S.L., Roberts, R.D., McGowan, L.T., Pugh, P.A., Smith, J.F., & Janke, A.R. (2005). Successful cryopreservation of Pacific oyster (*Crassostrea gigas*) oocytes. *Cryobiology*, 51, 142–151.
- Thorson, G. (1936). The larval development, growth, and metabolism of arctic marine bottom invertebrates compared with those of other seas. *Meddr. Greenland* 100, 1–155.
- Todt, C., & Wanninger, A. (2010). Of tests, trochs, shells, and spicules: Development of the basal mollusk *Wirenia argentea* (Solenogastres) and its bearing on the evolution of trochozoan larval key features. *Frontiers in Zoology*, 7(6).
- Tong, L.J., & Redfearn, P. (1985). Hatchery techniques and the culture of *Perna canaliculus*. MAF Fisheries Research Division. Marine farming seminar presented July 1985.
- Turnipseed, M., Knick, K.E., Lipcius, R.N., Dreyer, J. & Van Dover, C.L. (2003). Diversity in mussel beds at deep-sea hydrothermal vents and cold seeps. *Ecology Letters* 6, 518–523.
- Vakily, J.M. (1989). *The biology and culture of mussels of the genus Perna*. *ICLARM Studies and Reviews*, 17, 1–63.
- Verween, A., Vincx, M., & Degraer, S. (2009). Seasonal variation in gametogenesis and spawning of *Mytilopsis leucophaeata*, an invasive bivalve in Europe. *Journal of Molluscan Studies*, 75, 307–310.
- Voronezhskaya, E.E., Nezhlin, L.P., Odintsova, N.A., Plummer, J.T., & Croll, R.P. (2008). Neuronal development in larval mussel *Mytilus trossulus* (Molusca:Bivalvia). *Zoomorphology*, 127, 97–110.
- Waller, T. R. (1981). Functional morphology and development of veliger larvae of the European oyster, *Ostrea edulis* Linne. *Smithson Contrib. Zool.* 328, 70 pp.

- Wang, H., Li, X., Wang, M., Clarke, S., Gluis, M., & Zhang, Z. (2011). Effects of larval cryopreservation on subsequent development of the blue mussels, *Mytilus galloprovincialis* Lamarck. *Aquaculture Research*, 42, 1816–1823.
- Wassnig, M., & Southgate, P.C. (2012). Embryonic and larval development of *Pteria penguin* (Roding, 1798) (Bivalvia: Pteriidae). *Journal of Molluscan Studies* 78, 134–141.
- Watson, P.F., (1981). The Roles of Lipid and Protein in the Protection of Ram Spermatozoa at 5 Degrees C by Egg Yolk Lipoprotein. *Journal of Reproduction and Fertilisation*, 62(2), 483–492.
- Weiss, I.M., Tuross, N., Addadi, L., & Weiner, S. (2002). Mollusc Larval Shell Formation: Amorphous Calcium Carbonate Is a Precursor Phase for Aragonite. *Journal of Experimental Zoology*, 293, 478–49.
- Widdows, J. (1991). Physiological ecology of mussel larvae. *Aquaculture*, 94, 147–163.
- Wood, A. R., Apte, S., MacAvoy, E. S., & Gardner, J. P. A. (2007). A molecular phylogeny of the marine mussel genus *Perna* (Bivalvia: Mytilidae) based on nuclear (ITS1&2) and mitochondrial (COI) DNA sequences. *Molecular Phylogenetics and Evolution*, 44, 685-698.
- Xue, Q.Z. (1994). Cryopreservation of embryos of scallop, *Chlamys farreri*, in liquid nitrogen. *Marine Science*, 4, 44–47.
- Yankson, K., & Moyses, J. (1991). Cryopreservation of the spermatozoa of *Crassostrea tulipa* and three other oysters. *Aquaculture*, 97, 259–267.
- Young, T. (2009). Pharmacological induction of larval settlement in the New Zealand mussel *Perna canaliculus*. Thesis for the degree of Masters of Applied Science in Marine Environmental Sciences, Auckland University, New Zealand.
- Young, T., Alfaro, A.C., Ganesan, A.M., Brooks, J., Robertson, J., & Higgins, C. (2010). Chemosensory connections: Metabolism of microbe-induced behaviour in marine invertebrate larva. New Zealand Microbiological Society Conference. Auckland, New Zealand.

Young, T., Alfaro, A.C., & Robertson, J. (2011). Effect of neuroactive compounds on the settlement of mussel (*Perna canaliculus*) larvae. *Aquaculture*, 319, 277–283.

Zardus, J.D., & Martel, A.L. (2006). Phylum Mollusca: Bivalvia. In C.M. Young, M.A. Sewell, & M.E. Rice (Eds.), *Atlas of marine invertebrate larvae* (289–296). Amsterdam; Boston: Academic Press.